

December 2011

D3 Nozzle Characterization

Nicholas Andrew Fast
Worcester Polytechnic Institute

Rachel Adena Winsten
Worcester Polytechnic Institute

Follow this and additional works at: <https://digitalcommons.wpi.edu/mqp-all>

Repository Citation

Fast, N. A., & Winsten, R. A. (2011). *D3 Nozzle Characterization*. Retrieved from <https://digitalcommons.wpi.edu/mqp-all/2788>

This Unrestricted is brought to you for free and open access by the Major Qualifying Projects at Digital WPI. It has been accepted for inclusion in Major Qualifying Projects (All Years) by an authorized administrator of Digital WPI. For more information, please contact digitalwpi@wpi.edu.



D3 Nozzle Characterization

A Major Qualifying Project Report

Submitted to the Faculty of

Worcester Polytechnic Institute

in partial fulfillment of the requirements for the

Degree of Bachelor of Science by:

Nicholas Fast (ME)

Rachel Winsten (CE)

In Collaboration with Shanghai Jiao Tong University
Partners: Hao “Jonathan” Bohan, Chu “Stella” Yueshan

Date: 3 September 2011

Approved:

Professor Nicholas A. Dembsey

Melissa Avila

Project Number NAD TY11

Contents

Table of Tables	3
Table of Figures	4
Introduction.....	7
ABSTRACT:.....	8
INTRODUCTION:	9
BACKGROUND:	9
EXPERIMENTAL STUDY:	11
VALIDITY OF DATA:	16
RESULTS AND DISCUSSION:.....	17
Vertical PIV Results:	17
Horizontal PIV Results:	21
Shadowgraphy Results:	23
CONCLUSION:.....	25
FUTURE WORK:.....	25
ACKNOWLEDGEMENTS:.....	26
REFERENCES:	26
Appendix A: Pre Qualifying Project (PQP).....	28
Appendix B: Background	44
D3 Nozzle	44
Comparable Work.....	45
Dave Thomas Sheppard: “Spray Characteristics of Fire Sprinklers”	45
Ning Ren, Andrew R. Blum, Ying-Hui Zheng, Chi Do, and Andre Marshall: “Quantifying the Initial Spray from Fire Sprinklers”	47
G. Grant, J. Brenton, D. Drysdale: “Fire Suppression by Water Sprays”	48
TFRI Regulations.....	49
Shadowgraphy and PIV	51
Appendix C: Testing Setup.....	55

Appendix D: Calibration and Procedure.....	56
Appendix E: Testing Parameters	64
Appendix F: Encountered Problems	77
Appendix G: Data	82
Example Data Sets:	83
Vertical PIV Testing:	83
Horizontal PIV Testing:	84
Shadowgraphy Testing:	85
Appendix H: Results	88
Vertical Spray Angle Analysis.....	88
Horizontal Analysis	90
K-factor:	91
Pressure:	93
Height:.....	94
Ligament Distance	96
Shadowgraphy.....	105
Appendix I: Data Handling and Storage	113
Appendix J: Error Analysis.....	114
Appendix K: Tyco Scientific Presentation	116
Appendix L: Presentation for TFP President George Oliver	152

Table of Tables

Table 1: Parameters tested	12
Table 2: Spray Angle Validation	16
Table 3: Sprinkler List	40
Table 4: Example of Shadowgraphy Statistics	86
Table 5: Spray Angle Measurements	89
Table 6: 60° Rotation Angle Data.....	90
Table 7: 0 Degree Rotation Angle Data.....	90
Table 8: Ligament Distance Measurement (by group member)	98
Table 9: Average Ligament Distance Measurements	99
Table 10: Preliminary Shadowgraphy Picture Plan Based off Ligament Distance Data.....	102
Table 11: Ligament Distance Data	104
Table 12: Average Ligament Distance Breakup: 65° nozzle with a K-factor of 1.8.....	105
Table 13: Shadowgraphy Tests Conducted.....	106
Table 14: Shadowgraphy Results for 65 Degree Nozzle, 1.8 K-factor, 20 psi.....	106
Table 15: Pressure, K-factor, Nozzle Change Comparison	110

Table of Figures

Figure 1: PIV system, showing the orientation of the camera and the laser in relation to the flow of water ⁴	10
Figure 2: Shadowgraphy setup, showing the orientation of the light source and the camera in relation to the droplets being imaged ⁴	11
Figure 3: Underside of D3 nozzle, showing the deflector and the different rotation angles	13
Figure 4: 0° Rotation Figure 5: 45° Rotation	14
Figure 6: 60° Rotation Figure 7: 90° Rotation	14
Figure 8: Method Used to Measure the Spray Angle	18
Figure 9: Combined 500 Pictures of 65 Degree Nozzle with $0.1365 \text{ m}^3 \text{ s}^{-1} \text{ Pa}^{-1/2}$ K-factor at a pressure of 1.38 bar (20 psi)	18
Figure 10: Combined 500 pictures of 125 Degree Nozzle with $0.2277 \text{ m}^3 \text{ s}^{-1} \text{ Pa}^{-1/2}$ K-factor at a pressure of 1.38 bar (20 psi)	19
Figure 11: Combined 500 pictures of 180 Degree Nozzle with $0.5465 \text{ m}^3 \text{ s}^{-1} \text{ Pa}^{-1/2}$ K-factor at a pressure of 1.38 bar (20 psi)	19
Figure 12: Ligament Breakup Distance Measurement Technique	20
Figure 13: Spray Pattern Geometry	22
Figure 14: $0.1365 \text{ m}^3 \text{ s}^{-1} \text{ Pa}^{-1/2}$ K-factor, Figure 15: $0.1365 \text{ m}^3 \text{ s}^{-1} \text{ Pa}^{-1/2}$ K-factor, 22	
Figure 16 from source [1]	34
Figure 17 from source [1]	35
Figure 18: Droplet diameters and axial velocities a distance of 40 mm from the nozzle ^[2]	38
Figure 19: Mean and representative diameters and velocities for 40mm below the nozzle ^[2]	38
Figure 20: Transparent Calibration Plate ^[2]	39
Figure 21: D3 Nozzle.....	44
Figure 22: PDI System Setup (Sheppard, 44).....	46
Figure 23: PIV system setup (Sheppard, 46)	46
Figure 24: Ligament Distance (Ren et al., 3).....	48
Figure 25: Spray Angle Test Equipment	51
Figure 26: PIV system (LaVision).....	52
Figure 27: Shadowgraphy Setup (LaVision)	53

Figure 28: Tape Measure for Vertical Calibration.....	56
Figure 29: Styrofoam Calibration Board	60
Figure 30: Shadowgraphy Calibration Lens	62
Figure 31: 50 Pictures	66
Figure 32: 250 Pictures	66
Figure 33: 500 Pictures	67
Figure 34: 1000 Pictures	67
Figure 35: Comparison of Pictures	68
Figure 36: Spray Angle of 500 Pictures vs. 1000 Pictures (respectively)	69
Figure 37: Varying Nozzle Angles (65, 125, 180).....	71
Figure 38: Varying K-factors (7.2, 3.0, 1.8)	72
Figure 39: Rotation Angles.....	73
Figure 40: 50 Pictures at 20 psi.....	82
Figure 41: 250 Pictures at 20 psi.....	82
Figure 42: 500 Pictures at 20 psi.....	82
Figure 43: 1000 Pictures at 20 psi.....	82
Figure 44: 50 Pictures at 100 psi.....	83
Figure 45: 250 Pictures at 100 psi.....	83
Figure 46: 500 Pictures at 100 psi.....	83
Figure 47: 1000 Pictures at 100 psi.....	83
Figure 48: Example of Single Image	84
Figure 49: Example of Combined Images	84
Figure 50: Example of Single Image	84
Figure 51: Example of Combined Images	84
Figure 52: Example Shadowgraphy Picture	85
Figure 53: Example Velocity Map.....	85
Figure 54: Diameter vs. % of Max.....	86
Figure 55: Diameter vs. Volume Flux	87
Figure 56: Diameter vs. Mass Flux.....	87
Figure 57: Method Used to Measure the Spray Angle	88

Figure 58: Spray Pattern Geometry	91
Figure 59: K-factor Affect on Spray Geometry	91
Figure 60: K-factor Affect on Tine Spray Geometry.....	93
Figure 61: Pressure Affect on Spray Geometry	94
Figure 62: Height Affect on Spray Geometry.....	95
Figure 63: Height Affect on Spray Geometry.....	96
Figure 64: Ligament Distance (Ning Ren, et al.).....	97
Figure 65: Ligament Distance Breakup Measurement Technique	98
Figure 66: Average Ligament Distance Measurements of 0° Rotation	100
Figure 67: Average Ligament Distance Measurements of 45° Rotation	101
Figure 68: Average Ligament Distance Measurements of 60° Rotation	101
Figure 69: Average Ligament Distance Measurements of 90° Rotation	102
Figure 70: Edge, Middle, Under Representation	103
Figure 71: Ligament Distance with Varying Pressures	104

Introduction

This MQP is structured around a 15 page paper written for the sponsor, Tyco Fire Protection Products. The page limit was imposed in order to have the paper be eligible for submission to a fire protection conference so that the findings of the project may be shared with the rest of the fire protection community. Following the conference paper is found a series of appendices, which fully outline and explain the details of the project.

ABSTRACT:

Current sprinkler design and test methodologies could be dramatically improved with modern technology. With improvements in sprinkler characterization technology, it is possible to accurately measure sprinkler characteristics, including spray angle and droplet diameter that could streamline development and testing of sprinklers. In addition, the ability to accurately define sprinkler spray patterns is necessary to validate predictive modeling tools such as Fire Dynamics Simulator (FDS), leading to better predictions of the spray's impact on the fire environment. A state-of-the-art technology that is being used at Tyco Fire Protection Products to better define these characteristics is the LaVision™ laser system. The LaVision™ laser allows users to determine numerous sprinkler characteristics in a quick and efficient manner.

In order to obtain a thorough understanding of spray characteristics, two imaging techniques were used. These techniques were Particle Image Velocimetry (PIV), in both vertical and horizontal orientations, and High-magnification Shadow Imaging (shadowgraphy). Vertical PIV images were used to measure spray angle and ligament breakup distance, while horizontal PIV images displayed the flow. Shadowgraphy focused on a small section to magnify the water spray in order to determine droplet size and velocity.

As an initial step in using the laser, various nozzles were tested under numerous conditions and trends were observed and are reported. Using the Tyco D3 nozzle, three spray angles (65°, 125°, 180°) and three K-factors (0.1365, 0.2277, 0.5465 m³s¹Pa^{-1/2} (1.8K, 3.0K, 7.2K)). were chosen and tested under different pressures, heights and rotation angles. Care was taken to ensure that the effect of the frame arm, slots and tines were studied. The wide range of the different factors allowed trends in the sprinkler characteristics to be studied.

While the D3 nozzle was not completely characterized, there were several significant findings. The K-factor of the nozzle, for example, plays a role in the distribution of the water flow out of the nozzle. Additionally, pressure played a role in changes in the flow distribution. While both of these affected the overall distribution pattern, neither seemed to have an effect on the spray angle of a given nozzle. Depending on how the pressure or K-factor of a nozzle is changed, droplet size and droplet count vary based on the measurement location in the flow.

INTRODUCTION:

Fire models today have difficulty validating the effect a sprinkler spray will have on compartment fire dynamics, partly due to the lack of properly specified sprinkler characteristics. In response, some agencies and corporations in the fire protection engineering field are beginning to develop methodology to better specify sprinkler characteristics such as droplet size and velocity, spray angle and ligament breakup distance. Two methodologies being explored at Tyco Fire Protection Products are Particle Image Velocimetry (PIV) and High-magnification Shadow Imaging (shadowgraphy). As a first step toward development of a specific methodology for the techniques, multiple offerings of the Tyco D3 directional spray nozzle were studied. Different spray angle, pressure and K-factor nozzles were chosen from the D3 product family and the results from the PIV and shadowgraphy techniques were analyzed. Many interesting differences in the effects could be observed from the results based on the variations in the nozzles. The techniques can eventually be used to better characterize sprinkler and nozzle spray and aid in future development efforts. The current report will provide information on the background research conducted, a discussion on what methods were employed and an analysis of the results and conclusions.

BACKGROUND:

Although using a laser to determine sprinkler characteristics is a relatively new endeavor in the field of fire protection engineering, there has been some previous work by others on the subject. Along with the description of the comparable research, a short description of the types of nozzles that were studied and the instrumentation employed during testing is provided.

Comparable Research: David Thomas Sheppard's article, "Spray Characteristics of Fire Sprinklers," details work he completed with a similar PIV system to the one being used at Tyco.¹ Although Sheppard's projects are similar in their methods as well as their characterization of droplet size and velocity, a couple aspects of sprinkler spray characterization that Sheppard did not research are included in the current work. Ren, Blum, Zheng, Do and Marshall provided a key understanding of ligament breakup distance. Their work detailed the difference between the stages of the atomization process, including the formation of sheets, ligaments and separate droplets. The definition and explanation provided by Ren et al. on ligament breakup distance

became the foundation to measure the parameter.² The work by Grant, Brenton and Drysdale was essential to the study of droplet size. The data presented by Grant et al. was used to develop an understanding of how to accurately measure droplet size with a minimal level of error. With the provided information, a practical and functional procedure was applied for the shadowgraphy methodology.³

PIV and Shadowgraphy: PIV is a technique used to measure a full velocity field. For the known time interval, which has been set up in the system, the velocity of the droplets can be calculated using the distance that they travel in the interval. Since it is rather difficult to figure out the distance of specific droplets when each picture has hundreds of them, the camera and laser are designed specifically for the PIV technique. The camera can take two pictures in rapid succession in order to catch the same droplets within the camera's field of view. If any common lamp replaced the laser, the light it provides would be scattered in various directions. The laser light is more directed and also has a relatively higher power, allowing the system to accurately predict droplet velocity using PIV. The laser illuminates a plane of the flow, as shown in Figure 1 below.⁴

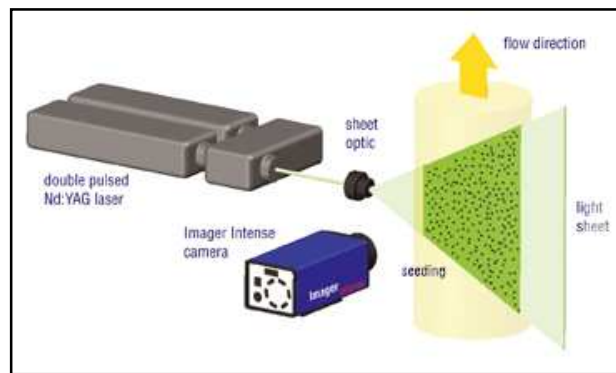


Figure 1: PIV system, showing the orientation of the camera and the laser in relation to the flow of water⁴

While PIV was designed to calculate velocity fields, the main focus for the technology in the current work was to measure ligament breakup distance and spray angle. In order to complete these tests, the pictures were taken in the exact same manner as velocity imaging. Ligament breakup distance was measured from individual pictures while the spray angle was measured by taking several pictures and averaging them to provide a more accurate representation of the spray

over time. These measurement techniques are described in more detail in the Experimental Study section below.

Shadowgraphy is mainly designed to measure the size and velocity of droplets that may be on the scale of micrometers. The system is composed of a long distance microscope with a high resolution Charge-Coupled Device (CCD) camera and a light source. Using two pictures taken in a short time interval, the velocity of the droplets can be calculated by measuring the distance the droplet moves. Using the laser system, the droplet velocity measured can be as high as 100 m/s (328.08 ft/s). Figure 2 below shows the shadowgraphy system setup.⁴ Refer to Appendix B in the D3 Nozzle Characterization MQP for more background information.⁵

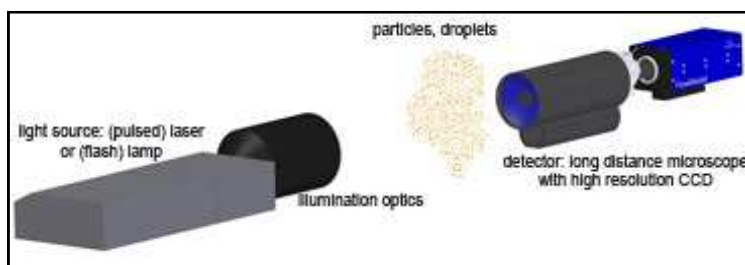


Figure 2: Shadowgraphy setup, showing the orientation of the light source and the camera in relation to the droplets being imaged⁴

EXPERIMENTAL STUDY:

D3 Nozzle: The Tyco D3 Protectospray nozzle is an open, external deflector type nozzle. It is effective in covering a wide range of surfaces and operates with the primary goal of preventing excessive heat absorption. A typical use of the D3 nozzle is protecting a large fuel tank from reaching dangerous temperatures in the event of a nearby fire. The D3 nozzle is available in numerous spray angles, orifice sizes and material types. The spray angle options range from 65° to 180°, while K-factors can be chosen between $0.0912 \text{ m}^3 \text{ s}^{-1} \text{ Pa}^{-1/2}$ (1.3K), and $0.5465 \text{ m}^3 \text{ s}^{-1} \text{ Pa}^{-1/2}$ (7.2K). The recommended pressure range for the nozzle is 1.38 bar to 4.14 bar (20 to 60 psi).⁶

Since there are so many K-factor, orifice size and pressure combinations to choose from, the number of nozzles to be studied had to be reduced to a suitable level. Preliminary tests were run to determine which nozzles would give the best pictures and thus would be suitable for further testing. With smaller spray angles, such as 65°, the whole flow was easily visible but the droplets

were very tightly packed, which made droplet analysis from PIV pictures more difficult. With wider angles, such as 180°, it was found that a wider-angle lens needed to be used in order to capture images of the entire flow. The wider angles did, however, provide a lower density of droplets, which made analysis a bit more clear. With these findings in mind, a sample range of nozzles was selected in order to provide a representative subset of the many differences across the full range of 56 possible nozzles.⁶ A maximum, minimum and median value was selected for the various parameters, as detailed in Table 1 below.

Table 1: Parameters tested

Nozzle Angle (°)	60	125	180
K-Factor ($\text{m}^3\text{s}^1\text{Pa}^{-1/2}$)	0.1365 [1.8K]	0.2277 [3.0K]	0.5465 [7.2K]
Pressure (bar) [psi]	1.38 [20]	6.89 [100]	12.07 [175]

Parameters: As an initial undertaking, a matrix of eight nozzles was selected. The range included spray angles at 65° and 125° with K-factors of $0.1365 \text{ m}^3\text{s}^1\text{Pa}^{-1/2}$ (1.8K), $0.2277 \text{ m}^3\text{s}^1\text{Pa}^{-1/2}$ (3.0K) and $0.5465 \text{ m}^3\text{s}^1\text{Pa}^{-1/2}$ (7.2K). Also included was the spray angle of 180° with K-factors of $0.1365 \text{ m}^3\text{s}^1\text{Pa}^{-1/2}$ (1.8K) and $0.5465 \text{ m}^3\text{s}^1\text{Pa}^{-1/2}$ (7.2K) (a K-factor of $0.2277 \text{ m}^3\text{s}^1\text{Pa}^{-1/2}$ (3.0K) was not studied due to availability of the nozzles). Vertical and horizontal PIV pictures were analyzed for all of the nozzles studied but only a subset of the matrix was analyzed using the shadowgraphy methodology.

PIV: A significant consideration in the selection of testing parameters was the number of pictures to acquire and analyze for horizontal and vertical PIV as well as shadowgraphy. In PIV, the images are taken by the computer and averaged to create a single image of the flow in order to more accurately measure spray angle. The number of pictures taken for the integration needs to be optimized to ensure that the final image is not too rough with individual droplets showing (i.e. too few pictures). The purpose of the integrated image is to show a solid profile of the shape formed by the flow of water out of the nozzle. If too few images are integrated, the final image is not clear enough and it is difficult to locate the solid edges of the flow. On the other hand, too many images require additional processing time and data storage while not adding much value. Upon examination of several different picture counts (50, 100, 250, 500 and 1000), it was

decided that 500 pictures would be sufficient for testing. Using 1000 images recorded a difference of less than 1° in the spray angle and required double the time for image capture and processing. On the other hand, integrating 250 pictures provided an image that lacked a clearly defined edge for measurement of the spray angle.

In order to define the location of the camera relative to the nozzle, the rotation angles were defined as shown in Figure 3 below. The base rotation of 0° was defined as the position at which the frame arms were in line with the camera, which allowed for easy visual alignment. To change the nozzle position, an automatic nozzle rotating system was used. The rotation system was attached directly to the pipe and nozzle and controlled via the computer. After visual analysis of the nozzle geometry, four rotation angles were chosen to be a sufficient representation of the spray. These angles were 0° , 45° , 60° and 90° , all rotated clockwise from the base 0° position.



Figure 3: Underside of D3 nozzle, showing the deflector and the different rotation angles

The 0° position provided an image of a vertical plane located on a tine with no effect from the frame arms. The 45° and 60° rotations both showed some influence from the frame arms, while also showing the flow through a slot and off a tine, respectively. Lastly, the 90° rotation angle displayed a plane with the full effect of the frame arms. The rotation changes are shown in Figure 4 through Figure 6 below.



Figure 4: 0° Rotation

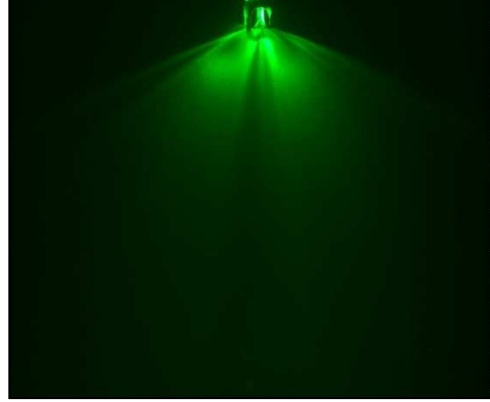


Figure 5: 45° Rotation



Figure 6: 60° Rotation



Figure 7: 90° Rotation

To analyze trends in spray angle with respect to pressure, a range of pressures were studied. According to the D3 data sheets, the recommended operating pressure range for the nozzle is 1.38 to 4.14 bar (20 to 60 psi) but the maximum pressure rating is 12.07 bar (175 psi).⁶ Therefore, the test pressures of 1.38 bar (20 psi), 6.89 bar (100 psi) and 12.07 bar (175 psi) were selected. The only issue encountered with these parameters was that the $0.5465 \text{ m}^3 \text{ s}^{-1} \text{ Pa}^{-1/2}$ (7.2K) K-factor nozzle at 12.07 bar (175 psi) required a flow rate of 360.75 lpm (95.3 gpm), which was unattainable with the test setup. As a result, only the pressures of 1.38 bar (20 psi) and 6.89 bar (100 psi) were tested for the $0.5465 \text{ m}^3 \text{ s}^{-1} \text{ Pa}^{-1/2}$ (7.2K) K-factor nozzle.

Vertical: The vertical PIV test setup consisted of the laser system and a high-speed camera, positioned perpendicular to each other. It allowed for the camera to capture images of the entire plane that the laser illuminated. While the laser could be positioned anywhere on the

perpendicular, the camera's distance needed to be considered to allow for testing to be reproduced. The camera was measured at a distance of 318.45 cm (124.375 in) away from the nozzle. The distance was chosen to allow the camera to be out of the flow of water and also obtain a picture of the entire flow, even on the larger spray angle nozzles. In order to calibrate the images, a tape measure was hung from the nozzle deflector and the camera lens was focused. Then with the computer, a 25.4 cm (10 in) range on the tape measure was selected and the distance was defined in the software to scale the view of the image.

Horizontal: In the horizontal PIV test setup, the laser light projected horizontally which illuminated a slice of the spray pattern at a specific height. The camera was mounted above the nozzle, which allowed the camera to capture images of the entire horizontal plane that the laser illuminated. Due to space and time considerations, the camera was mounted above the laser for the current study. The laser was positioned at a height of four feet above the ground so the camera was correspondingly focused on a piece of Styrofoam board four feet above the ground for calibration. A grid of 304.8 x 304.8 cm (12 in x 12 in) squares on the surface of the board was used as a reference point for the computer to define a measurement scale. The grid scale was used to remove the perspective distortion of the image, since the camera was not perpendicular to the field of view.

Shadowgraphy: In the background research for shadowgraphy it was discovered that a sample size of 1000 to 5000 droplets would yield 90-95% accuracy of droplet size. The spray produces a statistical distribution of droplets, which is why sample size is important. A sample with too few droplets may not give a true representation, as there can be an order of magnitude change between the diameters of droplets in a spray.³ It is important to collect a large enough sample to provide a true account of the droplets present in the flow. While it is desirable to be as accurate as possible, it takes close to 40,000 droplets in order to yield 97% accuracy.³ Considering that a sample size nearly 40 times larger is required to obtain a minimal increase in accuracy, a decision was made to capture between 1000 and 5000 droplets as the sample size. A count of 50 pictures was selected as it provided 1000-7000 droplets at different sample points in the flow for a 65° nozzle.

In order to account for the flow within the entirety of the spray, three testing positions were selected. The first position was the location directly below the deflector. Since the nozzle would be rotated at that point, the droplet count should not be affected by the rotation angle. The next position was located at the edge of the flow, which was estimated from the measured spray angle from the PIV testing. The last position was located in the middle of the flow, halfway between the edge of the flow and under the deflector. To properly locate the middle position, a protractor was held in place at the bottom of the deflector and a string was connected at that same point and pulled out to the correct radius at the correct angle. All three of the test positions were tested at nozzle rotations of 0°, 45° and 90°. Refer to Appendix C, D, and E in the D3 Nozzle Characterization MQP for additional experimental setup information⁵.

VALIDITY OF DATA:

Since the techniques are relatively new in the field of fire protection engineering, it was difficult to find information to validate the results. For measurements of spray angle, angles were originally determined using the laser images. To ensure that the laser did not affect the results obtained from the picture, related sets of photos were taken with a regular digital camera and the angles were re-measured. It was found that with both the laser pictures and the digital camera photos, the angles were similar. Table 2 below shows the results from both measurements. While a different pressure was used for the digital camera measurements and the laser measurements, it was found that pressure did not have an effect on the spray angle of the nozzle (see Results and Discussion section).

Table 2: Spray Angle Validation

Deflector Angle (°)	K-factor ($\text{m}^3\text{s}^1\text{Pa}^{-1/2}$)	Digital Camera Measured Angle (°)	Pressure (bar) [psi]	Laser Measured Angle (°)	Pressure (bar) [psi]
65	0.1365	90	3.45 [50]	95	1.38 [20]
65	0.5465	90	3.45 [50]	88	1.38 [20]
180	0.2277	176	3.45 [50]	174	1.38 [20]

180	0.5465	177	3.45 [50]	178	1.38 [20]
-----	--------	-----	-----------	-----	-----------

Other experiments could be compared against each other to validate results. In the horizontal pictures, it was found that at low pressures the area directly under the deflector appeared to have a decreased droplet count. The observation of the less dense area was verified through shadowgraphy, which showed that the droplet count under the nozzle was very low. At higher pressures, the area directly under the nozzle appeared to be dense with flow and the observation was again confirmed in the shadowgraphy statistical results.

Since there was little existing information on how to measure ligament breakup distance and the time for the project was limited, the ligament breakup distance measurements were not validated with redundant techniques. Refer to Appendix G in the ‘D3 Nozzle Characterization’ MQP for more information on the data.⁵

RESULTS AND DISCUSSION:

Vertical PIV Results:

Spray angle: Since there was not much literature on how to exactly measure spray angle, a method was developed which involved creating two points to define the line. To do so, it is necessary to set the first point at the brim of the deflector where the beginning of the water sheet exists. The other point sits at the position where the edge of the pattern makes an obvious change of direction due to gravity. After following the same procedure on the other side of the flow, the two lines can be used to measure the spray angle. The method used to measure spray angle is depicted in Figure 8 below.

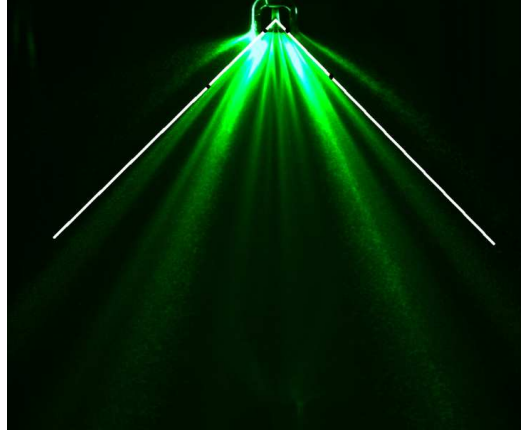


Figure 8: Method Used to Measure the Spray Angle

Although many different pictures were taken, only a representative few were analyzed and reported in the current work. The sample pictures that were analyzed include a 65° nozzle with a $0.1365 \text{ m}^3 \text{ s}^{-1} \text{ Pa}^{-1/2}$ (1.8K) K-factor, 125° nozzle with a $0.2277 \text{ m}^3 \text{ s}^{-1} \text{ Pa}^{-1/2}$ (3.0K) K-factor and 180° nozzle with a $0.5465 \text{ m}^3 \text{ s}^{-1} \text{ Pa}^{-1/2}$ (7.2K) K-factor. These samples are shown in Figures 9 through 11 below.



Figure 9: Combined 500 Pictures of 65 Degree Nozzle with $0.1365 \text{ m}^3 \text{ s}^{-1} \text{ Pa}^{-1/2}$ K-factor at a pressure of 1.38 bar (20 psi)



Figure 10: Combined 500 pictures of 125 Degree Nozzle with $0.2277 \text{ m}^3\text{s}^{-1}\text{Pa}^{-1/2}$ K-factor at a pressure of 1.38 bar (20 psi)

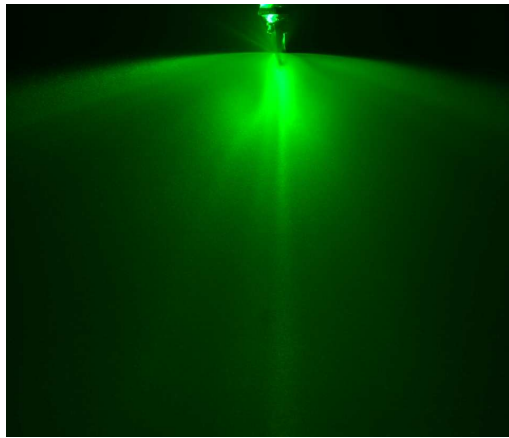


Figure 11: Combined 500 pictures of 180 Degree Nozzle with $0.5465 \text{ m}^3\text{s}^{-1}\text{Pa}^{-1/2}$ K-factor at a pressure of 1.38 bar (20 psi)

Upon analyzing the spray angle pictures, it was found that the varying pressures, which ranged from 1.38 to 12.07 bar (20 to 175 psi), did not affect the spray angle. For example, the spray angle ranged from 93.75° to 95° for the 65° nozzle for the full range of pressures, which is only a 1.25° difference. The 125° nozzle experienced a 5.5° difference between the minimum and maximum measured angle and the 180° nozzle had a 0.25° difference. Nozzle rotation angle was also analyzed in terms of its effect on spray angle but there appeared to be no significant effect. Spray angle measurement results are shown in Table 3 below.

Table 3: Spray Angle Results

Rotation Angle	$65^\circ (0.1365 \text{ m}^3\text{s}^{-1}\text{Pa}^{-1/2} \text{ K-factor})$		$125^\circ (0.2277 \text{ m}^3\text{s}^{-1}\text{Pa}^{-1/2} \text{ K-factor})$		$180^\circ (0.5465 \text{ m}^3\text{s}^{-1}\text{Pa}^{-1/2} \text{ K-factor})$
----------------	---	--	--	--	--

	1.3 8 bar	6.89 bar	12.07 bar	AV G	1.38 bar	6.89 bar	12.07 bar	AVG	1.38 bar	6.89 bar	AVG
0°	96°	94°	96°	95°	145°	153°	157°	152°	175°	176°	176°
45°	94°	94°	95°	94°	147°	150°	149°	149°	178°	177°	178°
60°	95°	96°	93°	95°	145°	151°	142°	146°	178°	177°	178°
90°	95°	94°	91°	93°	143°	148°	143°	145°	175°	175°	175°
AVG	95°	95°	94°		145°	151°	148°		177°	176°	

Ligament Breakup Distance: Due to the lack of an established method of determining ligament breakup distance and the difficulty in determining the exact location in the photographs, a new methodology was developed. Ligament breakup distance was measured vertically downward from the bottom of the nozzle using the pictures from the vertical PIV testing. The method used to determine ligament breakup distance is shown in Figure 12 below.

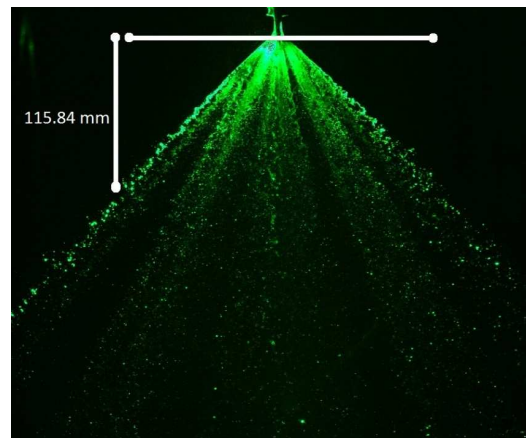


Figure 12: Ligament Breakup Distance Measurement Technique

Using the newly created definition, each group member (four) took measurements of the ligament breakup distance using a 65° nozzle with a $0.1365 \text{ m}^3\text{s}^1\text{Pa}^{-1/2}$ (1.8K) K-factor at each pressure and rotation angle and the average of the four distances is shown in Table 4 below. Whenever the droplets seemed to become separated is where ligament distance breakup was assumed to be. Each group member's measurement was within $\pm 10 \text{ mm}$ of each other.

Table 4: Ligament Breakup Distance using a 65 degree nozzle with a $0.1365 \text{ m}^3\text{s}^1\text{Pa}^{-1/2}$ k-factor at 20 psi.

Average Ligament Distance Breakup

	0°	45°	60°	90°
1.38 bar	116 mm, 4.57 in	97 mm, 3.81 in	126 mm, 4.96 in	108 mm, 4.25 in
6.89 bar	126 mm, 4.96 in	107 mm, 4.21 in	157 mm, 6.18 in	No Ligament
12.07 bar	142 mm, 5.59 in	114 mm, 4.49 in	180 mm, 7.09 in	No Ligament

From the table, it is noted that as the pressure increases, the ligament breakup distance also increases. Another pattern that was observed is in the rotation angle. Analysis of the 90° rotation did not match the observations at the other angles since there were no visible ligaments at higher nozzle pressures at that rotation. Recall from figure 3 that the 90° rotation was fully affected by the frame arms. The rest of the rotations were compared and it was found that on the slot (45° rotation), the ligament breakup distance was the smallest. On a tine (0° and 60° rotations), the ligament distance was longer than in the slot. Although both 0° and 60° were on a tine, the ligament distance at 60° was consistently larger. The reasoning for this was unable to be determined and requires future work. The difference between the slot and tine measurements was due to the flow of water in these positions.

Horizontal PIV Results:

Spray Geometry: When analyzing the horizontal pictures, the main point of interest was the spray geometry. To find how various parameters affect the spray pattern, numerous pictures were analyzed. Before going into a discussion of the results, it is important to understand the basics of the spray geometry. Figure 13 demonstrates how an inner and outer pattern is formed in horizontal testing. The water flowing through the slots creates the inner pattern, while the water flowing over the tines makes the outer pattern.

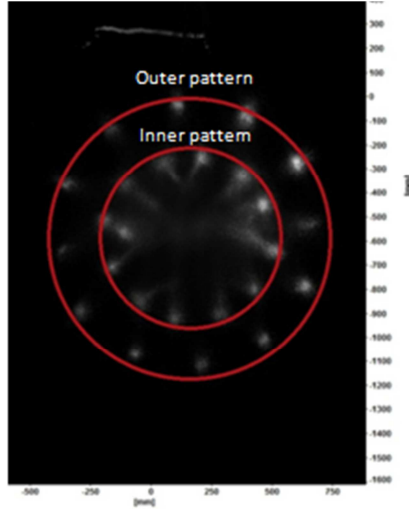
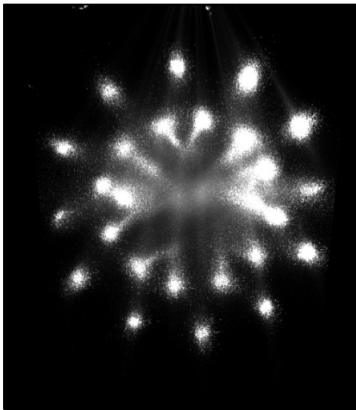
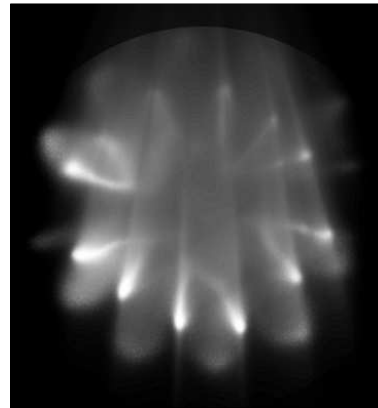


Figure 13: Spray Pattern Geometry

One of the most significant differences observed from the horizontal PIV images was a difference in droplet distribution between high and low pressure cases. At the lower pressure setting (1.38 bar), very neat circles could be seen around the edges of the flow where the water sprayed off of the deflector (Figure 14). The difference with pressure can be observed in Figures 14 and 15, where the pressure increases from 1.38 bar (20 psi) to 12.07 bar (175 psi).



**Figure 14: $0.1365 \text{ m}^3 \text{s}^{-1} \text{Pa}^{-1/2}$ K-factor,
65° D3 at 1.38 bar (20 psi)**



**Figure 15: $0.1365 \text{ m}^3 \text{s}^{-1} \text{Pa}^{-1/2}$ K-factor,
65° D3 at 12.07 bar (175 psi)**

Other observations made with horizontal testing are closely linked to the shadowgraphy results, which will be discussed in the following section.

Shadowgraphy Results:

After conducting a thorough analysis of the shadowgraphy pictures, charts and graphs, several interesting observations can be made. There were five different parameters that were tested when working with shadowgraphy. These include nozzle spray angle, height, location, K-factor and pressure. First, it is important to recognize how the number of droplets per picture changes with changing parameters. A general pattern that can be seen in the data is that the number of droplets increases as the picture is taken closer to the center of the spray pattern. In the center, water is flowing down through the slots and is also being pushed in by the flow of air, which leads to a greater concentration of droplets.

When it comes to nozzle rotation angle, there are also some patterns related to the number of droplets. At 0° , the lowest number of droplets is counted and steadily increases with the rotation angle of the nozzle. Even though the 90° angle is on the frame arms, many droplets were present. The height of the picture also affected how many droplets were found. When the camera was positioned at 30.48 cm (1 ft), the greatest number of droplets was counted. As the camera is moved farther away from the nozzle, the droplets become less dense, so the concentration per unit area is lower.

As the K-factor increases from $0.1365 \text{ m}^3\text{s}^1\text{Pa}^{-1/2}$ (1.8K) to $0.5465 \text{ m}^3\text{s}^1\text{Pa}^{-1/2}$ (7.2K), the droplet count drops significantly. The fewer droplets may be due to the fact that a higher K-factor allows for a wider spread of flow. In the small field of view (15 x 15 mm) that the pictures were taken, there may have been a more concentrated amount of water at the area when using the smaller K-factor nozzle. The nozzle spray angle does not seem to have a consistently significant effect on the droplet count. When the 180° nozzle is compared to the 65° nozzle with the same position, K-factor and pressure, the number of droplets decreased slightly.

Referring to figure 15 in the horizontal testing section, the inner and outer circles have a much more solid covering of the area at the higher pressure setting of 6.89 bar (100 psi). At higher pressures, the water jet will strike the deflector at a much higher velocity. The effect of the increased velocity will cause the droplets to shear and break apart into smaller droplets. The smaller droplets will then mix with the air and disperse more as they descend. In order to validate the hypothesis, a comparison was made between the number of droplets and the DV50 value at

different locations in the flow. The DV50, or the volume mean diameter, is the value at which half of the volume of water is contained in droplets with a diameter smaller than the DV50 value. Since the difference in droplet breakup should occur at the deflector, the results closest to the deflector were used. In table 5 below, the number of droplets is compared to the DV50 value for measurements taken at different locations in the flow for the 65° degree, $0.1365 \text{ m}^3\text{s}^{-1}\text{Pa}^{-1/2}$ (1.8K) K-factor nozzle at two different pressures.

Table 5: 65° D3 $0.1365 \text{ m}^3\text{s}^{-1}\text{Pa}^{-1/2}$ (1.8K) K-factor results at 30.48 cm (1 ft) radius

	Edge (Number of droplets/DV50 in mm)	Middle (Number of droplets/DV50 in mm)	Under (Number of droplets/DV50 in mm)
1.38 bar, 0°	3348/0.9241	3795/0.7231	6985/0.2817
6.89 bar, 0°	4504/0.2387	4036/0.4071	6211/0.5406

For the lower pressure, the number of droplets increases as you move in towards the middle of the flow. For the higher pressure, the trend is less clear but number of droplets generally still increased from the edge of the flow towards the middle. While the droplet count information does help to validate the theory about droplet distribution, the important detail is in the DV50 value, which is calculated by splitting the total volume of water passing through the control volume per unit time in half. The unit time period is the amount of time it takes for the pictures to be taken and is not a defined amount (i.e. it changes every time the test is run). Since droplets are typically spherical in shape, the droplet volume is proportional to the diameter cubed. If the DV50 number is small, the result is an exponentially greater number of small droplets.

Observing the DV50 values for 1.38 bar (20 psi), it can be seen that the droplets get smaller moving from the edge of the flow towards the middle. With the 6.89 bar (100 psi) case, however, the droplet size on the edge of the flow is extremely small in comparison to the 1.38 bar (20 psi) case. Instead of decreasing further similar to the 1.38 bar (20 psi) scenario, the droplet size tends to increase near the center of the spray pattern. The pattern of DV50 size shows a complete change between the low and high-pressure cases. This is most likely due to the higher pressure of water causing it to hit the deflector at a higher velocity causing shear and forcing the water to spread apart into smaller droplets. Refer to Appendix H in the ‘D3 Nozzle Characterization’ MQP for more in-depth results.⁵

CONCLUSION:

Even with the small number of nozzles studied, certain general trends and patterns can be derived from the results. The spray angle was not affected by changes in K-factor and pressure. In ligament breakup distance analysis, two trends arose. First, ligament breakup distance increases as the pressure increases. Also, ligament breakup distance occurred sooner on slots than on tines. Through horizontal PIV testing, it was found that pressure greatly affects the spray pattern. As pressure increased, the inner diameter became more dense with droplets while at low pressures; the interior of the flow was less dense. The same pattern emerged with increases in K-factor. Shadowgraphy was able to back up some of the finding of PIV testing, as well as providing useful data on droplet size, location, and velocity.

Through testing, processing and analysis, many interesting trends and patterns were found in the results from vertical and horizontal PIV as well as shadowgraphy. The data provided could be used for designing and modeling sprinklers in the future and can be a stepping stone toward learning more about sprinkler sprays with the current laser methodology and setup. All of the data is available upon reasonable request.

FUTURE WORK:

In order to complete an extensive study of the D3 nozzle, it would be beneficial to study each nozzle angle and K-factor. In the current work, only three different nozzles and K-factors were tested. These nozzles provided a general idea of trends and patterns but it would be interesting to see if the trends continue throughout the D3 nozzle family.

The computer program for the laser does offer techniques for measuring spray angle and creating vector maps, instead of measuring the spray angles by hand. In the future, it would be worthwhile to look into these methods to test spray angles to compare against the manually calculated values.

Ideally, the horizontal PIV pictures would have been taken from below to allow for direct comparisons between the derived results and the existing literature. In order to set up the pictures from below however, much more time, effort and materials would be required. It would be interesting to compare the two different perspectives on the flow.

There is a lot of work that could be undertaken looking further into droplet shearing at higher water pressures. Through the current study, it was found that a somewhat linear pattern is present for the DV50 values at different points in the flow. However, the direction in which DV50 increases changes between the two cases of 1.38 bar (20 psi) and 6.89 bar (100 psi). A select pressure may exist at which the change occurs, which could have a significant effect on sprinkler effectiveness. It would be beneficial to look further into whether or not there is a single pressure at which the droplet diameter change occurs for different nozzles. It is currently unclear how the change in flow geometry would affect the fire suppression capabilities of the nozzle, which could be another area of future research.

In the future, it may be possible to use the laser to determine differences in the spray geometry after the flow makes contact with the object it is intended to protect. The D3 nozzle would commonly be used to keep large fuel tanks cool in the event of a fire to avoid further fires and explosions. When the spray from the nozzle comes in contact with the surface of the tank, the geometry will most likely change, which could be very important for modeling.

ACKNOWLEDGEMENTS:

The authors of this paper would like to thank the extremely helpful and supportive employees at Tyco Fire Protection Products. In particular, George Oliver and Paul Piccolomini for making this project possible. Also, Melissa Avila at Tyco and Professor Nicholas Dembsey at WPI for giving very useful and helpful guidance throughout the project. Chad Goyette and Zach Magnone were always there to help answer questions, and explain the equipment. Patricia Beaulieu for creating the project. Lastly, the authors would like to thank Worcester Polytechnic Institute and Shanghai Jiao Tong University.

REFERENCES:

¹Sheppard, David Thomas. "Spray Characteristics of Fire Sprinklers." National Institute of Standards and Technology, NIST GCR 02-838, June 2002.

² Ren, N., Blum, A., Zheng, Y., Do, C. and Marshall, A., 2009. "Quantifying The Initial Spray From Fire Sprinklers." Fire Safety Science 9: 503-514. doi:10.3801/IAFSS.FSS.9-503

³Grant, G., Brenton, T., Drysdale, D. "Fire Suppression by Water Sprays." Progress in Energy and Combustion Science 2000: 79-130.

⁴ LaVision. Techniques. 27 7 2011 <<http://www.lavision.de/en/imprint.php>>.

⁵ Hoa Bohan, Nicholas Fast, Rachel Winsten and Chu “Stella” Yueshan. “D3 Nozzle Characterization.” Major Qualifying Project: Worcester Polytechnic Institute, 2011.

⁶ Products, Tyco: Fire Suppression & Building. Type D3 Protechtospray Directional Spray Nozzle, Open, Medium Velocity. Technical Data Sheet. Lansdale, 2009.

Appendix A: Pre Qualifying Project (PQP)

In order for a project of this caliber to be completed within the 7 week time frame that is the WPI term schedule, a large amount of background work was required. This period of time is referred to as the PQP or Pre Qualifying Project. While the project itself was completed during E-term (July and August) the PQP was completed before hand in D-term (March and April). During this time Tyco provided our group with a variety of different background material on related topics to our project.

Getting the work, assigned by Tyco, completed each week was a challenge in and of itself. While there was only 15 questions to be completed by the group, to coordinate between 4 busy college students, 12 time zones and roughly 11,000 miles apart (according to Google maps, which calculated Worcester to Shanghai as a ~38 day trip consisting primarily of a kayak trip across the pacific ocean with a pit stop in Hawaii) was quite a tricky task. Email and dividing the work up at the beginning of each week became the means in which this goal was accomplished. Every week everyone went through all of the assigned reading, and then focused on their few questions. After everyone answered their own specific questions they were all emailed to one person who combined all of the work, and edited the responses in a final draft which was then forwarded back out to the group as well as to Prof. Dembsey and Tyco. The morning after these questions were due the whole group would call in for a teleconference. The time that this was able to work out was at 10am EST, which ended up being 10pm for the SJTU students. During this meeting Prof. Dembsey would go through the questions from the previous week and try to help the group truly grasp the concepts behind the questions. His typical question was, “Alright, but what does that really mean?” The whole process of having to work as a team to answer questions and also to know the reading material well enough to defend your answers really helped the group to gain an understanding of the basics of fire suppression and sprinklers.

The first week of the PQP was focused on sprinkler operation. With the background reading for that week there was lots of information about the different types of sprinklers, and how each one of them operated. The three basic orientations of sprinklers are: upright, pendent, and sidewall. Upright sprinklers spray water upwards, and a deflector redirects the water downward in an umbrella shaped pattern. Pendent sprinklers are very similar, except that instead of being pointed

upwards, they are pointed down and the deflector just spreads out the spray of the water. With sidewall sprinklers, they spray water out from a wall and cover a large area both out and away from the sprinkler, as well as off to the sides. There are many more sprinklers with tons of different applications, but these are really the three basic types. In addition to learning about the types of sprinklers, the different operating elements were also studied. Several different designs are available, and they each function differently for different applications. It was very helpful to learn about these for a better understanding of sprinklers, but in terms of our project they were of little concern. The project was only to study characteristics of the flow pattern and not of the sprinkler deployment.

Week two of the PQP started to shift into more project specific work with some readings on PIV and shadowgraphy. While at the time it seemed as if shadowgraphy would be the main focus of the project, PIV did eventually play a very big role in the data collection process. PIV works by taking two pictures in rapid succession, and from the differences in those two pictures the velocity of droplets can be figured out. Shadowgraphy functions in a very similar manner, the difference being in the size of the picture captured. For pictures in shadowgraphy, they are very small and can very clearly capture individual droplets and obtain very precise information about their size and velocity. While PIV can capture information about velocity, it is less precise on a smaller level and would be more difficult to capture images of individual droplets. So for PIV the pictures are generally of a larger area of the flow. It was also noted in some of the readings that shadowgraphy can also be used for larger pictures in order to obtain data about the sheet breakup and ligament distance in the flow.

After that, in week three of the PQP, the discussion switched over to some basic fire dynamics. The material talked a little about how fires work, and then on how sprinklers utilize the attributes of fire in order to function effectively. The main concept that the sprinklers operating element (essentially a heat detector) draw from is a fire plume. When a fire burns, it produces energy in the form of heat which then causes hot gases to rise due to buoyancy; this movement is described as a fire plume. As the fire plume moves up from the point of origin, it will eventually come in contact with the ceiling and create a ceiling jet. From this point the smoke and heat moves out radially from the point of contact with the ceiling. When this happens the smoke and heat will

eventually be pushed over to where the sprinkler is located, in the event that the fire doesn't magically occur under a sprinkler. The heat in the ceiling jet can then cause the operating element of the sprinkler to deploy and water will be expelled downward in order to start suppressing the fire.

Moving into week four of the project the focus shifted again, this time towards writing the project proposal. The questions of the week were focused around technical writing techniques and citing the work of others. The main object of the week was to really start working on getting a solid proposal together for the work to be completed at Tyco. This work continued on until the end of the PQP with writing and editing the proposal until it was finally completed.

Below is found the PQP outline as provided at the start of the PQP by Tyco with a rough break down of each week, along with some general objectives. After that is found the final proposal submitted to Tyco for the project.

Shanghai Jiao Tong – WPI
PQP D Term 2011

Week	Date	Activity	Comment
1 March 13	3/16 10-11 am EST	Tele-conference with Tyco, WPI and SJTU	Team introductions & project overview discussion.
		It is expected that students converse with each other during the week. A hard schedule to be determined by students. Prof Dembsey and Dr. Beaulieu to be informed on schedule.	Assignment of "Introduction to Sprinklers" presentation plus videos. Homework assignment questions.
2 March 20	3/23 10-11 am EST	Tele-conference	Discussion of sprinkler components and types. K factor, operating elements and why choose one over the other. What affects their operation ?
		Students converse during the week.	Assignment of "An Introduction to Laser Imaging" and Marshall. Homework assignment questions.
3 March 27	3/30 10-11 am EST	Tele-conference	Discussion of Shadowgraphy, PIV, LIF, LII, PDI and parameters measured.
		Students converse during the week.	Assignment of "Why is Characterizing Spray Important?" Homework assignment questions. Assigned to start proposal.
4 April 3	4/6 10-11 am EST	Tele-conference	Review of student proposal and information to be included. Review of importance.
		Students converse during the week.	Assigned to fix proposal. Assignment of homework questions related to testing.
5 April 10	4/13 9-10 am EST	Tele-conference	Review of modified proposal. Discussion of testing conditions such as instrument calibration, data acquisition, data checks and safety issues.
		Students converse during the week.	Assigned to modify proposal again.
6 April 17	4/20 10-11 am EST	Tele-conference	Review of proposal. Questions taken from students on any topics. More discussion on safety topics.
		Students converse during the week.	Assigned to finalize proposal.
7 April 24	4/27 10-11 am EST	Tele-conference	Overall review of project. Details of phase 2 - MQP - logistics.
		Students converse during the week.	

Objectives

1. In general, obtain enough knowledge to successfully conduct the MQP in Term E, including
 - Basics of sprinklers including components, types, k factor, operating elements, temperature ratings, operation and how to choose one or the other.
 - Basics of different laser imaging methods
 - What parameters can be collected for sprinkler spray characterization
 - Why is understanding spray is important – how info is used
 -
 - An understanding of the instruments operation and what can go wrong.
 - How does one know if the readings are correct.
 - How to determine what can cause error.
 - Basics of data acquisition setup (type of signals, rate, calibration).
 - How to put together a basic research proposal including proper format, information to include and how to understand the big picture as to how the plan fits in as well as all the minute details needed.
2. Start to learn how to work in an “international” group across multiple time zones, cultures and language barriers.
 - Figure out how to video chat, e-mail and teleconference easily.
 - Learn how to put together one “report” or “work product” for a group while working as a team.
 - Learn how to speak up in a group to give opinions and not just let the professor “do all the talking”



Interoffice Memorandum

To: Tyco Fire Protection Products

From: - Hao Bohan

-Nicholas Fast

- Rachel Winsten

- Chu Yueshan

cc:

Date: 4/26/2011

Subject: To use a LaVision Shadowgraphy system to analyze the flow of water from a sprinkler.

Overview:

The work hereafter proposed aims to analyze the spray characteristics of the flow of different sprinkler heads. In order to accomplish this goal a Shadowgraphy system will be used in order to image the flow of water out of the sprinklers. Several images will be taken of each type of sprinkler, at each test pressure. These images will be analyzed to provide information on velocity and direction of the droplets in the flow. The information collected will lead to an improvement in testing measures, and as a result better performance based design of sprinklers. The proposed work will take place between July 6, 2011 and August 19, 2011.

Background:

Shadowgraphy:

A Shadowgraphy system, also known as High-magnification Shadow Imaging, is used to visualize particles, droplets, and other structures. The system is unique in that it allows the user

to analyze particles down to the micro scale. A Shadowgraphy system can measure particle size, particle position, particle shape, histograms, velocity, number density, and mass flux.

A Shadowgraphy system uses the basic principles of the focal plane and the depth of the field of imaging to measure the desired parameters. Using these principles, a Shadowgraphy system utilizes a light sources and an imaging system in order to capture images off of which calculations can be made. The light source, usually a laser, is placed behind the particles and pulses causing the particles motion to “freeze”. Once this occurs, the detector, or camera takes an image of the particles. From this image all of the parameters are able to be measured.

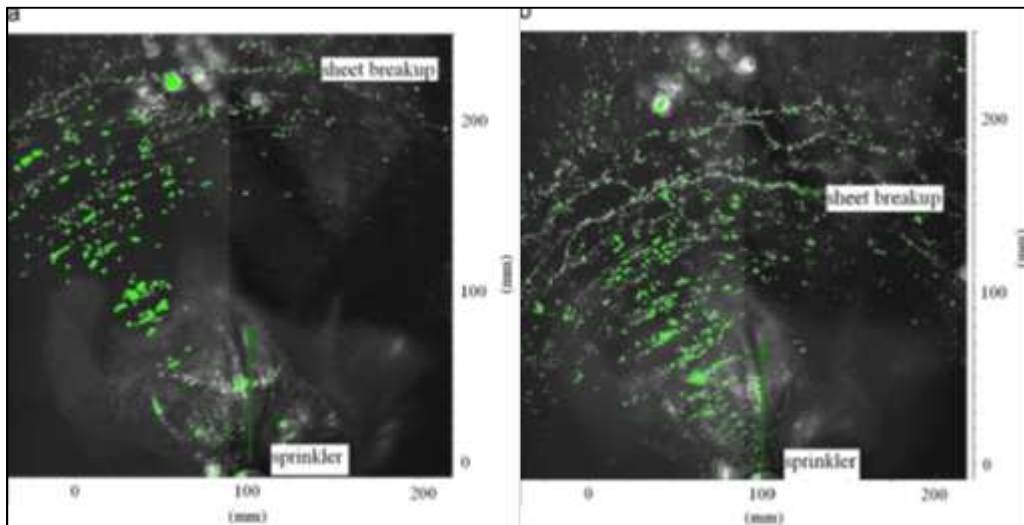


Figure 16 from source [1]

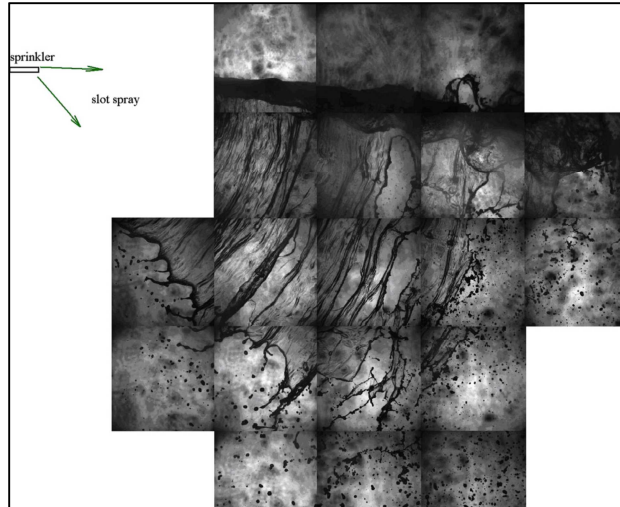


Figure 17 from source [1]

Some examples of the type of data that will be collected in this experiment can be seen in Figure 16 and Figure 17. The images that we will collect as part of this experiment will allow us to observe the flow as a whole out of the sprinkler, as well as to break it down more and analyze some of the smaller components of the flow. From here we could analyze droplet size and the general location of the droplets from the point of origin (the sprinkler head). As seen in Figure 16, you can observe the point at which the flow actually starts to break up into the smaller droplets. This would be a good example of the types of things we could look into analyzing.

Problem Statement:

Currently there is a shortage of information pertaining to sprinkler flow characteristics. This shortage of information has led to an inability to create better performance based designs for sprinklers.

Objective:

A obtain a comprehensive measurement of the discharge characteristics of the initial spray from sprinklers. This is to be illustrated by Tyco's new LaVision modular laser imaging system.

Results, Deliverables and Benefit:

The results could be documented through graphs of the information collected.

Some examples of this could be graphs of the following:

- Spray sheet thickness vs. radial distance
- Dimensionless sheet breakup distance vs. Weber number
- Slot spray angle vs. discharge pressure

Benefits:

This project will help to foster good working relationships between both universities as well as with Tyco. It will also help to provide a great opportunity for some students to receive some real world experience in working at Tyco, while working on solving a real life problem. This is also a great opportunity for Tyco to do some research that has not been explored yet. As a result the findings could help lead to improvement of the designs of sprinklers in order to help better assist in fire suppression techniques. There is not much in the way of past research conducted in this area. This is a problem that has just started to be explored within the community and our project will help to provide a good basis for others to go off of in continued research. This will be very beneficial to the Fire Science Community.

Technical Approach:

Overview/Plan:

Looking at the basic operation of sprinkler systems it can be seen that the shape of the water spray is that of an “umbrella”. The main purpose of having the water be deflected in this shaped flow is to be able to effectively suppress fire over a larger area. If the water were all to be expelled straight out of the nozzle of the sprinkler it would be very effective at suppressing fire directly under the nozzle. This would, however, require the ceiling of a given area to be covered in sprinklers to be effective in suppressing fire over that whole area. The sprinkler acts as a heat detector and can detect heat increases due to a fire, but has no way to detect the actual location of a fire. This is where the umbrella shaped flow comes into effect. The water is deflected from its originating source and falls over a larger area of the ground below. Well this is a much more effective way of suppressing the fire, there is little known about the flow other than its general shape, and the general area where the expelled water lands. The plan of this project is to take a closer look into the actual flow of water out of the nozzle and its spray pattern off of the

deflector afterwards. This will encompass different types of sprinklers as well as different types of deflectors in order to get a more specific picture of the nature of sprinkler system fire suppression.

Procedure:

To accomplish the goal of analyzing the water flow from the sprinkler orifice the following procedure will be used. In order to verify that the findings collected are going to be creditable, the Shadowgraphy system must be independently tested first. This is to ensure that the system is functioning properly and providing the images that it is expected to produce. If it is not functioning as anticipated then it will need to be calibrated properly to insure proper functioning. Some of the ways that the calibration of the laser can be tested are: replication of past experimental results, comparison of results to calibration sheets, and using an atomized or standardized spray.

One test that could be reproduced, in order to compare results, is documented in a paper by S. Wissell from the Aachen University of Technology. In this paper there are several graphs and a table of some results documented by a Shadowgraphy system at a distance of 40mm away from the nozzle of the sprinkler. In Figure 18 you can see the results for: droplet diameter vs. relative frequency, droplet diameter vs. cumulative volume, and axial velocity vs. relative frequency. In Figure 19 the diameters and velocities of the droplets recorded in this test can be found. While there are given results for a PDI test, and IMI test and a Shadow test, we would only be looking at the results produced by the Shadow test since that is the type of test to be completed in our study.

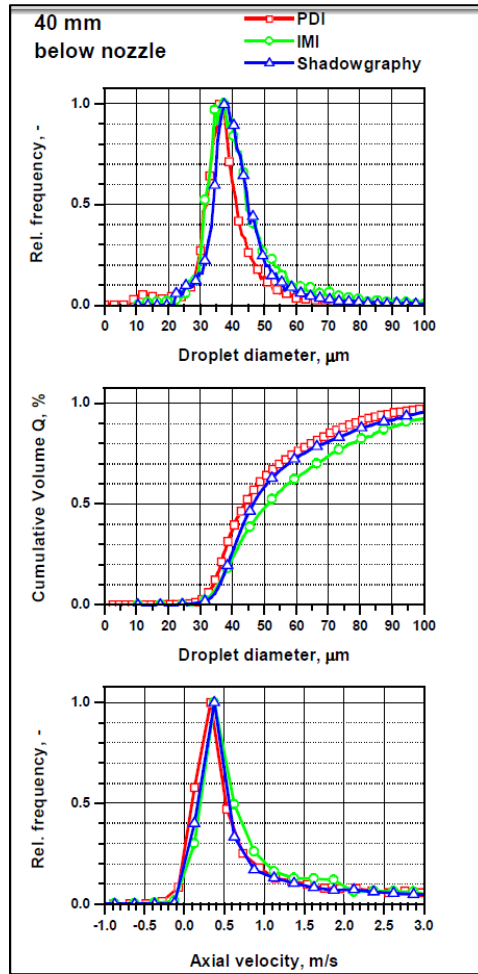


Figure 18: Droplet diameters and axial velocities a distance of 40 mm from the nozzle ^[2]

	PDI	IMI	Shadow
$D_{10}, \mu\text{m}$	38.8	42.7	42.4
$D_{32}, \mu\text{m}$	45.6	51.9	49.0
$D_{0.1}, \mu\text{m}$	34.0	35.7	36.0
$D_{0.5}, \mu\text{m}$	43.8	51.2	46.6
$D_{0.9}, \mu\text{m}$	78.0	93.4	85.4
samples	157220 (PVC)	10770	12272
$v_{\text{axial}}, \text{m/s}$	0.33	0.38	0.38
samples	25533	3159	9883

Figure 19: Mean and representative diameters and velocities for 40mm below the nozzle ^[2]

Another calibration technique that could be utilized is using calibrated sheets to compare the droplet sizes in the images collected by the testing. Calibrated sheets are often metal sheets with example sizes of droplets that can be compared to results obtained through an experiment. Calibration sheets are not limited to metal; some are transparent to allow for easier comparison. Figure 20 below shows an example of a transparent calibration plate.

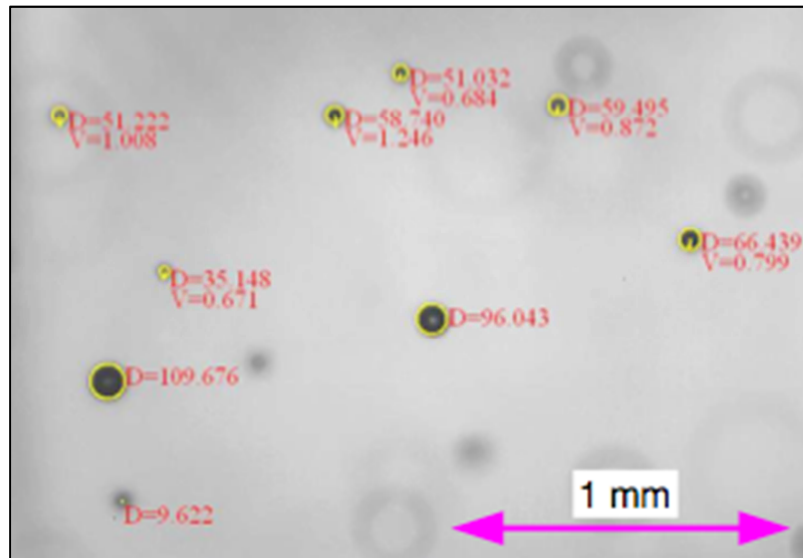


Figure 20: Transparent Calibration Plate ^[2]

In Figure 20, the calibration plate shows known sizes and distances. The dot diameters on the plate range from 10 μm to 200 μm. Under the plate, an image of the results from an experiment is shown. In this test, an image was taken at a distance of 100 mm from the nozzle. The droplet diameters and velocities were found, and then compared against the values shown on the plate. Calibration sheets are very useful to provide a way to determine whether the laser is functioning properly, as well as allow one to decide if major mistakes were made while conducting an experiment. Since there is not a large abundance of literature on these subjects, it is very useful to have calibration sheets to confirm whether data is correct ^[2].

A final testing procedure that could be used to check the calibration of the laser system is by using a standardized spray. In this type of testing, a material of known particle size is to be sprayed and imaged by the Shadowgraphy system. The resulting images can then be analyzed to checked against reference material, for example a calibration plate, to see if the particle sizes

match up with the actual size of the material. While this test seems in theory to be the best calibration method, little information is available regarding this test. It could be very beneficial for the group to look into this testing procedure for both use in this proposed testing, as well as for future testing.

Once calibration of the laser is completed then the actual imaging of the flow can go forward. The LaVision Shadowgraphy device will be set up near the base of the sprinkler to be studied. Once the sprinkler is activated the Shadowgraphy system will be used to take pictures of the water's flow pattern. Since the system is being used as a camera for this purpose, it will only be able to image one small area at a time. To be able to account for the flow in a 360 degree area around the sprinkler the Shadowgraphy system will need to be rotated around the outside of the flow, in order to create an image of the entire area. Ideally 4 larger images of the flow will be produced (approximately 300 mm by 300 mm) to create a big picture of the flow out of the sprinkler. These images will be arranged so there will be one of the "North" side of the sprinkler, one of the "West", one of the "South", and one of the "East" if you were to be looking down on the sprinkler from above. From these images the distance away that the breakup of the flow is occurring can be determined. In order to get a more precise image of the flow at this location several series of images will be recorded at this location (approximately 5 mm by 5 mm). The proposed series of images would include a 4 by 4 grid of images at each proposed location. It would be difficult to take images of this size around the entirety of the flow for each type of sprinkler, and pressure variation, and then analyze all of them. To combat this it is proposed that 3 representative areas be selected from each scenario. This would provide sufficient data to come to overall conclusions of the sprinklers flow characteristics around the entirety of the flow. This process will be replicated, for different operating conditions as well as for different types of sprinklers.

The proposed list of sprinklers that are to be used is as follows^[3]:

Table 3: Sprinkler List

Sprinkler Name	SIN	Type	K-Factor	Vertical adjustment
-----------------------	------------	-------------	-----------------	----------------------------

Series RFI	TY3531	Concealed Pendent	5.6	1/2"
Model TY-QRF	TY3261	Flush Pendent	5.6	3/8"
Series TY-L	TY3311	Sidewall	5.6	1/2"
Series TY-B	TY1151	Upright	2.8	1/2"
Series TY-B	TY1251	Pendent	2.8	1/2"
Series TY-B	TY3151	Upright	5.6	1/2"
Series TY-B	TY3251	Pendent	5.6	1/2"
Series TY-B	TY4151	Upright	8	3/4"
Series TY-B	TY4251	Pendent	8	3/4"
Series TY-B	TY4851	Upright	8	1/2"
Series TY-B	TY4951	Pendent	8	1/2"

This list brings in several different styles of sprinklers in order to help create a larger base model of results for laser imaging of sprinkler flow patterns. This will help to provide a good idea of how some of the more general types of sprinklers will perform. It also will set the ground work for more specified future testing of individual sprinklers. This proposed list of sprinklers includes not only different styles of sprinklers, but also several sprinklers with different K-factors.

Comparing the results that collected from these tests will help to provide a basis for how the K-factor helps to influence the sprinkler flow.

The next aspect of testing that needs to be varied in order to help provide a picture of the overall functionality of these sprinklers is the water pressure. Looking back to the equation for sprinkler flow, the two variables that play a role are the K-factor and the pressure. While the K-factor is fixed per the given sprinkler, we have provided a list varying K-factors based on the model of sprinkler. From each of these, the water pressure used for the testing will be varied and recorded. Since in the equation for sprinkler flow the square root of the pressure is taken, the graph that is produced is asymptotic in nature. In order to get a clear picture of the shape of the graph, and to create educated guesses as to other values based on our testing, several different pressures will need to be recorded in order to create the desired curve. From doing some research of past experiments an acceptable number of varied pressure points seems to be 6. The proposed pressures (in bar) for each sprinkler to be tested at are: 0.014, 0.034, 0.14, 0.28, 0.55, and 0.83. This proposed range should create a clear curve to analyze.

Analysis:

The first aspect to look at is the point where the flow begins to separate. As the water hits the deflector and begins to spread out from the point of origin, it starts off as a solid sheet of water. As it begins to pan out farther, however, it begins to separate into smaller droplets of water. The distance away from the deflector that this occurs will be considered in the analysis. Another aspect to consider is velocity at which these smaller droplets are flowing at. This can be done by taking multiple images in rapid succession. From these the rate of change in distance over the specified time period can be determined giving the droplets' velocity. After we know the location and velocity of the droplets of the flow their direction should be analyzed as well. This is an important area to look into because it is one of the big factors in figuring out how the water expelled from the sprinkler actually suppresses the fire below. From the old style "bucket tests" you could determine how much water ended up where after a sprinkler was on for a predetermined amount of time, but the specific nature of the droplets has never been explored. From determining where the different size droplets are being distributed off of the deflector it will provide a better picture of how exactly deflectors operate and help with future considerations of how to help make them more efficient. Ideally the larger droplets should be concentrated at the base of the fire, with the smaller "mist-like" droplets helping to cool down the surrounding area as well as the smoke coming off of the fire. The proposed test will allow the flow to be analyzed to find out how the flow actually operates and how it can be changed to reach its ideal state.

Schedule, Resources and Cost Estimate:

The proposed research study would be conducted over a 7 week time period. It would begin Tuesday, July 5, 2011 and be completed by Friday August 19, 2011. The research team will be made up of four students, two from Worcester Polytechnic Institute in Worcester, MA, USA and two from Shanghai Jaio Tong University in Shanghai, China. Additionally the students will be supervised by Chad Goyette of Tyco's New Technology Team. All of the students will be working full time, 40 hours per week, during this time period. Tyco already owns the equipment needed for the proposed work, and no further purchasing of equipment is requested.

Citations:

- [1] Zhou, Xiangyang, and Hong-Zeng Yu. "Experimental Investigation of Spray Formation as Affected by Sprinkler Geometry." *Fire Safety Journal* 46 (2011): 140-50. Print.
- [2] Berg, T., J. Deppe, D. Michaelis, H. Voges, and S. Wissel. "Comparison of Particle Size and Velocity Investigations in Sprays Carried Out by Means of Different Measurement Techniques." *ICLASS* 06-151 (2006). Print.
- [3] *Tyco Fire Suppression and Building Products*. Web. 25 Apr. 2011. <<http://www.tyco-fire.com/index.php?P=product>>.

Appendix B: Background

An important part of this project involved gathering information related to the project goals. To do so, literature in the form of journals, articles, and online web pages were used. In the field of fire protection engineering, working with a laser to determine sprinkler characteristics is a rather new technology; although, the basic idea of defining sprinkler characteristics has been around for many years. The two main methods that were researched were shadowgraphy, and PIV. Research was also conducted to find the work of engineers and professors in the field, to be used for comparison. It was also necessary to look into basic sprinkler rules and regulations. This investigation culminated into the 'background' section, which follows.

D3 Nozzle

Before delving too far into the project, it was necessary to learn about the nozzle that would be tested, the Tyco Type D3 Protectospray Nozzle. The D3 nozzle is an open, external deflector type nozzle. It is effective in covering a wide range of surfaces, and operates with the primary goal of preventing excessive heat absorption. The D3 nozzle is shown in Figure 21 below.



Figure 21: D3 Nozzle

The D3 comes in numerous spray angles, orifice sizes, and material types. The spray angle options range from 65° to 180°, while K-factors can be chosen from 1.2 to 7.2. The nozzle comes in bronze and stainless steel, and can be made with a natural finish, chrome plate, or lead coat. Certain design considerations should be considered when using the D3 nozzle. For instance, the recommended basic usage pressure is 20 to 60 psi, since any higher pressure will affect the spray

pattern. It was important to keep such design criteria in mind, since they would factor into how the results were analyzed (Tyco).

Comparable Work

A vital section of this project involved gathering background information regarding other research into the characterization of sprinkler flows. This investigation became combined into the ‘comparable work’ section, which follows. This section looks into the work of various engineers in the field of fire protection engineering. The articles and reports that were read became useful references as progress was made through the project. Not only did the information found in this section prove very useful, but it also offered an interesting look into previous work that has been done in the field.

Dave Thomas Sheppard: “Spray Characteristics of Fire Sprinklers”

First off, a noteworthy person in the field of fire protection engineering is David Thomas Sheppard. Sheppard wrote the article “Spray Characteristics of Fire Sprinklers” during his time at Northwestern University. His work was done in collaboration with the National Institute of Standards and Technology, a sector of the U.S. Department of Commerce. In this article, written in 2002, Sheppard describes his work with sprinklers and his methods to determine their characteristics (Sheppard).

Compared to this project, Sheppard’s work differed in many aspects. Since there is limited time period to complete this work, the group will not be going as in-depth as Sheppard did. Although these projects are similar in their methods, as well as their characterization of velocity and droplet size, the Tyco group looked into a couple aspects of sprinkler spray characterization that Sheppard did not research. For instance, laser images to determine spray angle and ligament distance were used. Sheppard did not characterize these, but he looked into water flux, which was not considered in this project. He also tested numerous sprinklers, and in this project only the D3 nozzle was used (Sheppard).

Sheppard’s work is unique in that, similar to this project, he used a laser-system. Sheppard describes this setup as “two complimentary laser-based systems used for experiments characterizing the droplet size and velocity distributions” (Sheppard). Northwestern University allowed Sheppard to make use of their Phase Doppler Interferometry (PDI) system, as well as

their sheet Particle Image Velocimetry (PIV) system in his testing. Light scattering interferometry techniques were used in the PDI system, which allowed Sheppard to measure particle velocity and size. The PDI system is shown in Figure 22 below (Sheppard).

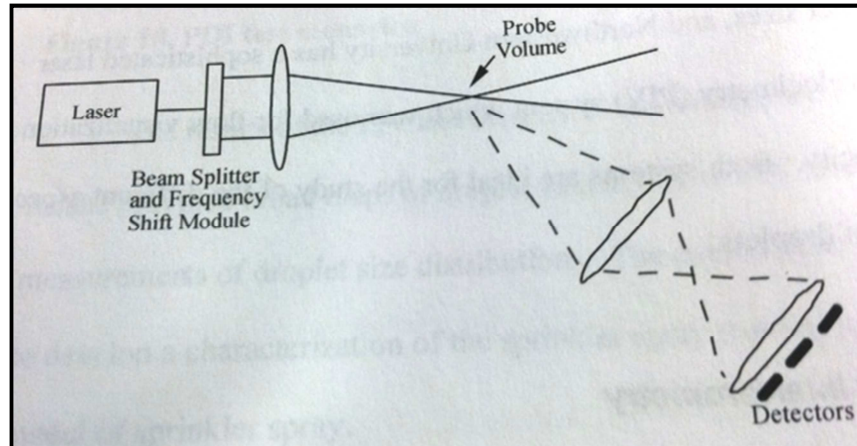


Figure 22: PDI System Setup (Sheppard, 44)

PDI systems do have some limitations though, which is why Sheppard also used the PIV system. PIV systems utilize the laser at a high-intensity in line with a certain plane of interest. In Figure 23, the PIV system is shown. The PIV was able to collect data on the velocity of particles over a plane, whereas the PDI could only determine the velocity at one point in the flow. With these methods, Sheppard was able to create an extensive report on these sprinkler characteristics.

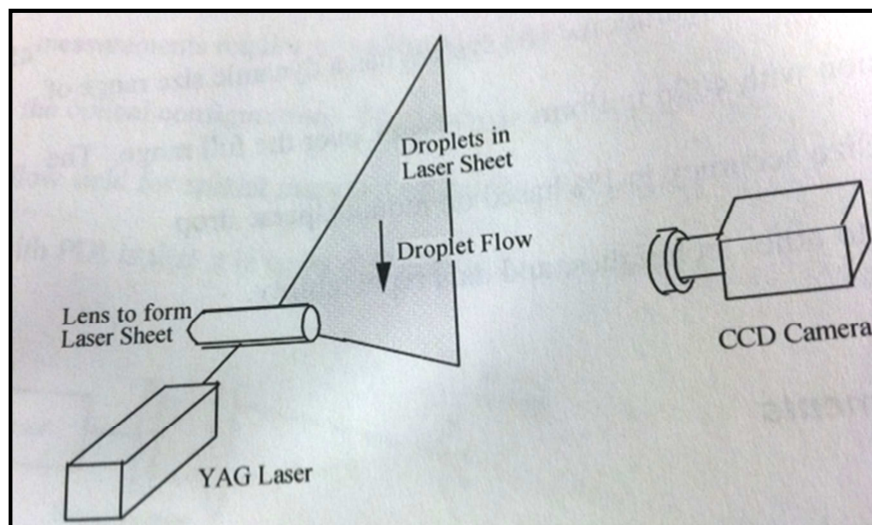


Figure 23: PIV system setup (Sheppard, 46)

Sheppard's dissertation details not only his methods, but also describes the foundations of sprinkler design, and includes a thorough discussion of his results. Sheppard noted the existence of numerous types of sprinklers, and with this, he tested a large number of sprinklers in both upright and pendant designs. He quantitatively came up with ways to verify his results, and provided numerous equations, charts, and graphs to back up his work. In conclusion of his report, he noted the importance of his investigation, and summarized his findings. Soon after its completion, Sheppard's work proved vital to the fire engineering community. It led the National Institute of Standards and Technology to modify their Fire Dynamics Software (FDS) to include input for sprinkler sprays. It is a hope that at the conclusion of this project, the work will also benefit the fire science industry (Sheppard).

Ning Ren, Andrew R. Blum, Ying-Hui Zheng, Chi Do, and Andre Marshall: "Quantifying the Initial Spray from Fire Sprinklers"

Ning Ren, Andrew R. Blum, Ying-Hui Zheng, Chi Do, and Andre Marshall wrote the article "Quantifying the Initial Spray from Fire Sprinklers." These individuals were colleagues at the University of Maryland, working in the Fire Protection Engineering sector of the university. Understanding the importance of analyzing spray characteristics, they put together an article and presentation regarding this subject. Their article describes their work through an extensive explanation of their objective, methodology, and results. In conclusion of their report, the findings are summarized, and some insight is given into the accuracy of the data (Ren et al).

Similar to this project, Ren, et al. used a laser to study sprinkler spray characteristics. In doing so, they made use of University of Maryland software known as a Sprinkler Atomization Model (SAM). Ren, et al. notes, "SAM provides the initial velocities, locations, and drop sizes that characterize the spray" (Ning Ren, 3). In addition to SAM, the authors of this article used Photographic and Planar Laser Induced Fluorescence (PLIF) techniques to determine spray characteristics. This method helped them find ligament distance and sheet size. This study is very similar to this project, where the vertical testing results were used to measure ligament distance. Figure 24 shows how Ren et al. defined ligament distance. This figure helped the group form an understanding of ligament distance, and became the foundation for the measurements.

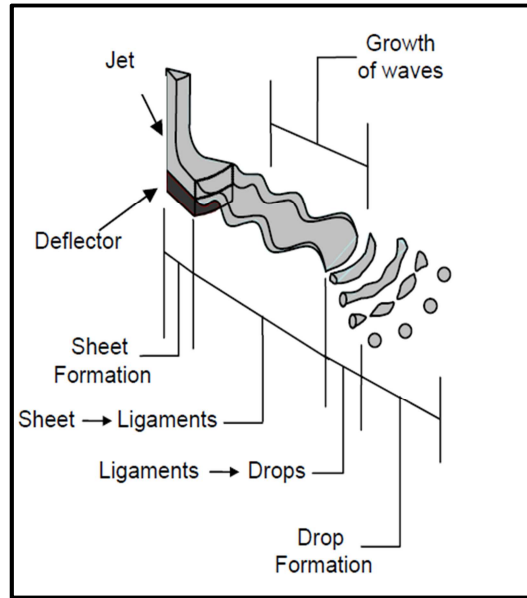


Figure 24: Ligament Distance (Ren et al., 3)

Contrastingly to this project, when taking pictures, Ren et al. only took about 20 pictures each time, while at Tyco 500 were taken. Although another similarity lied in Ren et al. finding droplet size. To do so, a Spraytec spray particle analyzer was used. This system used a laser to diffract light particles. Like Ren et al., droplet size was looked into at Tyco, but by use of shadowgraphy. It is interesting to see the similarities between their project and Tyco's work. Unfortunately, due to the differing methods the results section of this report does not directly compare to their's (Ren et al).

In the conclusion of the article written by Ren et al., a summary and analysis of the results is presented. Their project culminated in findings of flow geometry, ligament breakup, and droplet size measurements. They were able to relate these characteristics back to the nozzle geometry by use of various techniques described above. They made note of the fact that the tines and slots may have biased some of their results, and as a result plan to look further into those areas on future studies. Overall, their work provided interesting insight into sprinkler characteristics, and proved to be a useful reference throughout this project (Ren et al).

G. Grant, J. Brenton, D. Drysdale: "Fire Suppression by Water Sprays"

The article entitled "Fire Suppression by Water Sprays," written by G. Grant, J. Brenton, and D. Drysdale is based off a literature review on using water for fire suppression and extinguishing.

The article was presented in the journal called *Progress in Energy and Combustion Science* in 2000. The authors conducted this study in the United Kingdom, while two were employed in engineering companies and one at a university. Their article proved particularly important to this project, since it had a large section focusing on droplet size. Further, there was a plethora of information on fire and sprinklers in general (Grant).

Grant, Brenton, and Drysdale describe droplet size as a quantitative characteristic of water sprays. This part of the article was of great interest, as this project involved study into droplet size. Although, much of Grant et al. discussion was on formulas, which was not used in this project, much knowledge on droplet size was gained from their article. When working with shadowgraphy, it was necessary to figure out how many particles were required to make the pictures accurate. Grant et al. article had the exact information this project needed on this topic. A graph of error vs. sample size proved very useful, as it became the foundation for the groups rule throughout shadowgraphy testing. With this information, it was determined that 1000 particles were enough to give us 90-95% accuracy. This sample size information was essential to the testing, and provided a direct comparison to analyze results against (Grant).

Although the rest of this article was interesting, it did not directly relate to this project. The focus of the remainder of the article was on extinguishing fires, which the group did not work on during the time at Tyco. Even so, the information provided did give some knowledge on other areas of fire protection engineering, and may be of interest to Tyco for future work (Grant).

TFRI Regulations

The TianJin Fire Research Institute (TFRI), located in China is relevant to our project because they too conducted a study on the D3 nozzle. With this, it was important to get some information regarding their rules and regulations, to determine what tests are considered passing, and which would fail. Also, the TFRI tests were available to provide some comparison to the results found through this project. Disclaimer: Since the TFRI website is in Chinese, some translations may not be exact.

In the regulations from TFRI website regarding the automatic sprinkler system, there are several definitions that are important to understand. These are shown below:

Spray angle: the apex, formed from the mist from the nozzle, which forms a cone surrounding the axial line.

$D_{V0.90}$ drop diameter: in the total volume of the mist liquid, the droplets smaller than this diameter occupy 90% of the total volume (Chuo, Yang and Zhang).

Besides these definitions, there are some requirements and sample tests for the nozzles in the regulation, which can be useful to be the standing point on how the parameters were chosen. According to the regulations, the angles which are usually used include 45°, 60°, 90°, 120° and 150°. There are requirements for the angles to be in a specified scale. In detail, the spray angle of 45°, 60° and 90° should be located within plus or minus 5°, while the angle of 120° and 150° should be located within plus or minus 10°. Similarly, for any other angle not listed the measurement should be within plus or minus 5° for angles less than 100° and within plus or minus 10° for angles over 100°.

There is a very detailed and specified process for measuring the spray angle in the testing mentioned in the policy. A container to collect the water is used to measure the angle of the main flow. As the definition above, the angle would be accessible with the dial on the container. Before the testing, the nozzle should be placed in the middle line of the gyration, in order to make the apex of the flow cone superposition on the center of the dial. During the testing, the pressure should be kept at 0.35MPa to ensure the consistence of the results. Figure 25 below shows the test equipment in the spray angle test and lists the meaning of each label.

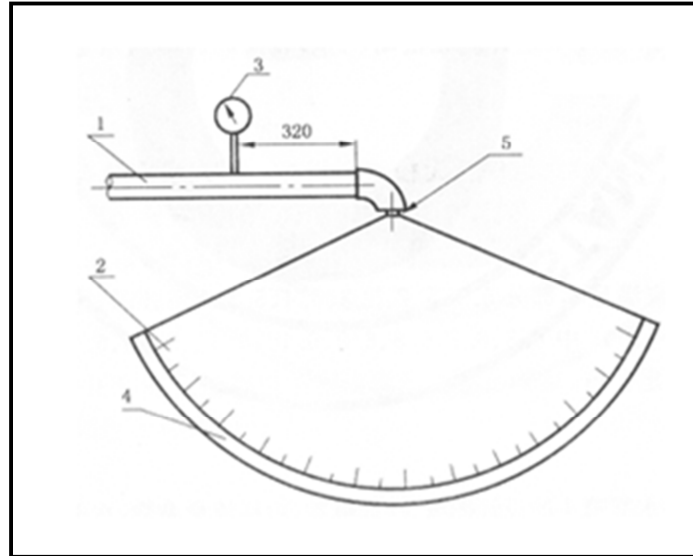


Figure 25: Spray Angle Test Equipment

Note: 1-- steel pipe, nominal diameter 65mm
 2-- dial (minimum scale 1 °);
 3-- pressure gauge, accuracy class 0.5;
 4-- then water trap (radius 500mm);
 5-- test samples.

Besides the rules and testing description about the spray angle, there is another important test for droplets size. In the regulation, it is pointed out in part 5.5 that $D_{V0.90}$ should be smaller than 1.000mm under the rated pressure. The test in part 6.5 of the regulation takes the data in two places to access the sprinkler. The first of these is on the axis of the deflector at a distance of 1m from the deflector of the nozzle. The other is at a radius of 0.25m from the first measured location for the spray angles of less than or equal to 60° , or at a radius of 0.5m for spray angles larger than 60° , or at a radius of 1m for spray angles larger or equal to 90° .

Shadowgraphy and PIV

Since PIV and shadowgraphy techniques were used throughout the project, it was necessary to do some background research into these techniques. From the LaVision website, detailed information was obtained on both of these systems.

First, Particle Image Velocity, also known as PIV, is a technique used to measure a full velocity field. This can be explained briefly by the relationship between speed, time and the distance. The velocity of the particles can be determined from the distance measured in the pictures of the particles movement over the interval. Being able to capture two images in rapid succession, in order to visibly observe the distance traveled of individual droplets, is no easy task. With countless droplets present in the flow at any given moment being able to find a droplet in one picture, and follow it into the next picture is very difficult. Thankfully the computer is used to identify key characteristics of droplets in each picture, and search for droplets of similar characteristics in the next image. This allows for the computer to fairly accurately figure out how far each droplet moves, and then by knowing the time allotted between the pictures the velocity can be determined. Another strength of the PIV system is its use of a laser as its light source. The laser is able to be directed into the path of a plane which can fairly accurately light up a small region of the flow of water instead of a typical white light which would illuminate the entire flow. Additionally, the laser's power can be controlled, and if needed turned up significantly, in order to penetrate through the entirety of the flow of water. This ensures that pictures of the flow will be clear instead of part of them not being illuminated (LaVision).

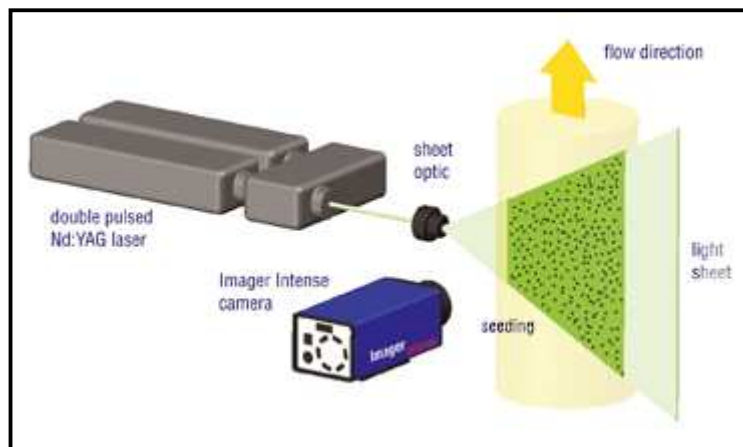


Figure 26: PIV system (LaVision)

Shadowgraphy, also known as High-magnification Shadow Imaging is mainly designed to measure the size of the droplets that may be on the micro level. The system is composed of two parts: the detector, which is a long distance microscope with a high resolution Charge-Coupled Device (CCD); and the light source, which provides light to illuminate the area. With the flash

lamp or a short laser if the droplets have a respectively higher velocity, the system can take pictures of the structures with high resolution. From these pictures the velocity of droplets is then calculated by their displacement. By using a shadowgraphy system to measure droplet velocity, velocities of up to 100m/s can be measured. Figure 27 below shows the shadowgraphy system setup (LaVision).

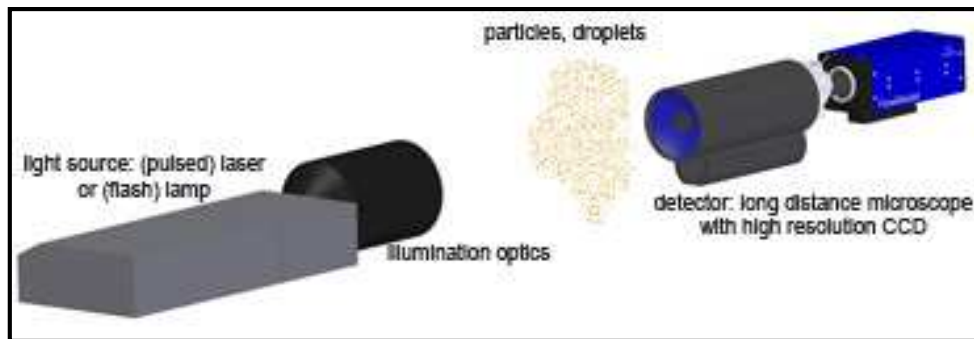


Figure 27: Shadowgraphy Setup (LaVision)

Citations:

Chuo, Fengyin, et al. "Automatic sprinkler systems Part 3: spray nozzle." 1 5 2004. standard information. 2 8 2011 <http://translate.google.com/translate?hl=en&sl=zh-CN&u=http://www.safetyinfo.com.cn/biaozhun/Biaozhun_2538.html&ei=og83TomUN8nx0gHu9JCLBA&sa=X&oi=translate&ct=result&resnum=1&ved=0CBsQ7gEwAA&prev=/search%3Fq%3D%25E8%2587%25AA%25E5%258A%25A8%25E5%2596%25B7>.

Ren, N., Blum, A., Zheng, Y., Do, C. and Marshall, A., 2009. "Quantifying The Initial Spray From Fire Sprinklers." *Fire Safety Science* 9: 503-514. doi:10.3801/IAFSS.FSS.9-503

Sheppard, David Thomas. "Spray Characteristics of Fire Sprinklers." National Institute of Standards and Technology, NIST GCR 02-838, June 2002.

Grant, G., Brenton, T., Drysdale, D. "Fire Suppression by Water Sprays." *Progress in Energy and Combustion Science* 2000: 79-130.

LaVision. Techniques. 27 7 2011 <<http://www.lavision.de/en/imprint.php>>.

Products, Tyco: Fire Suppression & Building. Type D3 Protectospray Directional Spray Nozzle, Open, Medium Velocity. Technical Data Sheet. Lansdale, 2009.

Appendix C: Testing Setup

Over half of our time at Tyco was spent working in the lab. The lab set up for working with vertical PIV testing consisted of the laser and camera directed at an intersecting angle (90° to each other). Both the laser and the camera were positioned so that the point where their directional paths overlapped was directly under the pipe where the different testing nozzles would be connected. The nozzle itself was set up with a special rotating device. This device allows for a user to control the nozzles rotational angle by means of a computer program and rotating motor on the actual device. This greatly reduces possible human error in angle positioning, and makes changing positions much more efficient. The horizontal PIV setup was similar to the vertical, the difference being the location of the camera. Instead of the camera being located on a camera stand on the ground, the camera was mounted on the ceiling, so it could look down over the flow.

When working with PIV, safety was a major consideration. The LaVision laser system made use of a Class 4 exposed laser light, which could be dangerous if handled incorrectly. With this, it was important to adhere to certain safety restrictions. Whenever the laser was on, users always wore protective safety glasses to protect their eyes from the light source. Also, protective tarps were set up surrounding the area.

Shadowgraphy called for a different setup. All the equipment used in shadowgraphy testing was connected to one stand. This stand was moved around the nozzle in desired positions, instead of moving the nozzle itself. The lightsource was mounted on the stand directly across from the camera. This allowed the lightsource to make shadows out of the droplets, which the camera took pictures of and sent to the computer.

Another integral piece of equipment in the testing area was the computer itself. Much of the time in the lab area was spent surrounding the computer analyzing results and processing information. Processing took a great deal of time, since we were working with large amount of pictures. Also, calibration was often done through the LaVision software on the computer.

Appendix D: Calibration and Procedure

Vertical PIV Calibration and Procedure: One of the first decisions that was changed between the original project proposal (PQP) and the actual testing was the sprinklers that were used. The original plan was to use several different types of sprinklers, however, upon arrival it was decided between Tyco and the group that the using different D3 nozzles would be the easiest and most beneficial for Tyco.

In order to learn how to do the required calibration and to run through the testing procedure, a 160° D3 nozzle with a K-Factor of 4.1 was used as a practice nozzle. Calibration was able to be completed without running any water through the nozzle, but in order to run through the whole procedure a nozzle was required.

Calibration is a very important step in the testing process as it allows the software to do more than simply take pictures. When adjusting everything for shooting in Vertical PIV mode, calibration is fairly straightforward. A tape measure was the main tool used to calibrate. It helped us gain focus and determine the distance we would obtain our pictures from. This calibration tool is shown in Figure 28 below.

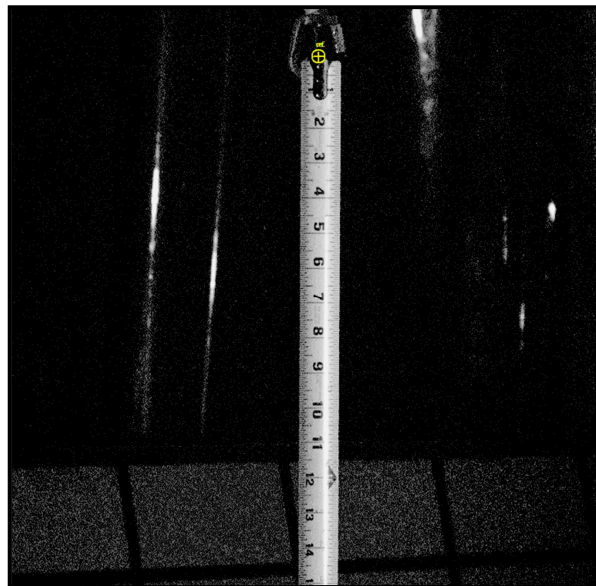


Figure 28: Tape Measure for Vertical Calibration

In order to calibrate the system for vertical PIV, a tape measure was hung from the nozzle directly down to the floor (Figure 28). Once this was completed a picture would need to be taken of the nozzle in order to check its position in the picture as well as its clarity. An important detail to keep in mind is that during initial calibration the laser is not turned on. Since for the testing the laser acts as the light source for the pictures there is not much external light present in the room. In order to get a viewable picture of the tape measure for calibration an external light source needed to be brought in. After this was completed, and the pictures were bright enough to view, the computer was set to take continuous pictures. While this live feed of the set up was being displayed on the computer, the camera could slowly be adjusted into the proper position, and similarly the proper focus. Since this process is done by hand, and is subjective, it was up to the operator to judge the position at which the image appeared to be most clear.

Once the camera appeared to be in focus, and correctly positioned, the computer was taken off of continuous shooting mode. At this point, a single image was captured in order to run the computer's calibration procedure. With an image of the nozzle and tape measure taken, going into the calibration function of the software, distances could be determined. A 10" range was selected in the picture (from 3" to 13" on the tape measure as to avoid any issues with selecting the end of the tape measure). With the computer now recognizing that the amount of pixels it was seeing in a span that we had defined as 10" proper scales for all of the pictures could then be determined.

After these steps were completed the external light source could be removed and the cameras lens filter could be attached. The filter was in place to cut out light outside of the wavelength of the laser. This was able to help produce a higher quality final image.

To start the actual testing procedure, Teflon tape was used to cover the threaded end of the nozzle. This was done in order to help assure a tighter seal was made between the pipe and the nozzle. With this, the water flowing through them would be directed out of the orifice and not through the threaded connector. Another step that helped to ensure this tight connection involved using a wrench to screw in the nozzle, which made a tighter connection than with simple hand tightening. Once the nozzle was tightly secured, it needed to be oriented into the correct position. The piece of piping that the nozzle is connected to is also connected to a motor capable of

rotating it at very precise increments. This is extremely helpful in order to change the angle of the nozzle for each set of pictures to be captured. In order to properly calibrate it to the correct position, a little bit of work was required. The software controlling the rotating motor could be zeroed at any position in order to denote a new angle of zero degrees. The one problem was the angle referenced as zero needed to be the same in each test. To do this, one orientation of the sprinkler needed to be chosen to denote zero degrees. This position was chosen to be the angle at which the two frame arms of the sprinkler were in line with the camera, and perpendicular to the laser. Positioning the sprinkler in this way was done by first lining it up as close as possible by hand. After this was done, the camera was used to take a picture of the nozzle in a similar manner to the original calibration of the camera set up. From using the picture of the nozzle, and the motors software, the position of the laser could be adjusted the final few degrees to the zero degree position. Once the nozzle was at the correct angle, the software's angle reading was reset to zero which would allow for control of the angle off of that base position.

Once the nozzle was tightly fastened, and correctly positioned, the flow of water could be turned on. In the pipe directing the flow of water to the nozzle, the pressure was set to 100 psi. Since the testing was planned to be done at a pressure of 20 psi, the flow rate needed to be throttled down. Using a program installed on a separate laptop computer, the known K-Factor of the nozzle (4.1) and our desired pressure (20 psi) were able to be entered. Then using a variation of the Bernoulli equation, the program showed the Flow Rate that was needed in order to satisfy these other two variables. For this particular nozzle, a Flow Rate of approximately 18.4 gpm was required. Using one of the turn valves in the piping leading to the nozzle, the flow of water (measured from a flow meter connected into the system) was able to be turned down to reach this required Flow Rate.

After this setup was complete, testing was almost ready to start. One concern was in varying the power of the laser for different pressures. In order to see if one power setting could be used for the laser, a test was run at the 50% power setting with a water pressure of 20 psi. The original concern with doing this was that it would over-saturate the white balance in our pictures causing them to be unclear and essentially unusable in terms of analysis. Upon a quick test of the 50% power setting, it was apparent that this would not be too high of a power setting for the lower

pressure. It was then decided that 50% power would be the official test power for the laser during the entirety of testing.

From here, test of all of the angles (0° , 18° , 36° , 54° , 72° , 90° , 108° , 126° , 144° , 162° , and 180°) were completed for the 160° D3 nozzle at 20 psi, at 250 pictures per angle. Although later the rotation angles and number of pictures were changed. A more detailed description of this change is found in Appendix E: Testing Parameters.

Horizontal PIV Calibration and Procedure:

Calibration for horizontal PIV testing is very crucial in being able to provide useful images for analysis. The camera needs to be focused in on a horizontal plane of a known height in order to be able to change the point in the flow that the images are captured. In addition to that, the computer needs to know at what angle the pictures are being taken from in order to properly resize them to simulate a flat plane. In order to run any of this calibration, the first step that needed to be taken was orienting the camera. For horizontal PIV the camera can either be mounted on the ceiling looking down at the flow, or on the ground looking up into the flow. There are advantages and disadvantages to both ways, so this had to be carefully considered. While mounting the camera from the floor looking up at the flow would give a much clearer picture, the camera was also much more prone to getting bumped in this location. That would have the potential for throwing the calibration completely off. Instead of this, a decision was made to mount the camera up on the ceiling. This ended up being very easy to work out as a camera mount, which could be connected to one of the brackets on the ceiling supporting the tarps that surrounded our test area, was available. This set up kept the camera up and out of the way, but did have the downside of also having all of our piping in the picture. It also had the potential for distorting images because of the high concentration of water at the nozzle, which would also be present in the images. Upon further investigation it appeared that there was minimal concern associated with this and the images would be clear and without any visible distortion or blurring from this angle.

Once the camera was properly mounted it needed to be focused on a specific plane. In order to accomplish this, a Styrofoam board was laid flat and leveled at a height of 4 feet above the ground. This board is shown in Figure 29 below.

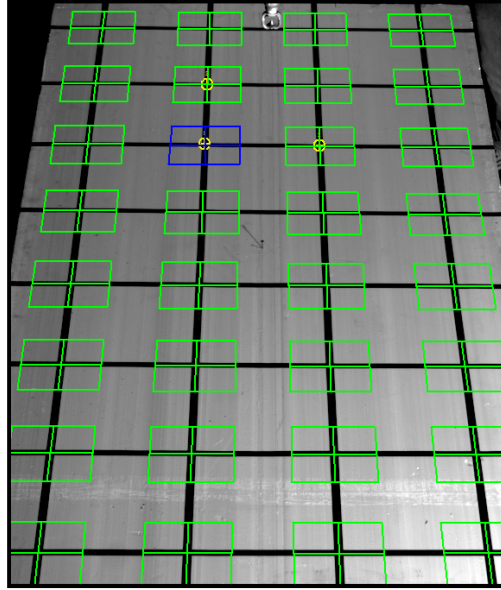


Figure 29: Styrofoam Calibration Board

A screw was then placed in the middle of the Styrofoam board; this was placed directly under the nozzle providing a point on which the camera could be focused on. Similarly to the calibration of vertical PIV testing, the camera was dialed in to the correct focal length by observing the images on the computer and changing the focus until the clearest picture was visible. Once this was completed, the tricky part of the calibration began. In order for the pictures to appear as if they were taken from directly above the flow looking down the pictures needed to be resized in processing. This process would resize the pixels of the picture by shrinking one side of the image in order to account for the offset angle of the camera. In order for this to be effective, however, the computer needed know the size of different locations in the viewing plane; to do this the Styrofoam board was utilized again. On the surface of the board there was a grid of 1ft by 1ft squares. With this grid a picture was taken, and on the computer three corners of one of the boxes closer to the middle were selected. These reference points were defined as all being 1ft away from each other, and then from there the computer attempted to find all of the corner point of the grid. After locating all of these points, the computer then knew how to resize the picture as necessary.

The one last thing that needed to be completed for calibration was positioning the laser. In the vertical mode this was fairly easy to do as there was a line drawn on the floor that the laser could

be positioned on. In order to position the laser for horizontal PIV, there was a need to ensure that the laser was at a constant height all around. It was known that the laser needed to be positioned at four feet above the ground so the lasers stand was adjusted to match that height. At that point the lens was rotated on the laser so that it would direct the light in a horizontal pattern instead of a vertical one. Next, the laser was turned on, as well as turned down to its lowest power and put in “adjustment mode”. At this point one of the students put on protective laser glasses and got a tape measure. They then walked around to different points in the lasers path while pointing to the 4ft mark on the tape measure. This was safe to do because the laser was positioned at a height close to 4ft, while eye level was above this height. The safety glasses were still worn as a precaution. While this was being done one of the technicians was able to match the laser up to the different points to ensure that the plane was truly horizontal.

Once calibration was completed, data collection was able to begin. The only real difference between the vertical and horizontal procedures was in the offset angles for each nozzle. In horizontal PIV, because the image captured the entire flow at a given height, rotation of the nozzle would not be beneficial. Instead, the height in the flow was varied in order to produce different results. In order to quickly change heights for the testing, several pipes of different lengths were used. This allowed for heights of 2ft, 4ft, and 6ft below the nozzles deflector. The thing that really made this process beneficial was that neither the camera, nor the laser needed to be adjusted each time. The new pipe could simply be moved into place and testing could continue. This was extremely beneficial in utilizing to use the short amount of time available for this project, in the best way possible.

With the exception of height, all of the same nozzles, and same pressures were tested and the results recorded at a picture count of 500. One parameter that did need to be defined in the procedure was how to orient our nozzle so that we could make sense of the images after they were collected. It was decided to place the frame arms of the nozzle perpendicular to the angle of the camera; this angle was defined as 0° .

After all of the pictures were taken, processing began. Through talking with some of the people from Tyco about processing it was discovered that the best order to process in was to create the summation of the 500 pictures, and then after that was completed the final image could be

adjusted to simulate a shot from directly above. The images that the resulted from processing provided a very clear picture of what the geometry was for the whole flow at different heights.

Shadowgraphy Calibration and Procedure:

In order to calibrate the camera for shadowgraphy, the process was very similar, but the approach changed slightly. The set up of shadowgraphy consisted of a single mounted structure. On this mount the camera lens as well as the illuminating backlight were positioned facing each other (see Figure 27, Appendix B). Since shadowgraphy focuses on very small areas, the tape measure used in PIV calibration was not precise enough. Instead, a special calibration lens was used. This lens (Figure 30) has a laser etching, which contains 200 lines across a 5 mm span. In order to focus on this spot the camera could be moved in and out, and then once secured in the desired location could be focused in using the similar PIV method. By using the known span of 5 mm, and the same technique used for PIV calibration the computer software can figure out specific distances at the focal length of the lens. Since the calibration is for the specific plane of the lens, that position needed to be marked for the actual testing. In order to do this, a piece of tape was put down on the mount at the point where the lens was located. After this was completed the calibration lens could be removed.

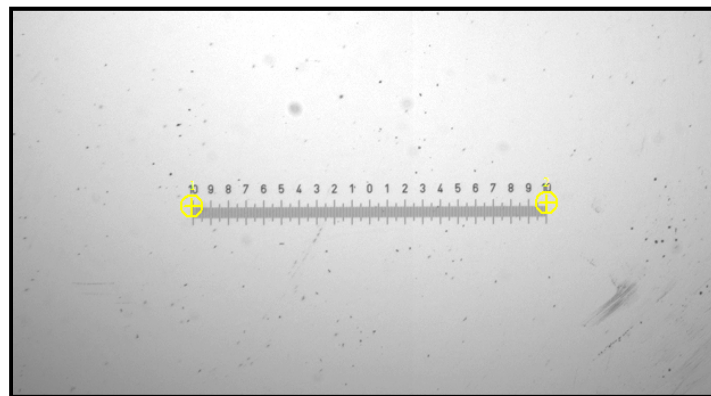


Figure 30: Shadowgraphy Calibration Lens

After calibration, the shadowgraphy mount needed a way to be placed into the flow of water. The easiest way to do this was by attaching the mount to a tripod, which could be moved around, and the height adjusted in order to achieve the desired height and position. The next step was to locate the actual positions in which to take the pictures. It was decided that the positions would

be at different locations into the flow, at different radii from the deflector (described in more detail in Appendix H; Shadowgraphy). In order to measure out these positions a string and protractor were utilized. A loop was tied in the string and looped over the deflector of the sprinkler nozzle. Then, the 1ft and 3 ft distances were measured on the string and marked with a Sharpie. This string could then be pulled to different positions in the flow using the protractor to find the angle. By holding the string in the correct position the tripod holding the shadowgraphy mount could be moved around to fit into the proper location. Once the equipment was all in place then testing could begin.

For the actual testing of shadowgraphy the process was along the same lines as for PIV. The power to the laser needed to be adjusted to a point that did not provide too much, or too little light to the picture. If the laser was turned down too low the whole picture ended up appearing dark, but if the power was too high then the whole image appeared white and no drops were visible. There was a very small region in between the two extremes in which the light would function properly and cause the droplets to appear as shadows in the pictures.

Once the laser's power was correctly calibrated images could be collected. At each location 100 pairs of images were taken and analyzed by the computer. The software would make judgments based on the size and brightness of droplets in order to determine their displacement across the pair of images. All of the information was recorded in several different formats in order to be used for our analysis. This is described in more details in Appendix G: Data.

Appendix E: Testing Parameters

Upon arrival at Tyco one of the first things that had to be accomplished was learning how to use the required software for testing. The computer program that Tyco uses to operate the camera and the laser is DaVis 8.0. In order to understand how to use this program, and also to figure out how the nozzles would actually be tested, some preliminary tests were run. The following includes information about these preliminary tests, and analysis based off the limited data acquired at the beginning of the project.

One of the first big concerns was that there were many options available for testing parameters and the list needed to be narrowed down. One of the first things looked into, was which type of nozzle to use. The testing was to be done on a D3 nozzle, but there are several different spray angles available, as well as a wide range of different K-factors for each spray angle. Several different D3's were tested in order to get an idea of the possible spray patterns. The spray angles that were tested were 65°, 80°, 140°, and 160°. All of the tests were done at a pressure of 100 psi. After some brief background about the D3 design, and with observing several being tested, it appears that they are designed to cover the same base area. Smaller spray angle nozzles can be placed farther away from their intended area of contact, and the wider spray angles can be placed much closer in order to have the same coverage. In testing the 65° D3 with a K-factor of 3.0, there was a very concentrated flow of water close to the nozzle's orifice. This appeared to be less ideal for testing as it seemed it would be much more difficult to observe all of the individual droplets so close together. Another nozzle that was tested was the 160° D3 with a K-factor of 4.1. With this wider spray angle the water droplets were more spread out after contact with the deflector than they had been with the 65° nozzle. This allowed for a much clearer view of the spray pattern. After observing this range of different spray angles, it was decided to focus on the 180° D3 nozzles, as this should allow for the largest distribution of spray. It seemed that it would be easiest to keep the same spray angle and vary the K-factor of the nozzle for testing. This would allow for a variation in the flow to be seen without having a need for analyzing completely different shapes of flow patterns. By limiting the number of variables that needed to be analyzed it would better focus the study.

Once a decision had been reached on which nozzles to study, the other parameters for the testing still needed to be selected. One of the first big things to consider was the water pressure at which the nozzle was to be operated at. Originally, the pressure of the system set to run at 100 psi. In the first couple of pictures that were captured, it became apparent that this pressure may be too high to observe a high detail in droplet definition. With this information, the pressure of the system was lowered down to 20 psi. Consequently, the pictures received a much higher clarity in droplet definition.

One of the features of the software is an averaging technique. This feature can combine a series of pictures and sum them all together in order to create a crisper image of the total water distribution. The fewer pictures that are averaged together, the better the individual droplets can be seen. As the number of pictures is increased, the individual droplet definition is decreased, leaving a more solid picture of the distribution. From this averaged picture, the spray angle off the nozzle can be more clearly seen. While a larger number of pictures create a much better image, it also takes much more time and computer power to process. Therefore, there was a need to find a number of pictures that would optimize picture quality and required processing time. In order to assess this different picture counts were experimented with. A water pressure of 20 psi was selected to start and series of images with the counts of 50, 100, 250, 500 and 1000 were captured. The following images depict these changes.

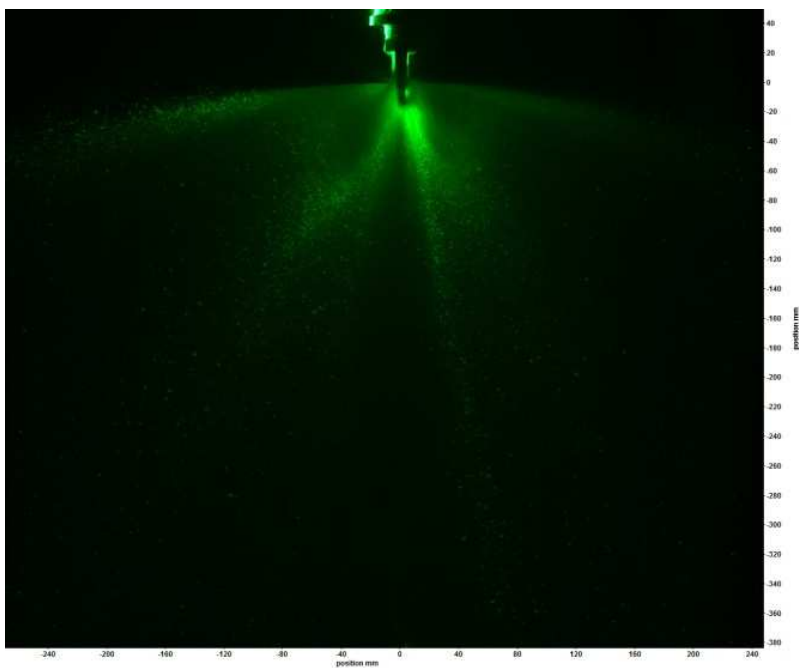


Figure 31: 50 Pictures

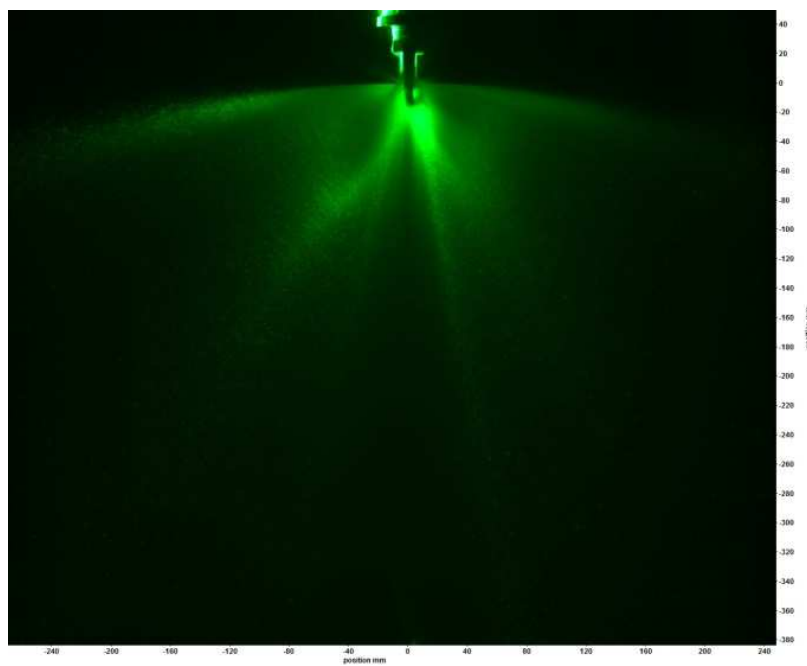


Figure 32: 250 Pictures

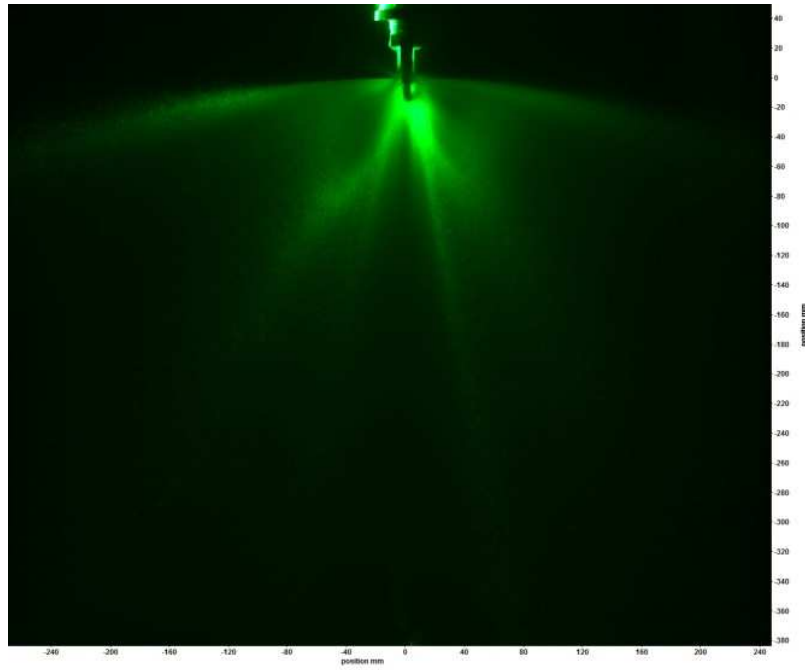


Figure 33: 500 Pictures

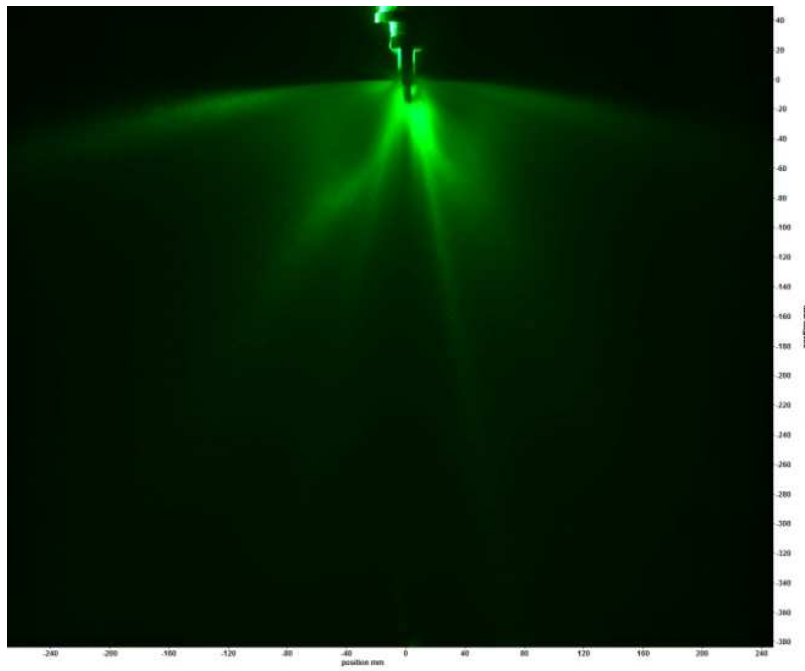


Figure 34: 1000 Pictures

Next, the pressure was increased back to 100 psi and the same picture counts were captured. In comparing the two sets of picture counts at the different pressures, it was decided that running

tests at 20 psi and capturing 250 pictures would be optimal. Figure 35 below demonstrates the difference between the 20 psi and 100 psi on a 160° nozzle, where 250 pictures were taken. On the left hand side, the 100 psi photo is shown, while the 20 psi picture is on the right. As previously discussed, the higher pressure gives a wider distribution and less droplet definition.

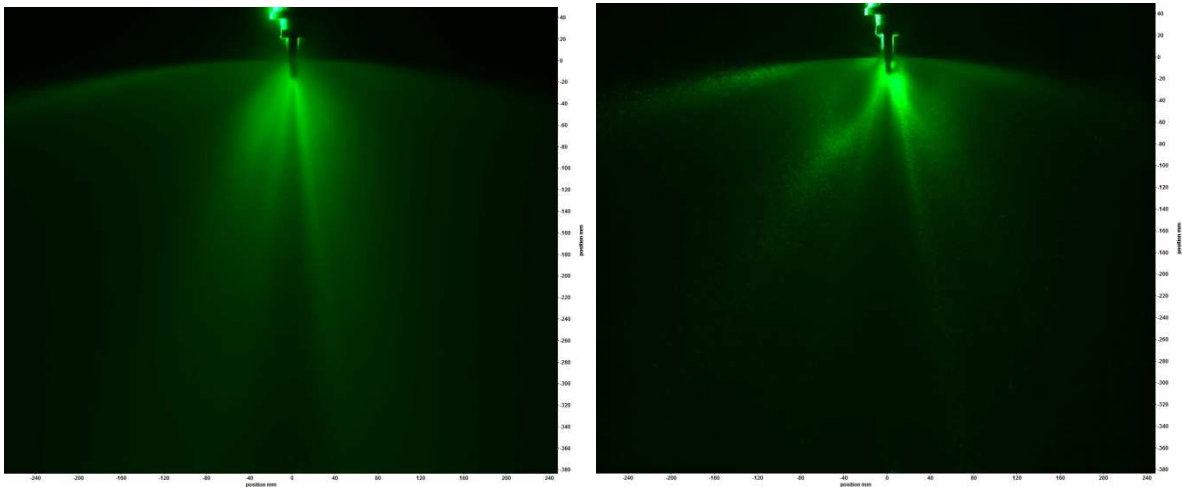


Figure 35: Comparison of Pictures

A trend was noticed as the number of pictures increased; with increasing pictures droplet definition decreased, as spray angle shape became more apparent. After discussing this concept with various Tyco employees, it was found that more pictures are considered to be more appropriate than fewer pictures. Keeping in mind the time limitations, and computer space issues, a balance needed to be created between number of pictures taken and the time table for the work schedule. Although this could not be a deciding factor, it was one consideration. Initially, it was felt that 250 pictures would provide a good enough spray angle, but after measuring the pictures, it was found the 500 and 1000 pictures were easier to analyze. Therefore, it was decided to either use 500 or 1000 pictures in the testing. In order to make a final decision, the pictures were all printed out and the angles measured. A ruler and protractor were used to manually determine these measurements. If the angle measurement did not drastically change between 500 and 1000 pictures then it would be acceptable to use 500 over using 1000. For these measurements the 160° nozzle at a pressure of 20 psi, and a K-factor of 3.0, was used. Figure 36 below shows the final measurements of the 500 pictures and 1000 pictures. As shown, the angle

is 174° in both pictures, which provided the proof that the 500 pictures would be acceptable to use. Taking this into consideration, the decision was finalized to use 500 pictures in the testing.

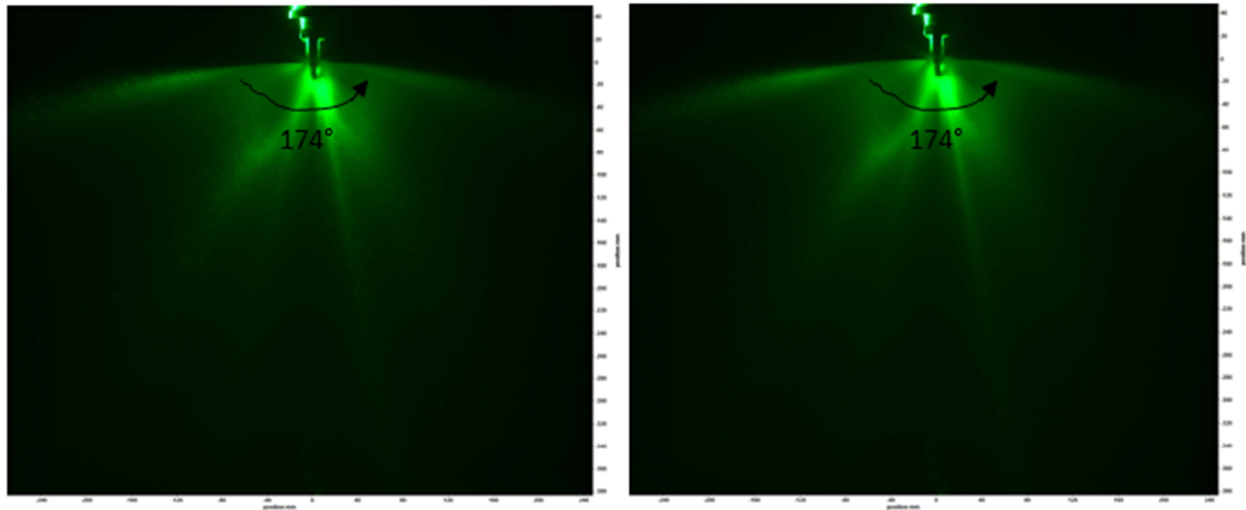


Figure 36: Spray Angle of 500 Pictures vs. 1000 Pictures (respectively)

Another important detail to consider was the power at which to run the laser for the testing. The laser is throttled, so that when the computer control settings are set to 100% the laser is really only operating at 10% of its capability. For this discussion all references to the lasers power will be in terms of the computer control settings. Upon initial considerations of looking at the lasers power settings tests were being run at 20 psi. The lowest possible setting for the laser is 10%, and this was not adequate lighting to display the water droplets in this flow. The laser was then increased to 20% power and this provided a good picture of the flow. Later on, when the water pressure was increased to 100 psi, running the laser at 20% power was still able to give an image of the whole flow; however, the power was increased to 50% to provide an even clearer picture. The water pressure was then lowered to 20 psi again, and the laser power sustained at 50%. At this setting the pictures were still very clear and there appeared to be no negative effect from this increased power setting. As such, 50% appeared to be the best setting for this application, and was selected for testing purposes.

The next consideration for testing was the number of planes to test on. The way the laser works is that it diffuses the light from a single point, at an angle, in order to form a plane. This allows for the camera to capture an image of all of the water droplets present on this plane. In order to

get a more complete idea of the whole flow of water, the plane that is imaged will need to be rotated. What needed to be considered was what a practical number of rotation angles would be. The nozzle is connected to a rig that is attached to a motor and controlled by a computer. It has the capability of being precisely controlled to move by very small angles of rotation. This was set up to change in increments of 1° , although it has the capability to allow for smaller rotations. While tests could be run for every 1° , many of the same droplets would be captured between shots. This would provide repetitive data, and simply far too much data to practically analyze. In order to collect of reasonable amount of data it was decided to move in 18° increments. This will hopefully allow for images of the different areas of the water distribution to be captured. The goal is to not have all the planes end up in-between the tines, or on the edges of the tines. By moving at this increment the hope is to capture a variety of different sprinkler orientations in order to get a more complete picture of the flow patterns.

Updates: While the original testing plan that was developed provided a good starting point, once testing began the need for several changes was discovered. One such change was the number of nozzles to include in the test. The D3 nozzle comes in a variety of angles ranging from 65° to 180° . In testing this nozzle, it was important to choose a wide range of angles to fully understand the nozzle's characteristics. Therefore, it was decided to conduct the tests with a minimum, maximum, and middle angle. With this, the nozzle angles of 65° , 125° , and 180° were chosen. The 65° nozzle will provide an understanding of how a smaller angle affects the sprinklers characteristics, while the 180° nozzle will demonstrate how a larger angle compares. Clear comparisons should be able to be made between these two extremes, since they will likely be very different. Testing the 125° nozzle will provide a middle point between the 65° and the 180° nozzles. Also, it will show how a less drastic degree has different characteristics than the two boundary values. Testing this range of nozzles should help to provide a clearer picture of the overall spray characteristics of the D3 nozzle. The different Spray Angles tested are shown in Figure 37 below.



Figure 37: Varying Nozzle Angles (65, 125, 180)

After some discussion with our supervisor at Tyco, and discussion within the group it was decided that testing multiple pressures would be beneficial to helping to characterize sprinkler flow. In looking at the data sheet for the D3 nozzle (Tyco) it can be noted that the low end of the D3's working pressure range is 20 psi, while its maximum working pressure is 175 psi. By testing both ends of the available pressure spectrum is important, but another pressure in the middle was also needed in order to have a more complete test. So while the original planned test pressure of 20 psi would still be utilized, the test pressures of 100 psi and 175 psi were also added.

Once testing of these pressures with the different nozzles actually began it was discovered that 175 psi was not able to be reached on the K-Factors of 7.2. The required flow rate through our system would have to be 95.247 gpm in order to reach the desired pressure. When the pump providing water to our test pipe was turned all the way up, it was only able to obtain a flow rate of approximately 88.6 gpm, providing a pressure of 151.5 psi. When the flow of water was observed at this pressure, however, it appeared to be a solid cloud of mist. The pictures of the flow simply looked white, and there was no distinguishable droplets seen. In order to alleviate this problem, it was decided that the 7.2 K-Factor nozzles would only be tested at 20 psi and 100 psi as these pressures provided more useable data.

The original range of K-Factors was to include 1.2, 2.3, 4.1, and 7.2 of each nozzle to be tested. While this seemed to provide a good range of data (including the lowest and highest available K-Factors, and 2 in the middle), it required a lot more testing. As the total number of nozzles and other factors started to increase the number of tests required, total available time became a serious consideration. With a 6 week schedule for testing, we were tight on time. Therefore, we decided to cut back the number of K-Factors to be tested. Since most of the testing parameters had been changed to three, this seemed like an appropriate number to examine for K-Factors as well. Using the 1.8, 3.0, and 7.2 K-Factors for each angle of nozzle still provided a large range of data, while also cutting down on the required testing time. The different K-factors tested are shown in Figure 38 below.



Figure 38: Varying K-factors (7.2, 3.0, 1.8)

Changing the angle of rotation by 18° in order to get a clearer picture of the entire flow was also part of the original plan. After realizing how much time was required to run testing at 11 different places for each of the nozzles, we realized this was unreasonable. A closer look was taken at the spacing of the tines on the different nozzles in order to come up with a more concise set of testing angles. Upon further examination, it was discovered that outer edges of the tines are approximately 24° of the deflectors outside diameter. With this, we calculated the spacing in-between the tines would be about 6° . Using this information, we noted that most of our angles were on tines, with a few ending up close to the edges. With each of the deflectors being oriented slightly different between various nozzles, it was uncertain if any of the angles captured would actually be spaced in between any of the tines. In order to account for this, and to help save time overall, we cut the number of angles down to four. The angles to be imaged were 0° , 45° , 60° , and 90° . The angles of 0° and 90° provided a plane without direct influence from the frame arms,

as well as one that split both of the frame arms down the middle. The angle of 45° provided a plane that was located in-between two tines, while also showing the influence of both frame arms. Likewise, the angle of 60° showed a plane located on a tine, while showing the influence of both frame arms. Upon running a test of the 45° and 60° angles we found that they were in fact lined up where we had anticipated. Figure 39 below shows where each angle lines up on the nozzle.

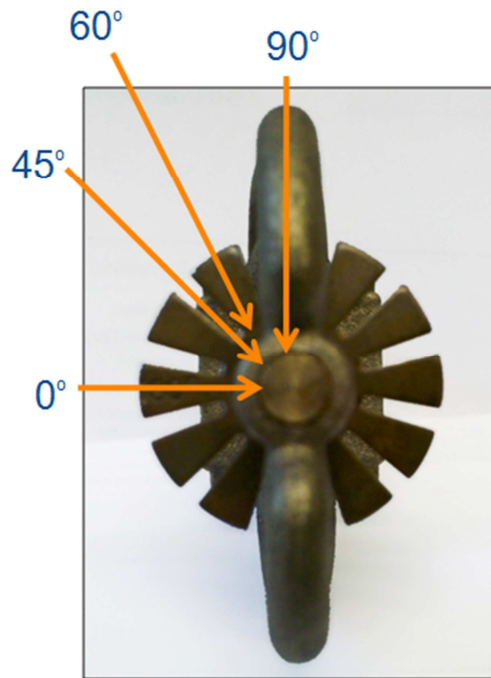


Figure 39: Rotation Angles

From here on our testing continued with these 4 angles for each nozzle in order to capture the most planes in the fewest images as possible.

Shadowgraphy:

The original plan for shadowgraphy testing consisted of 3 different radii being tested at 3 different positions in the flow (see Figure 70 in Appendix H: Results). The Proposed radii to be tested were at 2ft, 4ft, and 6ft in order to correspond with the data collected in PIV testing. Due to a request from Tyco, however, the radii to be tested were changed to 1ft, 2ft, and 3ft. It was decided that this would be a positive change to the testing. Having a smaller test radius would

allow for more information to be obtained from our test area, because the droplets would have less distance to spread out in.

In order to account for the flow from the areas under the nozzle, in addition to the areas on the edge of the flow, three testing positions were selected. The first position was the location directly below the deflector; since the nozzle would be rotated at that point the droplet count should not be affected by the rotation angle. The next position was located at the edge of the flow; this position was estimated from the measured spray angle results from PIV testing. The last position was located in the middle of the flow, half way between the edge of the flow and under the deflector. The edge position was estimated from the measured spray angle results from PIV testing. For the 65° nozzle a spray angle of 90° was assumed, for the angle for 125° a 140° angle was assumed, and lastly for the 180° nozzle a 175° angle was assumed. From each of these angles, the point at which the edge would lie was measured as half of the total spray angle starting from below the deflector and out to the appropriate angle. To complete this measurement a protractor was held in place at the bottom of the deflector and a string was connected at that same point and pulled out to the correct radius at the correct angle. The angles from below the deflector out to the position for each nozzle were as follows:

65°: Edge - 45°; Middle - 23°; Under - 0°

125°: Edge - 70°; Middle - 35°; Under - 0°

180°: Edge - 88°; Middle - 44°; Under - 0°

The first nozzle to be tested for shadowgraphy was a 65° nozzle with a 1.8 K-factor at 100psi. After the test was run, and the pictures were processed the data was quickly analyzed. One of the things that observed was that for the tests on the edge of the spray, farther away from the nozzle (2ft and 3ft tests) there was really no useable data. Gravity affects the flow of water and causes it to start to drop off from its original spray angle. So, while closer to the nozzle it was easy to take tests on the edge, as you drop lower into the flow it became much more difficult to locate the actual edge. With this in mind the decision was made to drop the testing of the edge at the heights of 2ft and 3ft. There was a hope that at the 3ft range there may be some better pictures taken due to the water being more spread out. Due to this finding and time considerations, the decision was made to not test the 2ft height. The last change made to the original testing method

was the tests underneath the nozzle. Since the nozzle was rotating around the same point, the data collected there should be comparable between different nozzle rotation angles. This led to the decision to only test underneath at the 0° rotation angle. With these cuts to the testing positions, the final list of places to test dropped down to: edge, middle for all rotations at 1ft, and underneath at the 0° rotation; and middle for all rotations at 3ft, and underneath at the 0° rotation.

With the time left for the project really starting to wind down at this point some more decisions needed to be made on how to cut down the required number of tests while still collecting useful data. The amount of time needed to really analyze all of the pictures and compare different tests to each other was really one of the biggest factors. In order to alleviate some of this required time, the number of nozzles actually tested was lowered. By testing every spray angle at 2 K-factors, and 2 pressures general trends in the differences would be able to be noticed. For each spray angle the 1.8 K-factor nozzle would be tested at both 20psi and 100psi in order to show the differences in pressures. The same spray angles would also all be tested with a 7.2 K-factor at 20psi in order to compare the difference of K-factors with the 1.8K nozzle.

The next important detail to look into was the number of pictures required for each test. In the background research for shadowgraphy it was discovered that a sample size of 1000 to 5000 droplets would yield 90-95% accuracy. A sample with too few droplets may not give a true representation as there can be an order of magnitude change between the diameters of droplets (Grant). It is important to collect a large enough sample to give a true accounting of the droplets present in the flow. While it would be more desirable to have a higher percent accuracy it would take close to 40,000 droplets in order to yield just 97% accuracy (Grant). With minimal increase of accuracy for a sample size nearly 40 times larger it was decided to try to capture between 1000 and 5000 droplets as the sample size. Upon initial analysis of the required picture counts to produce the number of droplets, 50 pictures seemed an appropriate number as it produced results of 1000-7000 at different sample points in the flow for a 65° nozzle. The decision was made to move forward the picture count of 50 for all of the sample areas.

Citations:

Grant, G., Brenton, T., Drysdale, D. "Fire Suppression by Water Sprays." Progress in Energy and Combustion Science 2000: 79-130.

Products, Tyco: Fire Suppression & Building. Type D3 Protechtospray Directional Spray Nozzle, Open, Medium Velocity. Technical Data Sheet. Lansdale, 2009.

Appendix F: Encountered Problems

As with any project, our work was not free of setbacks. Some minor, as well as more major problems presented themselves throughout our time at Tyco. We viewed these issues as opportunities to get a better understanding of our project, and attempted to find innovative ways to solve them. We were fortunate in that we found ways to remedy most of our problems, which are described in the following section.

Blinking Laser: Although all the images appeared to be getting taken correctly, the laser seemed slightly off visually. Whenever the laser appears to flash, it is actually doing two, extremely fast pulses. Along with each one of these quick pulses, a picture is taken. With these pulses being so quick it appears to be one solid flash of the laser, with several of these going off every second. The problem that seemed to arise, however, was that the flashes did not seem to be in any sort of methodical pattern. There were random breaks occurring during the course of the image capture process.

While this is an odd occurrence, it did not seem to actually present a problem for our testing. As long as the camera is still correctly timed with the laser, it will capture images when the laser actually does go off. If this alignment was affected, it would become obvious, as there would be no light source present for the camera taking the picture, and we would have black images. The manufacturer was contacted about this problem. One possible thought about it was that it could be an error with the circuit board. If that were to be the case, though, an error message would have appeared on the controller for the laser. As none of these errors had appeared to occur, testing continued on as normal. If this problem continues to arise, further inquiry into its solution will be conducted.

Mist: Another issue that arose on this day was when we adjusted pressures. As we adjusted the pressure from 20 psi to 100 psi and to 175 psi, we noticed some minor issues that called for procedural changes. With higher pressures, our pictures became blurry and unclear. We realized this was due to the increased mist with increased pressures. With this, it became necessary to wipe the camera lens between each set of pictures. Upon doing so, much care needed to be taken. First, we had to be careful not to press too hard and change the focus on the camera. Also, we needed to be very gentle to ensure the position of the camera did not change. If either the focus

or position was changed, we would have a big problem. We would no longer be able to make equitable comparisons between pictures because an outside factor would come into play. If this situation occurred, we may have to redo a great amount of work. Lastly, we needed to keep in mind that the camera is an expensive, fragile piece of equipment. Knowing this, we used a soft cloth to gently, but thoroughly clean the lens. Cleaning the camera lens solved the problem of blurry pictures, so we continued to do this throughout testing with the higher pressures.

Motor Rotation: One final problem that we found on this day when we were conducting the test with the 180° sprinkler dealt with the motor which controlled the nozzle rotation. When we began the testing with a pressure of 100 psi, it seemed that the nozzle did not rotate at the correct angle. We noticed the pictures we took at 108° seemed to be very similar to those of the 90° angle. After comparing the pictures taken at 100 psi with the pictures taken at 20 psi at the same angle before, we found that the error happened at the beginning of the testing of 100 psi, but that the pictures of the 20 psi were correct. With this, we realized that the high pressure affected the motor. We found that the motor skipped degrees when it was rotating under the high pressure. Therefore, we decreased the rotating speed in order to make the motor more stable and to make the rotation more precise. After we adjusted the rotation speed, the pictures seemed to be accurate and we continued the remainder of the testing. However, the motor failed to rotate again when it was supposed to reach 72°. Once again, we increased the power of the motor. Unfortunately, it did not help this time, so we needed to figure out another way to prevent this occurrence. We decided to shut down the water before rotating the nozzle every time. We would then restart the water when we took pictures. This solved the problem, allowing us to prevent the motor being affected by the high water pressure.

Flow Limitations: On July 12th, we continued to run into some issues. First off, it is important to understand that, as nozzles K-factor increases, so does the diameter in which water enters before hitting the deflector. This means that with larger K-factors, more water hits the deflector at a quicker rate than on nozzles with small K-factors. As we went through the usual testing procedures on this day, we ran into a dilemma when dealing with the 180° nozzle with a K-factor of 7.2 at 175 psi. Since this was our maximum pressure, and largest K-factor, the two did not work well together. First off, the combination of the high pressure and large K-factor created an

inward suction of air, which pulled the tarps toward the sprinkler system. After readjusting the tarps so they would not move, we noticed another problem: the camera was getting covered in water. With this, we attached an extended lens piece on the camera, which protected it from the water, while still giving us a clear image. Finally, we realized testing the 7.2 K-factor nozzle at 175 psi was not even practical due to the flow rates limitations. The flow rate could only be increased to around 83 gpm, but the 175 psi called for a flow rate of 92 gpm. With this, we realized we could not test the 7.2 K-factor nozzle at the maximum pressure. Therefore, we made note of it, and moved on with our testing keeping in mind the possibility for this problem to reoccur with other nozzles.

Camera Focus: After working with smaller angles, we realized the 180° nozzle may present a problem. Due to the fact that it has a wider spray pattern, the complete distribution did not completely fit into the cameras focus. This may present a problem in the future when we are working with velocity and vector maps. With these parameters, we will want to see the entire distribution, and therefore, will need to make some type of adjustment to fit the 180° spread into the picture. There are two ways to do so; first off, we could change the camera lens. There is a wider focus lens that can be attached to the camera to produce a larger picture. Unfortunately, it is commonly used for extremely wide spreads, so the 180° may be too small to work well with this lens. If this is the case, the distribution will end up appearing very small, and will be of no use. The second option to remedy our problem is to only take a picture of half the spray. Upon doing so, we can mirror the image over to the other side to create a complete spread. Since, in theory, both sides of the spray should be equivalent, this method is very practical for completing our objectives. It was eventually decided to go with the wide angle lens in order to capture the entire flow in the picture.

Light Artifact: An important lesson was discovered in making sure to check what the laser is actually doing. While from a safety standpoint it is extremely important to wear the appropriate safety glasses to shield your eyes from potentially straying laser lights, it is also good to take safe, quick peeks at what occurring in your lasers plane. When running the tests, a beam of laser light was discovered cutting through the lasers plane. This phenomenon is referred to as a “Light Artifact”. The cause of this problem turned out to be a drop of water present on the lens of the

laser. This resulted in something comparable to the beam of a laser pointer being directed from our laser, at a downward angle through the flow. While this problem did have the potential to distort some of our images taken by over saturating the light at those points in the pictures, in processing the images collected it did not appear to be an issue. This problem was fixed by stopping the series of pictures that was being collected, and wiping down the laser's lens, much like what had been done with the camera lens at higher water pressures, and flow rates.

Pin Hole: About two weeks into running tests, we ran into a major setback. When taking trial pictures, we noticed a spot on the picture that looked out of place. We attempted to wipe the camera lens, thinking the mist problem was to blame, but this did not work. Therefore, we realized it was a bigger problem. Chad explained that the pipe was likely causing the problem, so he went onto the ceiling to find out. He was correct; there was a "pin hole" in the pipe, which means a small hole existed due to erosion inside the pipe. Over time, as pipes are exposed to high pressures and flows, their insides begin to wear away. This is especially true for the bottom of the pipes, where water begins to collect. Once the bottom layer is very thin, this sitting water will eventually make a small hole, the "pin hole." For us, this was a major problem, because the only real fix would be to replace the pipe, which we did not have the time or resources to do. Therefore, we resorted to a quick fix, duct tape. This worked for the low pressure of 20 psi, but once the pressure was increased, the tape was pushed off, and the "pin hole" was once again exposed. With this, we gave up testing for the day, and plan to move into a different testing area before resuming.

Testing Location: One of the first issues we ran into with testing was conflict over who got to use the water for their testing. While there are two separate systems to pump water through Tyco's testing labs, our test pipe was connected to the same manifold as another group's test pipe. Through the first two weeks of testing the solution to this problem was splitting lab time. Every morning our group had water for the morning and took as many pictures during that time as we could. Then, each afternoon the other group took the water, and we were able to use that time to process our data.

From the time that our project started, Tyco had plans to move the laser testing over one bay. While this would allow for us to use both pump system at the same time, a new manifold needed

to be constructed. On our first day at Tyco, we were shown where the laser was currently set up, and then a room full of other equipment that was where we were to move to. Needless to say, it took several days for the area to be cleared, and then piping construction was able to begin. There was already a pipe across the ceiling leading to where we needed, but this needed to be rerouted through a different piping manifold. By Friday of our second week all of the construction for the piping was completed, as well as several new ceiling tracks which were used to support the tarps used to enclose the testing area.

Wide Lens → Light Artifacts: On the first day of horizontal testing, we made significant progress. We began testing with the 65° and 125° nozzle, and the pictures were turning out well. Once we got to the 180° nozzle, we realized the spread was too wide to fit in the picture. Since the distribution was essential for our analysis, we realized a change needed to be made. We ended up changing the camera lens to a wider focus. This allowed us to fit the entire spread into the picture without a problem. Unfortunately, in doing so, a new problem emerged. With this wider picture, more wall space could be seen, which led to light artifacts showing up in our picture. The laser's light was reflecting off the back wall, and causing two lines in the photos. One was on the initial reflection off the wall; another was from that line reflecting downwards onto the ground. The lower reflection was our main concern, as it created a line through the spray pattern. After much discussion regarding how to solve this dilemma, it was decided that the best option would be to cover the back wall with a tarp. Upon doing so, the reflection on the ground was greatly reduced. In order to completely get rid of this reflection, we needed a non-reflective surface to put over the wall. With this in mind, we ordered a cloth tarp in both tan and green. The next day the tarps arrived, and we put the tan tarp against the wall. This tarp completely eliminated the reflection off the ground, and slightly reduced the one off the wall. We came to the conclusion that this was the best option we had at this point, and ran through the entire horizontal testing with this tarp in place.

Appendix G: Data

Pictures with a 160° D3-nozzle with K-Factor of 4.1. Images of different ranges collected in order to show difference in picture clarity between different numbers of summed images ranging from 50 pictures to 1000 pictures. This section is in reference to the discussion of parameters on how many pictures to take to accurately measure spray angle.

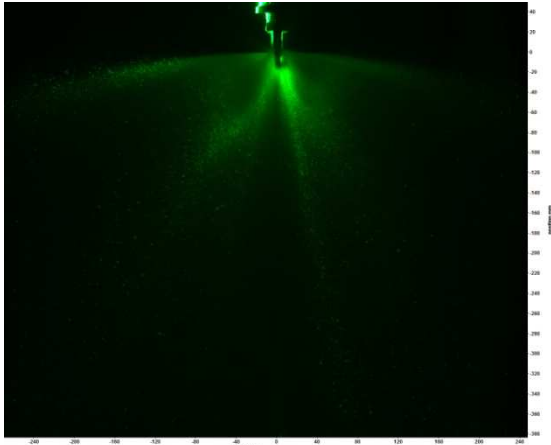


Figure 40: 50 Pictures at 20 psi

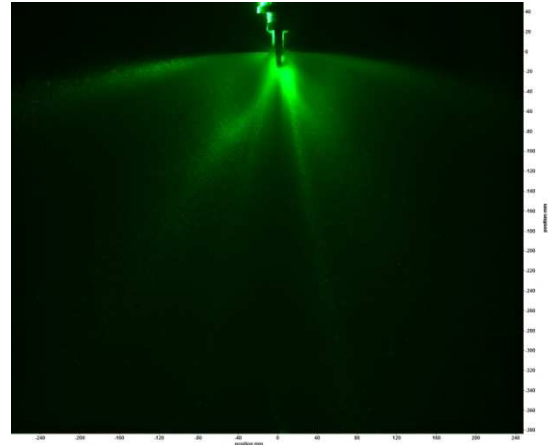


Figure 41: 250 Pictures at 20 psi

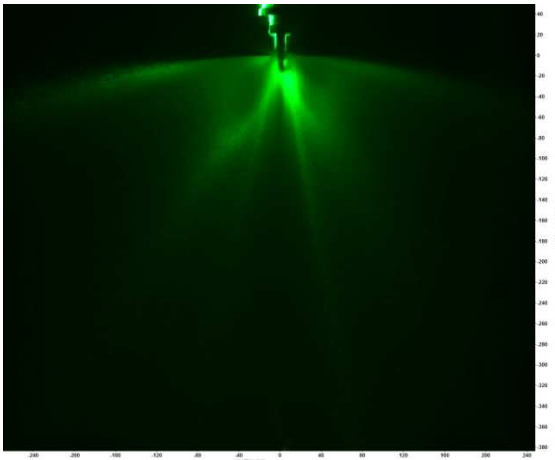


Figure 42: 500 Pictures at 20 psi

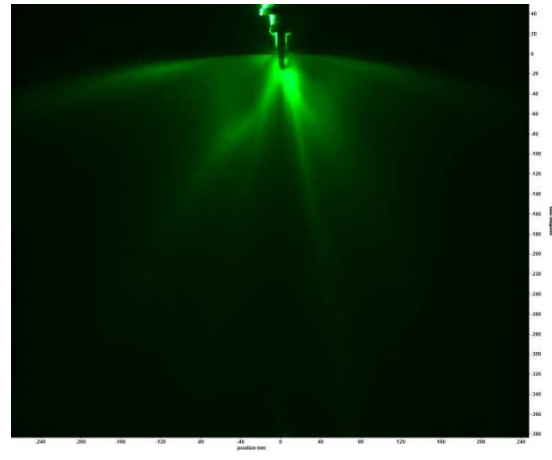


Figure 43: 1000 Pictures at 20 psi

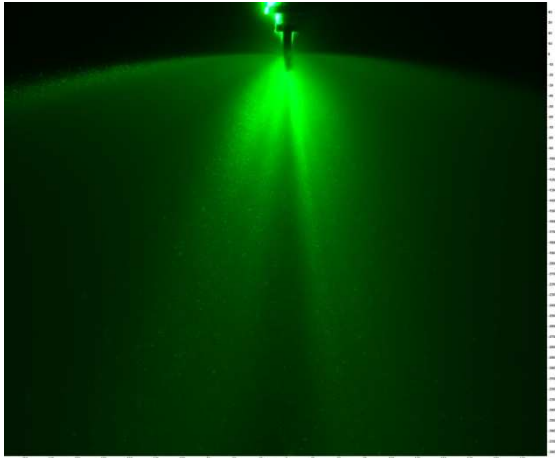


Figure 44: 50 Pictures at 100 psi

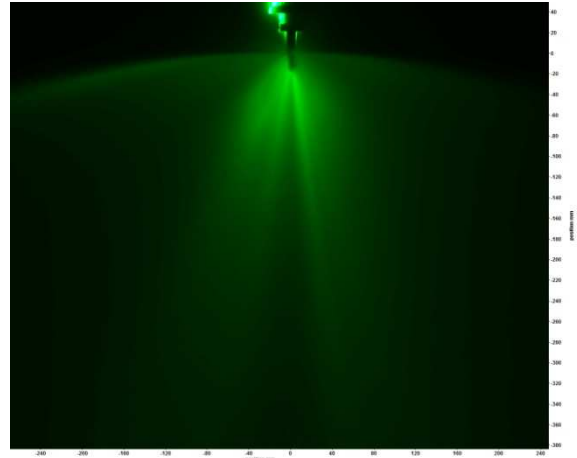


Figure 45: 250 Pictures at 100 psi

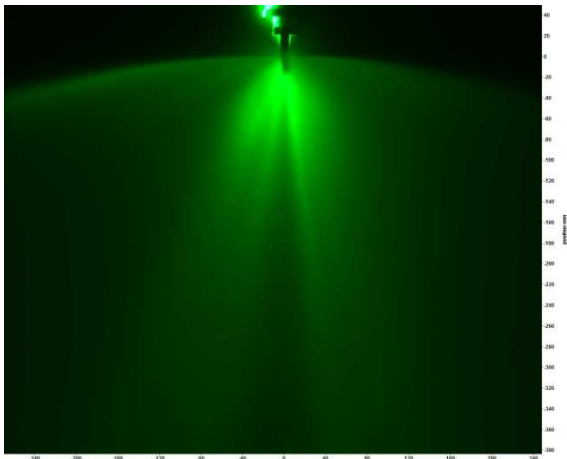


Figure 46: 500 Pictures at 100 psi

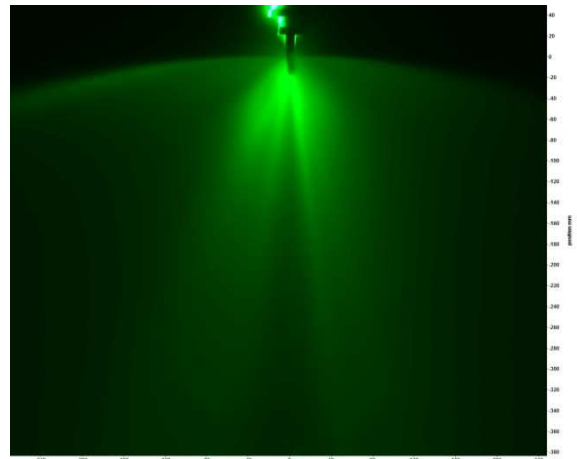
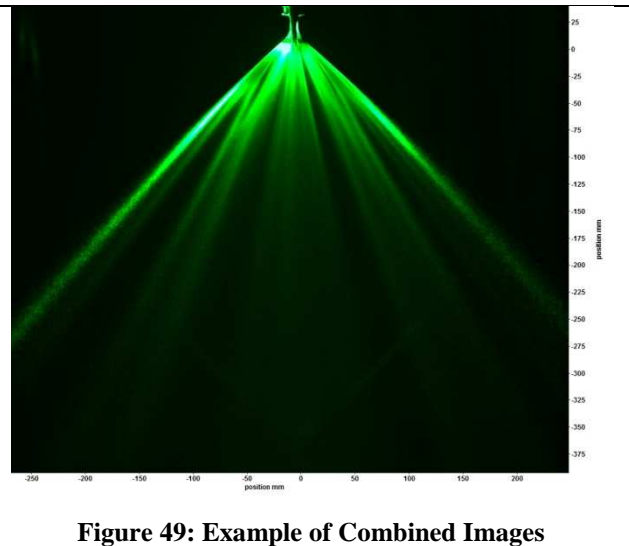
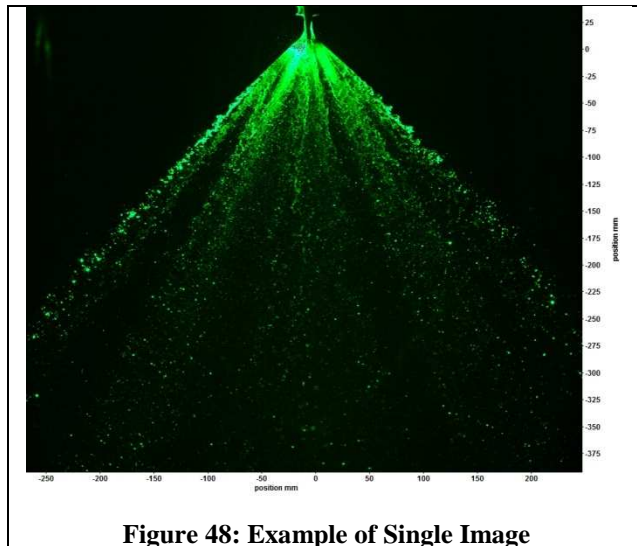


Figure 47: 1000 Pictures at 100 psi

Example Data Sets:

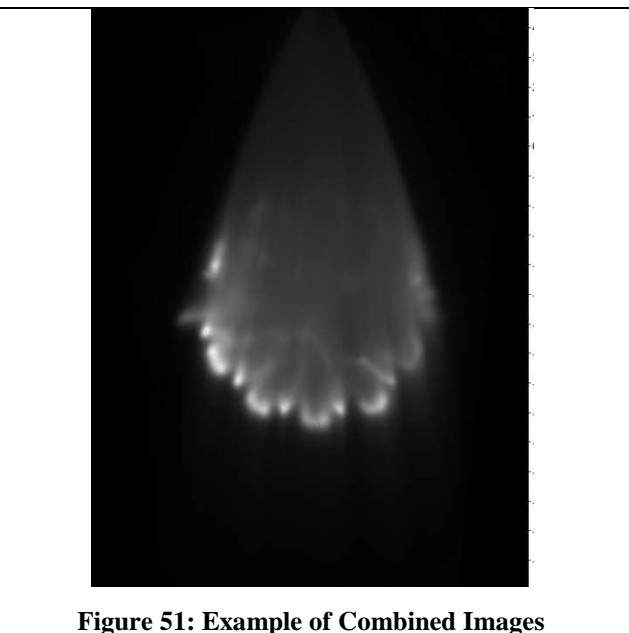
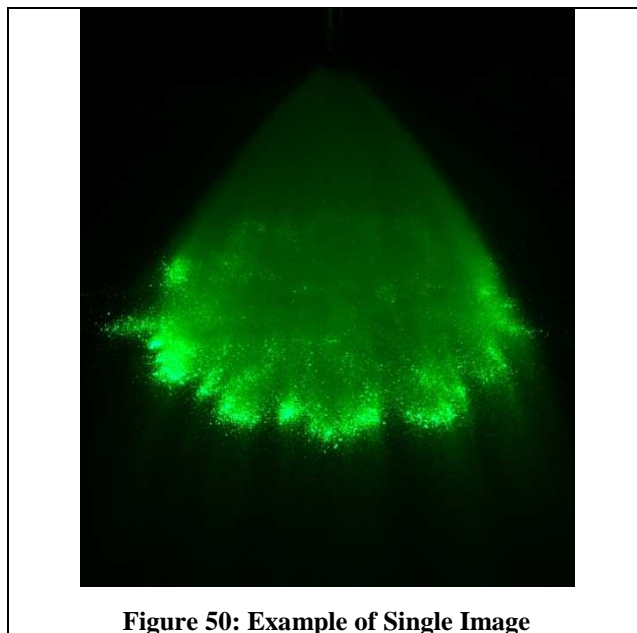
Vertical PIV Testing:

When working with vertical PIV, the computer created two types of pictures. The first type is single images of the flow. Each time the nozzle was changed, 500 pictures were taken, so the computer gave us 500 single images. A single image example is shown in Figure 48. When we processed them, the computer combined each image to create one final picture of all 500 overlaid. An example of the combined picture is shown in Figure 49. Using the single images, ligament distance could be found. From the combined images, we could determine spray angle.



Horizontal PIV Testing:

Similar to vertical PIV testing, horizontal gave us single and combined images. Instead of showing the entire flow, the pictures were taken from above. The single images were not used for analysis, but the combined ones allowed us to find the spray pattern. Once again, both types of pictures we could derive from horizontal PIV testing are shown below. The single image is seen in Figure 50, while the combined is shown in Figure 51.



Shadowgraphy Testing:

Shadowgraphy testing provided some unique information which was unable to be obtained by PIV testing. Since shadowgraphy focused on a very small area, the entire flow could not be seen. Instead, it was used to analyze tiny particles. With this, the computer gave us pictures of droplets showing their size and velocity, which is shown in Figure 52. The yellow circles designate droplets that the computer could clearly identify. Although other droplets may be present, they were too unclear for the computer to select. Also, processing allowed us to obtain vector maps, showing the magnitude and velocity of droplets. An example vector map is shown in Figure 53. In the velocity map, different colors stand for different velocities, and varying sizes show changes in magnitude.

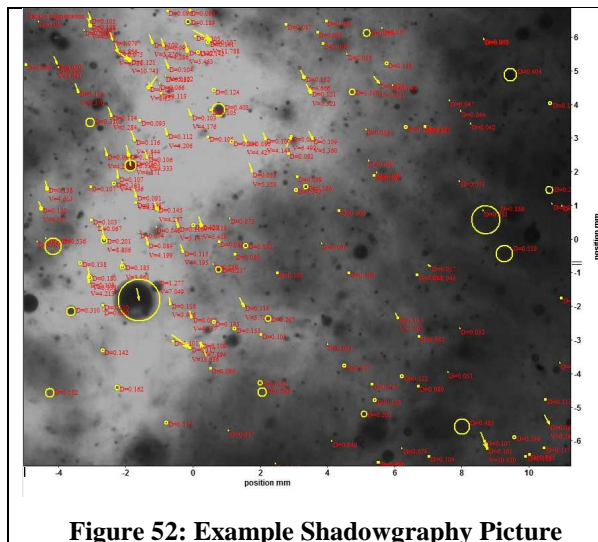


Figure 52: Example Shadowgraphy Picture

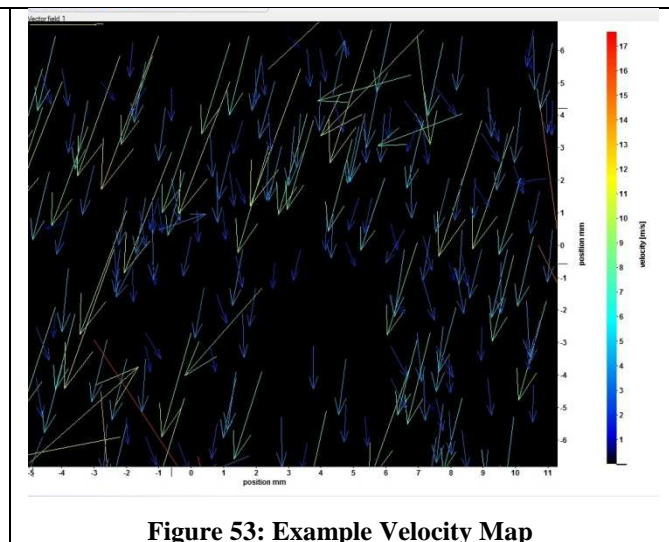


Figure 53: Example Velocity Map

Besides actual pictures, shadowgraphy gave us numerous statistics for analysis. Table 4 below shows an example of the statistics provided by the computer after processing. The 'N' shows the number of particles identified by the computer. 'N Corrected' identifies the number of droplets after corrections were made. 'D10' shows the mean diameter value, while 'D32' displays the surface volume diameter. 'DV__' deals with the mean volume diameter. With this, 'DV50' was of most interest to us, since it showed the value of the volume that was in the 50th percentile.

Table 4: Example of Shadowgraphy Statistics

N	3993
N_Corrected	4839.73
D10	0.084294 mm
D32	0.388611 mm
DV10	0.166426 mm
DV50	0.695759 mm
DV90	0.996216 mm
RMS	0.079953 mm

Other than the table above, the computer gave us large lists of statistics for each particle. These were not used in our analysis, since we did not have time to analyze every particle separately. Some other interesting data that was shown through shadowgraphy testing was in the form of graphs. Although we did not make great use of these graphs in our project, it would be useful to analyze these in future work. Figure 54 through Figure 56 each show different data related to some of the statistics previously explained.

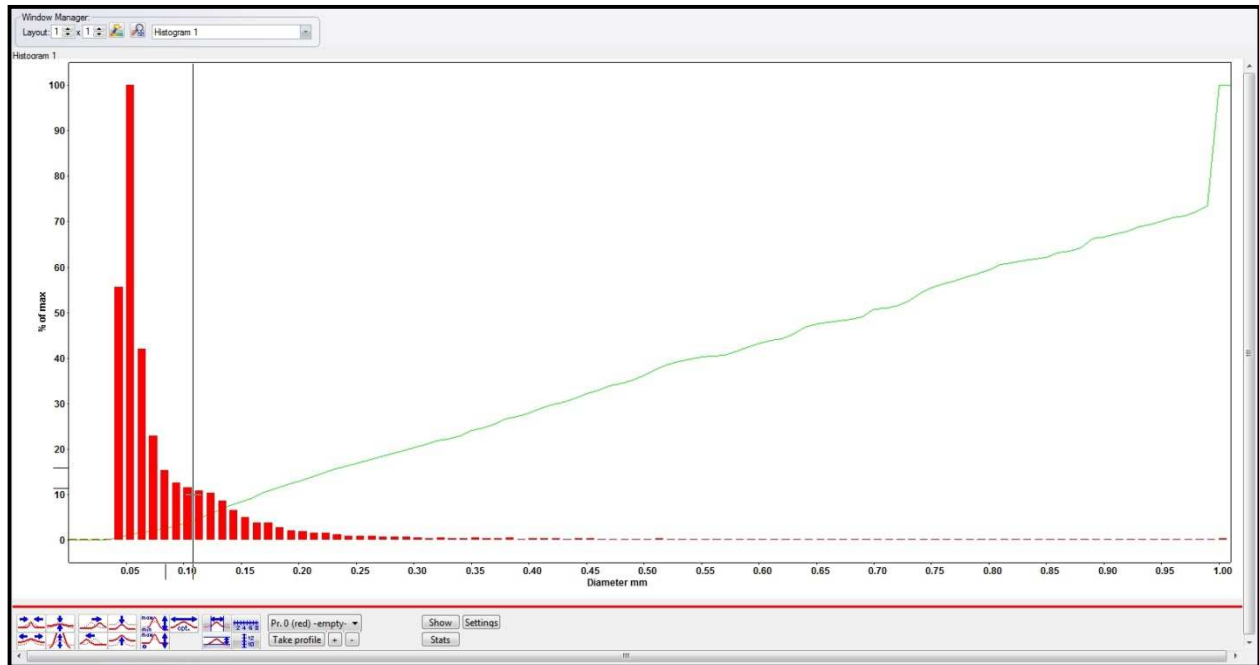


Figure 54: Diameter vs. % of Max



Figure 55: Diameter vs. Volume Flux

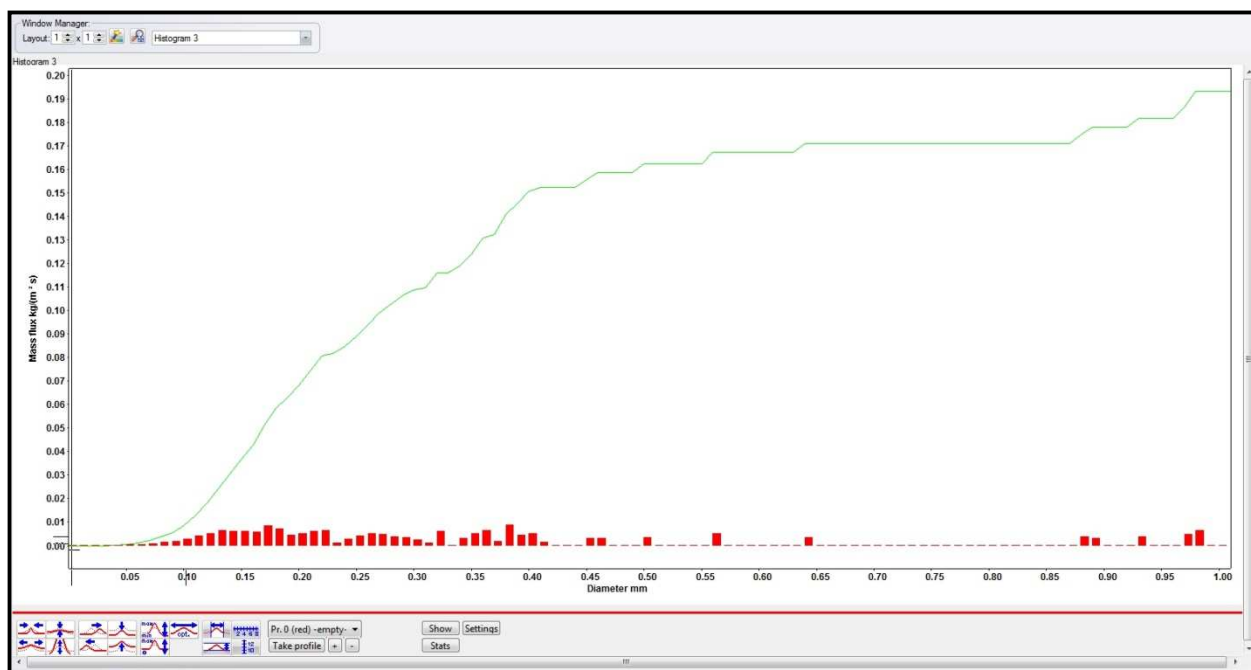


Figure 56: Diameter vs. Mass Flux

Appendix H: Results

Vertical Spray Angle Analysis

In order to measure spray angle, a definition needed to first be laid out. After talking to several people at Tyco about spray angle, and how it was measured, and then by observing some of the images we collected we came to a working definition of spray angle. The water flows through the nozzle and off of the deflector, and then initially travels for a distance in a straight line. Soon after this, gravity starts to affect the flow of water to the point where the stream begins to be redirected downward. Two points can then be found; the points where this change occurs on both sides of the flow, and then the point in the nozzle where the flow begins to be redirected. By measuring the angle between all of these points (the nozzle being the apex) the spray angle can be determined. This can be seen in Figure 57, below.

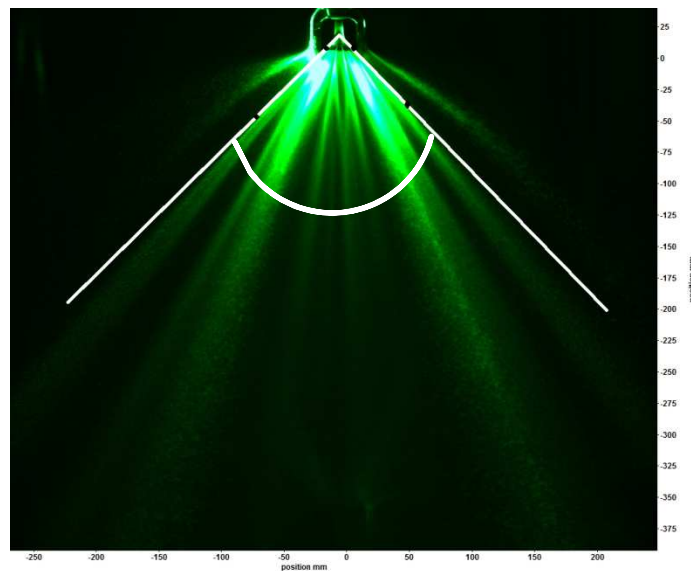


Figure 57: Method Used to Measure the Spray Angle

The measurements found by use of a protractor and ruler was used to create Table 5 below.

Table 5: Spray Angle Measurements

	65° (1.8)				125° (3.0)				180° (7.2)		
	20 psi	100 psi	175 psi	AVG	20 psi	100 psi	175 psi	AVG	20 psi	100 psi	AVG
0°	96°	94°	96°	95.33°	145°	153°	157°	151.67°	175°	176°	175.5°
45°	94°	94°	95°	94.33°	147°	150°	149°	148.67°	178°	177°	177.5°
60°	95°	96°	93°	94.67°	145°	151°	142°	146°	178°	177°	177.5°
90°	95°	94°	91°	93.33°	143°	148°	143°	144.67°	175°	175°	175°
AVG	95°	94.5°	93.75°		145°	150.5°	147.75°		176.5°	176.25°	

In the table, the first column is rotation angle with average of spray angle from same pressure. The first line is a different designed spray angles with their designed K-factor in the bracket. The second line is three different pressures at each nozzle. The “AVG” refers to the average of spray angle from three different pressures at one rotation angle.

Upon analyzing this information, the average results for one nozzle with different pressure have no significant change. For example, in the 65° spray angle, the range of the averages is 1.25° (Max: 95°, Min: 93.75°). The other two nozzles have differences of 5.5° and 0.25°. That shows the influence of pressure on the spray angle is not very significant, so can be ignored.

Since limited time was given to complete this project, cutting down the data for further analysis was necessary. Therefore, it was decided to choose a certain rotation angle to check the influence of other parameters. In the chart, the highlighted numbers are the results which are closest to the average; it can be found that the results from 60° rotation are consistently closer to the average. Thus, the 60° rotation was chosen to be a representation for all the nozzles and pressures. Using a 60° rotation, different pressures and angles data were used to create Table 6.

Table 6: 60° Rotation Angle Data

Spray Angle	65°			125°			180°	
K-factor	1.8	3	7.2	1.8	3	7.2	1.8	7.2
20psi	95°	95°	88°	144°	145°	146°	174°	178°
100psi	96°	98°	93°	145°	151°	149°	175°	177°
175psi	93°	97°		148°	142°			
Avg	94.67°	96.67°	90.5°	145.67°	146°	147.5°	174.5°	177.5°

In Table 6, the “Avg” (average of spray angle from different pressure) increased a small amount in the 125° and 180° nozzle. However, this trend is not consistent in the 65° nozzle. With this, it was necessary to look at another rotation angle. Therefore, the 0° rotation angle was chosen to double-check this prediction. The data collected from this analysis is shown in Table 7.

Table 7: 0 Degree Rotation Angle Data

0 degree	65°			125°			180°	
	1.8	3	7.2	1.8	3	7.2	1.8	7.2
20psi	96°	91°	99°	145°	146°	143°	179°	174°
100psi	95°	95°	94°	144°	150°	149°	177°	175°
175psi	94°	98°		152°	156°			
Avg	95°	94.67°	96.5°	147°	150.67°	146°	178°	174.5°

The trend of the average results in Table 7 seemed random, so this data cannot prove the previous hypothesis. For example, in the 125° and 180° nozzle, the average has no trend of either increasing or decreasing. Thus, the conclusion is that the K-factor does not have a consistent pattern or trend that can be correlated to the spray angle.

Horizontal Analysis

In analyzing the horizontal pictures, the main point of interest was the spray geometry. To find how various parameters affect this pattern, numerous pictures were analyzed. It was important to find how K-factor, pressure, and nozzle angle influenced the spray geometry. Upon doing so, different trends and patterns could be found. Before going into a discussion on the results, it is important to understand the basics of the spray geometry. Figure 58 demonstrates how an inner and outer pattern is formed in horizontal testing. The inner pattern is created by the water flowing through the tines. The outer pattern is made by the water flowing over the tines.

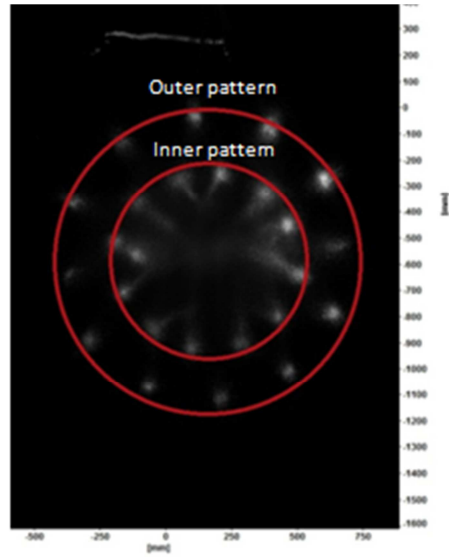


Figure 58: Spray Pattern Geometry

K-factor:

When analyzing how K-factor affects the spray geometry, several interesting points can be made. Figure 59 below will be used to demonstrate how an increase in K-factor affects the geometry.

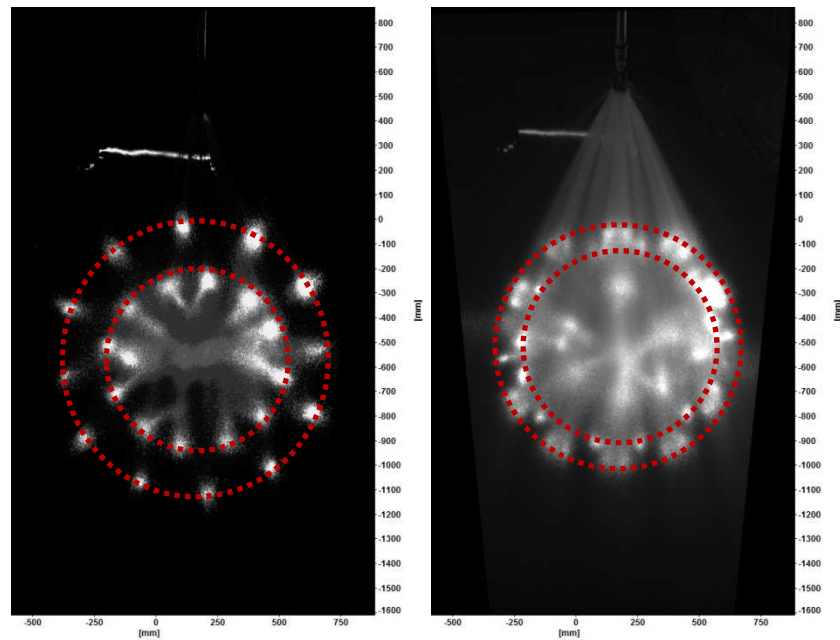


Figure 59: K-factor Affect on Spray Geometry

Left Side: 65°, 20psi, 1.8 K-factor, 2ft; Right Side: 65°, 20psi, 7.2 K-factor, 2ft

In order to measure the diameter of the inner and outer pattern, estimates were used. Although the geometry may not be a perfect circle, for the purpose of measuring the diameter it was assumed to be so, as can be seen in Figure 59 above. For the picture on the left, the outer diameter was found to be 1150 mm, while the inner diameter was measured as 860 mm. In the right sided picture, the outer diameter was found to be 1000 mm, and the inner was measured as 850 mm. With this, it is clear that with an increase in K-factor, the outer diameter decreases, while the inner diameter increases. As K-factor increases more flow can pass through the opening at a quicker rate. This leads to an increase in water being pushed inward rather than outward. Due to this occurrence, it makes sense that the outer diameter would decrease with an increase in K-factor, and that the inner diameter would increase.

This event also affects the overall spray geometry of the pictures. When the K-factor is lower, there is less water in the middle of the picture. When K-factor increases, there is more flow in the middle. This creates a star-like pattern in the middle of the flow in the picture on the right. On the left picture, there is an absence of flow in this area. Also, as K-factor increases there is more water spread overall. The definition in the tines and slots becomes blurred with an increasing K-factor. In the lower K-factor, this definition can more easily be seen, with dots and spaces clearly present.

Another interesting point that can be made is related to the flow over the tines. Figure 60 shows how the shape changes with increasing K-factor. In both pictures, dots can be seen where water flows over the tines. Although, when the K-factor is lower these dots are smaller and circular. When the K-factor increases, the dots become more spread, and form an oval or even square shape.

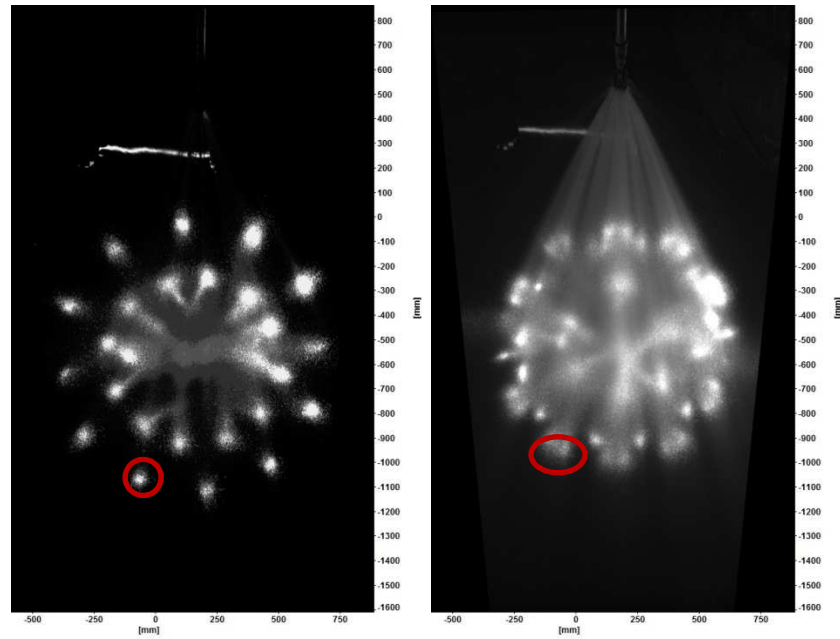


Figure 60: K-factor Affect on Tine Spray Geometry

Left Side: 65°, 20psi, 1.8 K-factor, 2ft; Right Side: 65°, 20psi, 7.2 K-factor, 2ft

Pressure:

When determining how pressure affects the spray geometry, several points were found. First off, in general, with an increase in pressure, definition is lost in the tine and slot pattern. Figure 61 below demonstrates this occurrence.

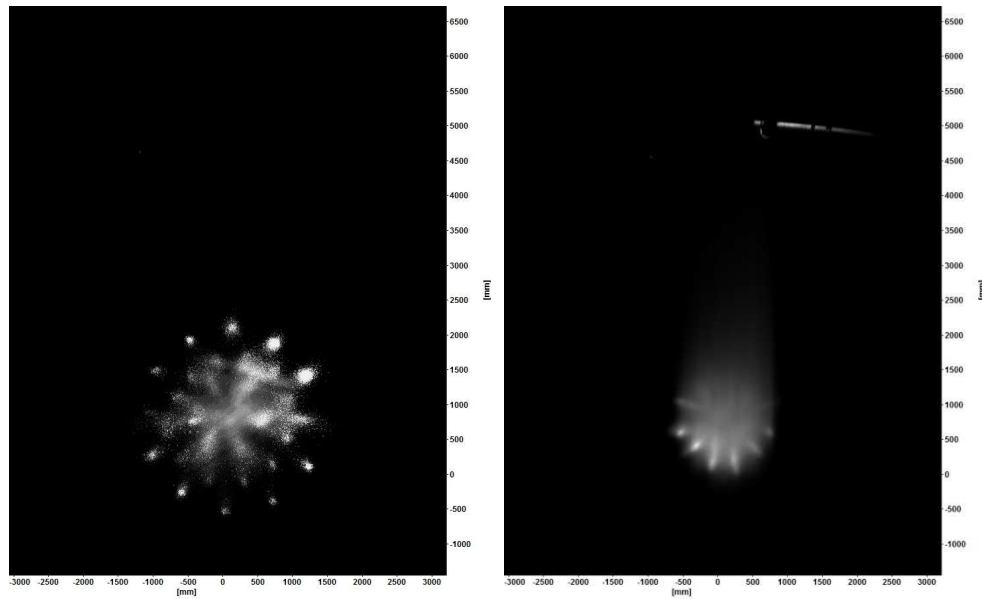


Figure 61: Pressure Affect on Spray Geometry

Left: 65°, 20psi, 3.0 K-factor, 6ft; Right: 65°, 175psi, 3.0 K-factor, 6ft

As shown in Figure 61, as the pressure increases from 20 psi to 175 psi, the picture becomes much less defined and more blurred. The overall pattern in the higher pressure looks more rounded off and combined than in the lower pressure. This is due to the fact the water flow rate increases with pressure increase. The water hits the deflector with a higher speed making it become more spread through the tine and slot. Thus, these two areas begin to mix together, creating a connected, blurred result.

Height:

Unlike K-factor and pressure, changing the height does not have a significant effect on spray pattern geometry. In Figure 62 below, the picture on the left is at 2ft, and the picture on the right is at 6ft. There is no difference in the tine and slot flow distribution, level of clarity, or overall geometry.

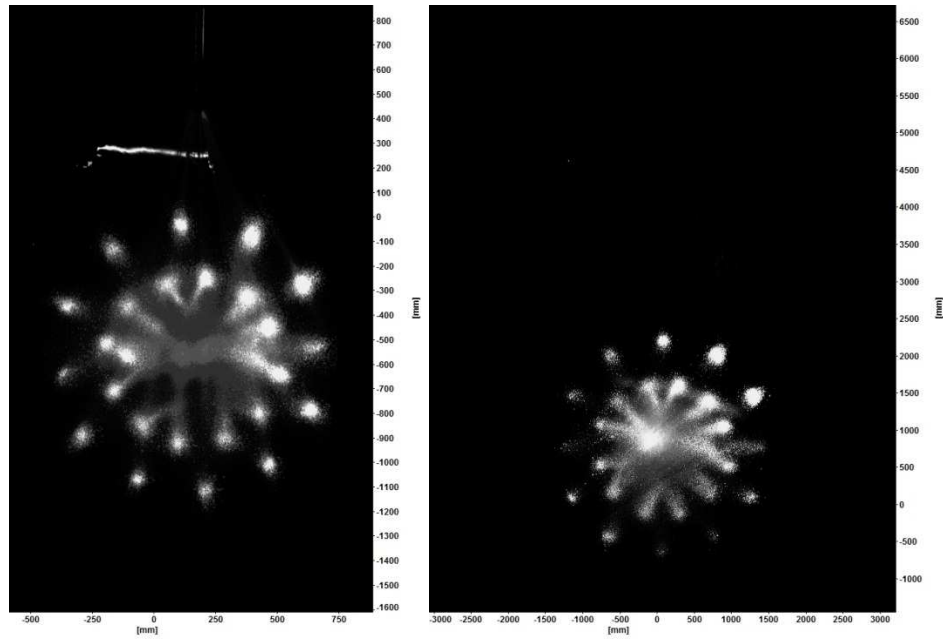


Figure 62: Height Affect on Spray Geometry

Left: 65°, 20psi, 1.8 K-factor, 2ft; Right: 65°, 20psi, 1.8 K-factor, 6ft

Figure 63 below shows pictures at the same pressure of 175 psi, but at different heights. On the left, the height is 2ft, and on the right it is 6ft. These pictures show how an increase in pressure at lower heights changes the distribution. At a higher pressure, there is a loss of definition. This is due to the force of the water flow blurring the differences between the position of the slot and tine. As the camera is moved down from 2ft to 4ft to 6ft, at higher pressures the picture will be more and more blurred.

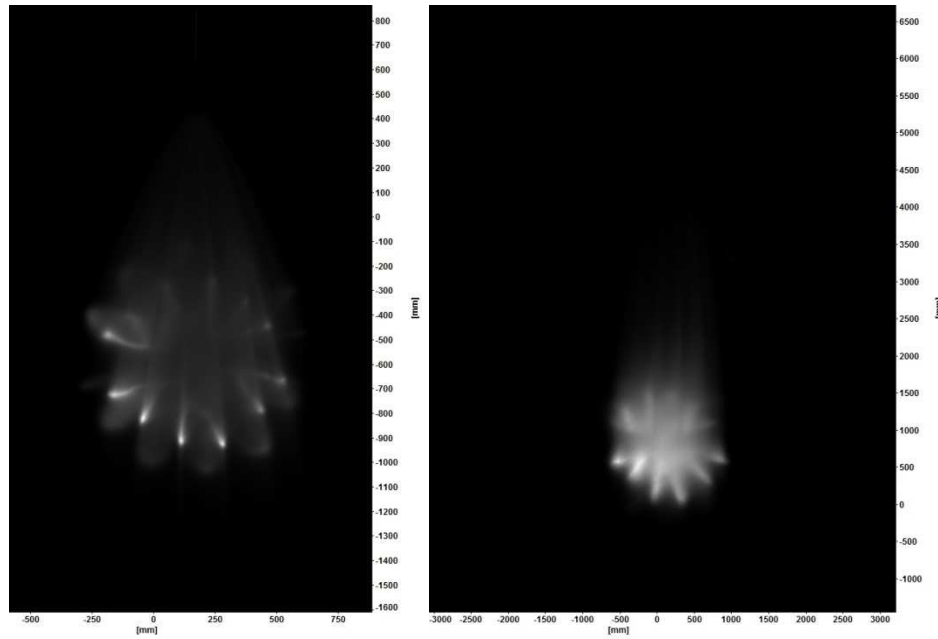


Figure 63: Height Affect on Spray Geometry

Left: 65°, 175psi, 1.8 K-factor, 2ft; Right: 65°, 175psi, 1.8 K-factor, 6ft

Ligament Distance

Droplet Breakup Distance: Once setup for shadowgraphy was completed, a decision needed to be made on where to take the pictures. This led right back to the literature to start trying to find examples of any other test that had been done previously. While some results of work done with shadowgraphy were found, there was not much that really related back to what was trying to be accomplished. To get a better idea of where to focus the pictures, PIV data needed to be analyzed to draw some conclusions. The distance from the bottom of the deflector, to the point of droplet breakup was measured on a 65° nozzle with a 1.8 K-factor at 20 psi. Four different pictures of this nozzle were used at each rotation: 0°, 45°, 60°, and 90°. In order to get the most accurate data out of these pictures measurements of the distance on the outside edges of the flow were made. This was more creditable since they were on the plane that the camera was focused on. Using this data, the best heights and distances to take shadowgraphy pictures was found.

Procedure: Measuring ligament distance was an interesting procedure for the group. We used Figure 64 as a basic guideline of where ligament distance could be measured at. It was known that when water leaves the nozzle, it starts out in a sheet-like formation. The water is complete, and unseparated. Once gravity and pressure begin to take their affect, the water splits into lines,

called ligaments. Finally, these ligaments will be broken up into separate droplets, and this is the point where ligament breakup has occurred.

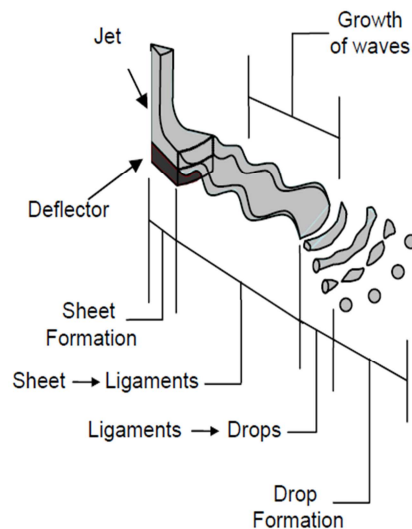


Figure 64: Ligament Distance (Ning Ren, et al.)

Since there was no defined way to measure ligament distance in the literature, we made a method of our own after speaking with Tyco employees. We decided to measure the outer edges of the flow to reduce error, and measure the ligament distance breakup downwards from the end of the nozzle. First, we would draw a horizontal line across where the nozzle ended. Then, we would figure out the best place to mark the end of the ligament. With this, we would measure down to that point to get our final measurement. Our method is shown in Figure 65 below.

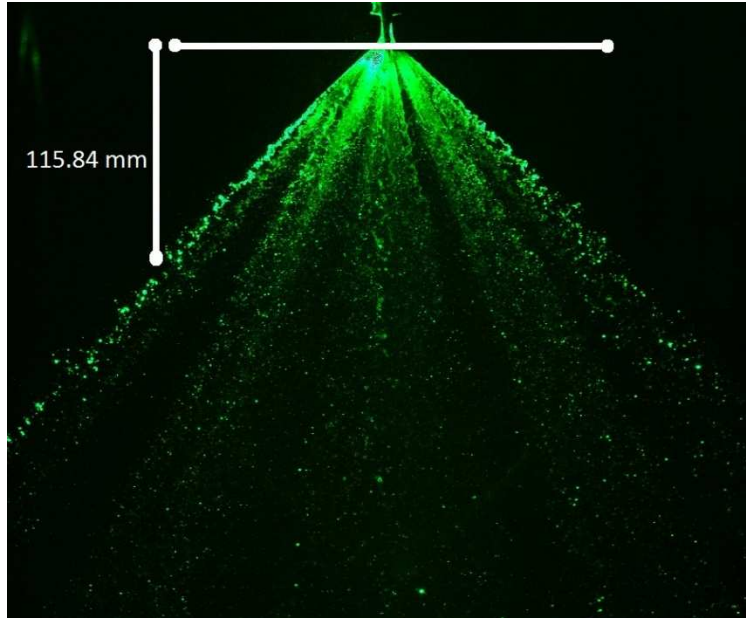


Figure 65: Ligament Distance Breakup Measurement Technique

Everyone agreed on the basic definition of ligament distance, but soon realized there was some subjectivity to this measurement. Everyone saw the ligament breakup at slightly different areas, since each perspective on when the droplets formed was different. Therefore, to reduce error as much as possible, each group member measured the ligament distance separately on every picture. Table 8 below shows the results of this process.

Table 8: Ligament Distance Measurement (by group member)

	Ligament Distance Measurement (mm)		
Rotation (°)	Rachel	Nick	Jonathan
0	109.73	101.25	110.67
	128.02	128.87	124.95
	114.3	128.87	114.24
	118.87	105.86	99.96
	108.58	128.87	117.81
	114.3	128.87	124.95
	97.16	119.66	99.96
	120.02	138.07	96.39
45	102.89	101.25	86.4
	102.89	105.86	97.2
	91.44	101.25	86.4

	102.89	101.25	93.6
	91.44	101.25	90
	102.89	96.65	90
	102.89	96.65	86.4
	102.89	101.25	93.6
60	108.58	115.2	100.8
	108.58	111.6	115.2
	114.3	122.4	115.2
	125.75	129.6	115.2
	120.02	146.3	132.09
	137.16	137.16	142.8
	137.16	155.45	121.38
	142.88	137.16	139.23
90	87.84	118.87	89.25
	102.89	128.02	78.54
	87.84	128.02	110.67
	87.84	118.87	110.67
	97.16	128.02	99.96
	102.89	109.73	107.1
	114.3	100.58	110.67
	114.3	118.87	110.67

After gathering this information, a way to display it in a more clear manner needed to be found, and final conclusions on where the average ligament distances were needed to be decided. In order to do so, Table 9 was created. Table 9 shows the averages of each group members measurements, and a final average of the separate averages combined.

Table 9: Average Ligament Distance Measurements

	0°	45°	60°	90°
Rachel	113.87	100.03	124.3	99.38
Nick	122.54	100.68	131.86	118.87
Jonathan	111.12	90.45	122.74	104.44
Final Average	115.84	97.05	126.3	107.56

Results: Once the data was compiled, it was decided to create charts out of the data to better display the information. On analyzing the charts, it was interesting to see how each persons measurements varied. As previously explained, everyones own perceptions influenced their measurements, which is why there is some variation in the numbers. In the end though, everyone was able to come to final averages which allowed a determination on where to take the shadowgraphy pictures. Therefore, even though measuring ligament distance was a long process, it was worth the efforts. It was found that the average ligament distance for the 0° rotation was around 115.84 mm. For the 45° rotation it was approximately 97.05 mm. The 60° rotation had an average ligament distance of 126.3 mm. Finally, the 90° rotation was around 107.56 mm. Figure 66 through Figure 69 show the average ligament distance data compiled into charts.

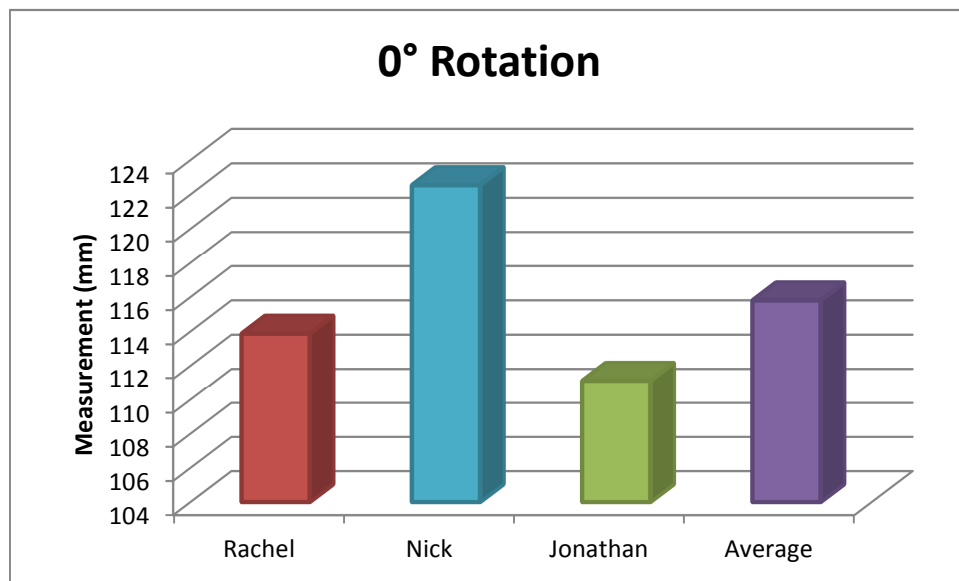


Figure 66: Average Ligament Distance Measurements of 0° Rotation

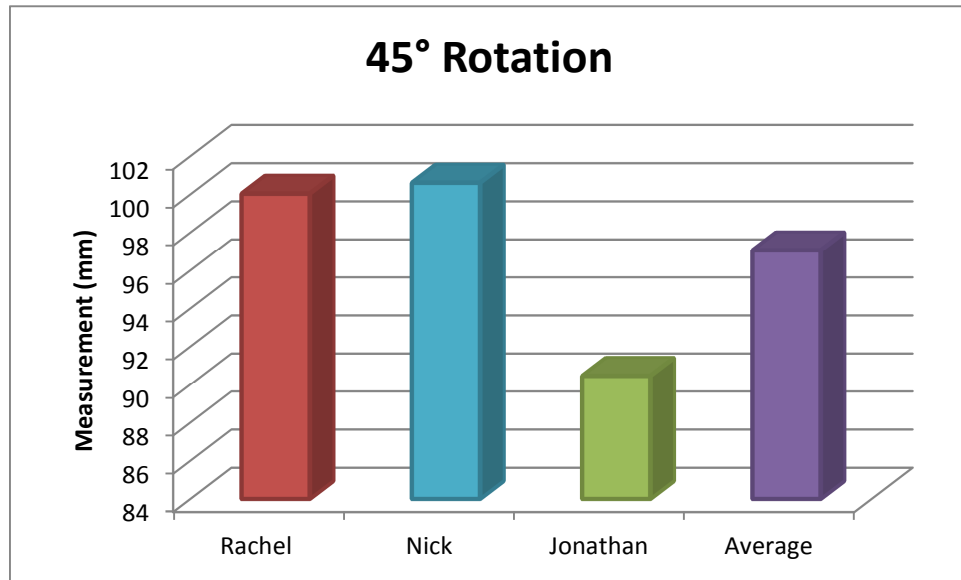


Figure 67: Average Ligament Distance Measurements of 45° Rotation

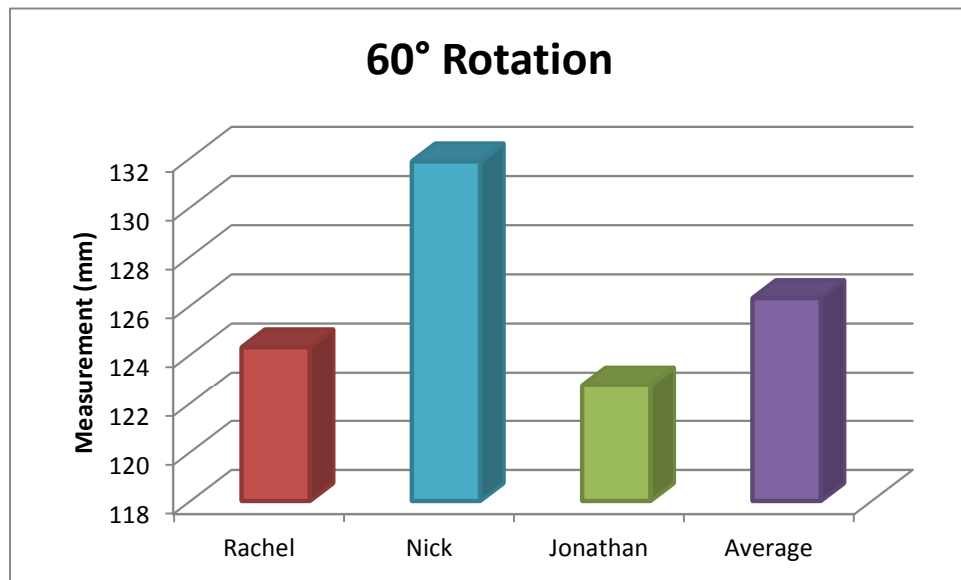


Figure 68: Average Ligament Distance Measurements of 60° Rotation

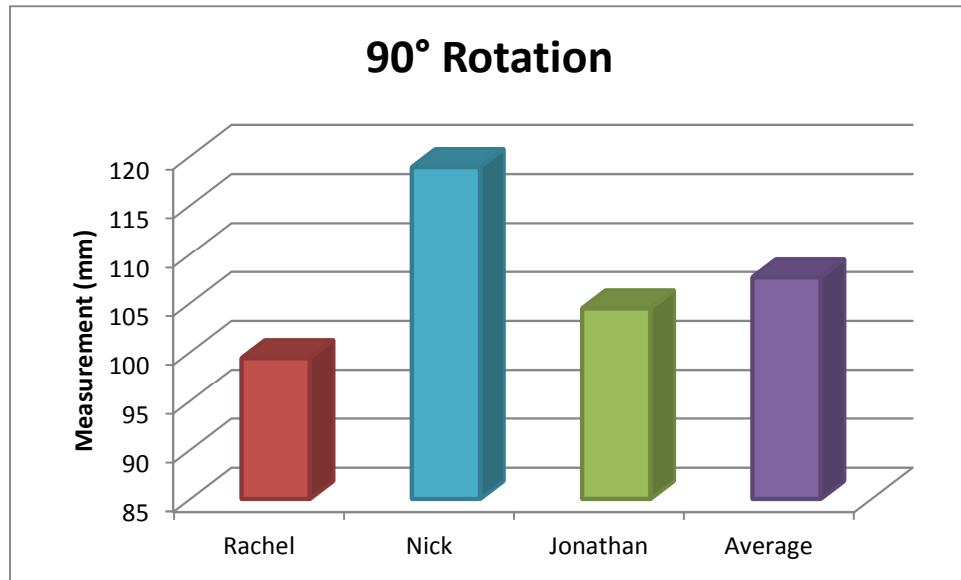


Figure 69: Average Ligament Distance Measurements of 90° Rotation

It was interesting to see how the ligament distance changes with varying rotations. With this understanding, a matrix for the preliminary shadowgraphy testing was created, which is shown in Table 10 below. Heights were decided based on previous procedures with the horizontal testing. After these preliminary tests are completed, there was hope to eliminate any repetitive or useless pictures for the remainder of testing.

Table 10: Preliminary Shadowgraphy Picture Plan Based off Ligament Distance Data

65 degree, 1.8 K-Factor, 20 psi	Height (middle of picture)	Depth of shot	Rotation Angle
	2ft	edge of flow	0 degrees
	2ft	edge of flow	45 degrees
	2ft	edge of flow	90 degrees
	2ft	quarter depth of flow	0 degrees
	2ft	quarter depth of flow	45 degrees
	2ft	quarter depth of flow	90 degrees
	2ft	middle of flow	
	4ft	edge of flow	0 degrees
	4ft	edge of flow	45 degrees
	4ft	edge of flow	90 degrees
	4ft	quarter depth of	0 degrees

		flow	
	4ft	quarter depth of flow	45 degrees
	4ft	quarter depth of flow	90 degrees
	4ft	middle of flow	
	6ft	edge of flow	0 degrees
	6ft	edge of flow	45 degrees
	6ft	edge of flow	90 degrees
	6ft	quarter depth of flow	0 degrees
	6ft	quarter depth of flow	45 degrees
	6ft	quarter depth of flow	90 degrees
	6ft	middle of flow	
rooster tail	0ft	To the side of the flow	left side
rooster tail	0ft	To the side of the flow	right side

The way we defined edge, middle, and under is shown in Figure 70 below.

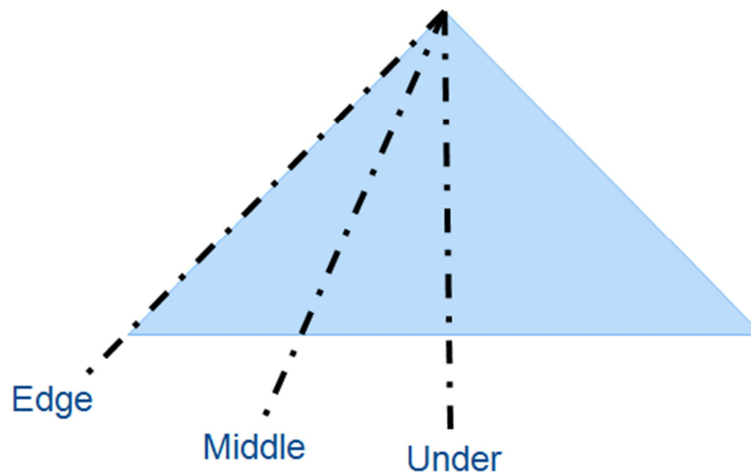


Figure 70: Edge, Middle, Under Representation

To verify the ligament distance results were true in all cases, another analysis was conducted. Using a 65° nozzle with a 1.8 K-factor, different pressures and rotation angles were compared to create Table 11 and Figure 71.

Table 11: Ligament Distance Data

Rotation Angle	Pressure	Top				Button				Average (mm)
		Left		Right		Left		Right		
0 degrees	100 psi	42.5	153	31	111.6	37.1	133.56	28.5	102.6	126.225
		40	144	37.5	135	33.4	120.24	30.5	109.8	
45 degrees	100 psi	30.5	109.8	29.7	106.92	31	111.6	28	100.8	106.155
		31.5	113.4	26.7	96.12	31.5	113.4	27	97.2	
60 degrees	100 psi	46.2	166.32	27	97.2	51.5	185.4	41	147.6	156.78
		47	169.2	40	144	51.2	184.32	44.5	160.2	
0 degrees	175 psi	53.5	192.6	32.7	117.72	47.6	171.36	29	104.4	141.75
		50.1	180.36	23.7	85.32	48.7	175.32	29.7	106.92	
45 degrees	175 psi	35.2	126.72	24	86.4	33.2	119.52	30.1	108.36	114.075
		39.8	143.28	31.5	113.4	29.8	107.28	29.9	107.64	
60 degrees	175 psi	35.8	180.2			40.5	183.1			179.525
		42.5	178.4			39.2	176.4			

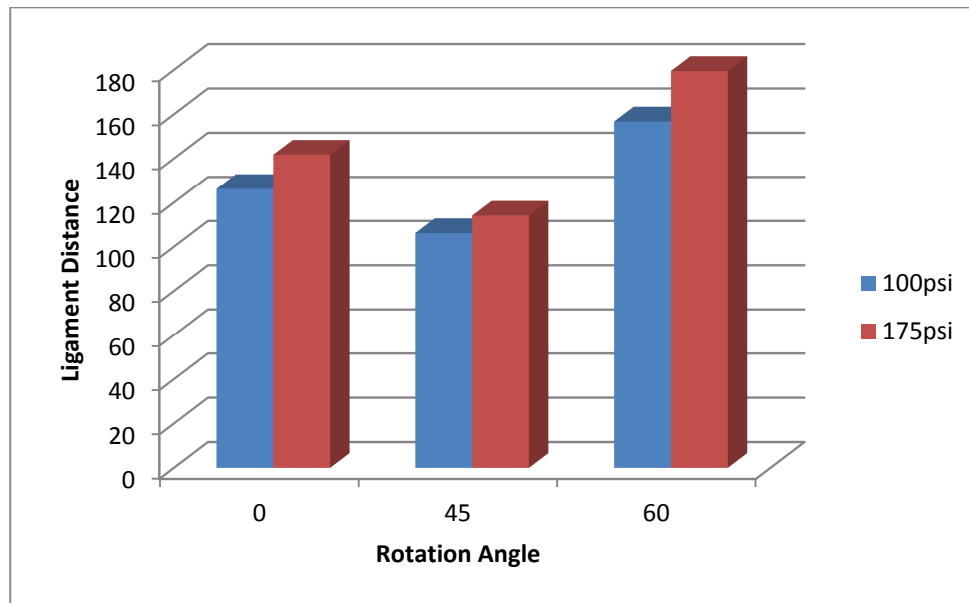


Figure 71: Ligament Distance with Varying Pressures

The figure above demonstrates the change in ligament distance breakup under different pressures and different rotation angles. As shown in the figure, when the pressure increased, the ligament distance also increases. Also, for the average of the three rotation angles, the data of the 45° rotation was consistently smallest. This data proves the previous analysis on ligament distance is accurate. With this, it can be decided that these two samples of data will be representative for the rest of the ligament distance pictures. The results from both ligament distance analysis were combined to create Table 12 below.

Table 12: Average Ligament Distance Breakup: 65° nozzle with a K-factor of 1.8

	0°	45°	60°	90°
20 psi	115.84 mm	97.05 mm	126.3 mm	107.56 mm
100 psi	126.23 mm	106.56 mm	156.78 mm	No Ligament
175 psi	141.75 mm	114.08 mm	180 mm	No Ligament

A couple general trends on ligament distance can be seen in Table 12. First off, as pressure increases, so does ligament distance breakup. As pressure increases from 20 psi to 175 psi, the ligament distance breakup consistently increases. Also, at a 45° rotation angle, the ligament distance breakup is always smaller than at 0° and 60° rotation.

Shadowgraphy

The following section includes an in-depth look into the shadowgraphy testing. This is a preliminary analysis, and is not completely representative of all the shadowgraphy data sets. Following sections will include a deeper look into the shadowgraphy results.

Numerous tables are presented in order to give the reader a clear look into the results, since shadowgraphy produces an excess of intricate statistics and pictures. However, shadowgraphy was an important part of this project since it produced valuable information on droplet size, which PIV does not show.

Since a limited time period was given to complete this project, and because shadowgraphy analysis could take quite a long time, not every K-factor and pressure was tested. Table 13 below shows each test that was conducted. The red represents a test that was left out. It was decided

that 3.0 K-factors would not be tested, as well as 175 psi. Further, measuring at a height of 2 feet was decided to be unnecessary after finishing the 65° nozzle tests.

Table 13: Shadowgraphy Tests Conducted

65 Degree Nozzle			
K-Factor	1.8	3.0	7.2
Pressure	20	100	175
Height	1	2	3
Angle	0	45	90
Location	Edge	Middle	Under
125 Degree Nozzle			
K-Factor	1.8	3.0	7.2
Pressure	20	100	175
Height	1	2	3
Angle	0	45	90
Location	Edge	Middle	Under
180 Degree Nozzle			
K-Factor	1.8	3.0	7.2
Pressure	20	100	175
Height	1	2	3
Angle	0	45	90
Location	Edge	Middle	Under

When working with shadowgraph, over 100 pictures were taken. Three nozzles were tested at numerous K-factors, pressures, locations, heights, and angles. This made the statistical results quite long and complicated. Therefore, in this section, only a summary of the results will be shown in tabular form. The results below were derived from the 65° nozzle with a K-factor of 1.8 at a pressure of 20 psi. The height, location, and angle were variable in the table shown below. Although this is only a sample selection of data shown in this section, it represents how the remainder of the tests was performed. For example, the same pattern of tests was run for the 65° nozzle at different K-factors and pressures. This is also true for the 125° and 180° nozzle.

Table 14: Shadowgraphy Results for 65 Degree Nozzle, 1.8 K-factor, 20 psi

65 Degree Nozzle, 1.8 K-factor, 20 psi, 1 ft, 0, Edge		65 Degree Nozzle, 1.8 K-factor, 20 psi, 1 ft, 45, Edge	
N	3348	N	2564
N_Corrected	3519.3	N_Corrected	2939.12
D10	0.098739 mm	D10	0.08989 mm

D32	0.653792mm	D32	0.572903 mm
DV10	0.368627 mm	DV10	0.303339 mm
DV50	0.924091 mm	DV50	0.806458 mm
DV90	0.997776 mm	DV90	0.997502 mm
RMS	0.133032 mm	RMS	0.10979 mm
65 Degree Nozzle, 1.8 K-factor, 20 psi, 1 ft, 0, Middle		65 Degree Nozzle, 1.8 K-factor, 20 psi, 1 ft, 90, Middle	
N	3795	N	4397
N_Corrected	4998.1	N_Corrected	3649.83
D10	0.07736 mm	D10	0.125036 mm
D32	0.381742 mm	D32	0.628003 mm
DV10	0.152647 mm	DV10	0.284228 mm
DV50	0.723107 mm	DV50	0.943909 mm
DV90	0.996935 mm	DV90	0.997835 mm
RMS	0.069344 mm	RMS	0.138112 mm
65 Degree Nozzle, 1.8 K-factor, 20 psi, 1 ft, 0, Under		65 Degree Nozzle, 1.8 K-factor, 20 psi, 1 ft, 90, Under	
N	6985	N	5276
N_Corrected	9863.58	N_Corrected	5762.85
D10	0.071738 mm	D10	0.093678 mm
D32	0.178628 mm	D32	0.552224 mm
DV10	0.068458 mm	DV10	0.203215 mm
DV50	0.281731 mm	DV50	0.991141 mm
DV90	0.990102 mm	DV90	0.998228 mm
RMS	0.041949 mm	RMS	0.0857 mm
65 Degree Nozzle, 1.8 K-factor, 20 psi, 2 ft, 0, Edge		65 Degree Nozzle, 1.8 K-factor, 20 psi, 2 ft, 45, Edge	
N	1165	N	1223
N_Corrected	1418.65	N_Corrected	1626.18
D10	0.084664 mm	D10	0.076907 mm
D32	0.594559 mm	D32	0.481936 mm
DV10	0.329842 mm	DV10	0.243939 mm
DV50	0.89927 mm	DV50	0.829676 mm
DV90	0.997568 mm	DV90	0.997486 mm
RMS	0.11025 mm	RMS	0.083329 mm
65 Degree Nozzle, 1.8 K-factor, 20 psi, 2 ft, 0, Middle		65 Degree Nozzle, 1.8 K-factor, 20 psi, 2 ft, 45, Middle	
N	1026	N	1098
N_Corrected	1381.9	N_Corrected	1440.86
D10	0.076176 mm	D10	0.078021 mm
D32	0.71929 mm	D32	0.527613 mm
DV10	0.362462 mm	DV10	0.245569 mm
DV50	0.992697 mm	DV50	0.964236 mm
DV90	0.998539 mm	DV90	0.997885 mm

RMS	0.094445 mm	RMS	0.087621 mm
65 Degree Nozzle, 1.8 K-factor, 20 psi, 2 ft, 0, Under		65 Degree Nozzle, 1.8 K-factor, 20 psi, 2 ft, 45, Under	
N	3085	N	2717
N_Corrected	4037.76	N_Corrected	3628.96
D10	0.077465 mm	D10	0.076011 mm
D32	0.210425 mm	D32	0.281133 mm
DV10	0.081064 mm	DV10	0.096732 mm
DV50	0.393237 mm	DV50	0.637485 mm
DV90	0.996437 mm	DV90	0.997089 mm
RMS	0.044244 mm	RMS	0.052901 mm
65 Degree Nozzle, 1.8 K-factor, 20 psi, 2 ft, 90, Edge		65 Degree Nozzle, 1.8 K-factor, 20 psi, 3 ft, 0, Edge	
N	935	N	1244
N_Corrected	1174.02	N_Corrected	1529.26
D10	0.082541 mm	D10	0.085074 mm
D32	1.24535 mm	D32	0.909079 mm
DV10	0.620195 mm	DV10	0.574526 mm
DV50	0.993848 mm	DV50	0.99277 mm
DV90	0.99877 mm	DV90	0.998554 mm
RMS	0.125355 mm	RMS	0.146215 mm
65 Degree Nozzle, 1.8 K-factor, 20 psi, 2 ft, 90, Middle		65 Degree Nozzle, 1.8 K-factor, 20 psi, 3 ft, 0, Middle	
N	1411	N	622
N_Corrected	1728.71	N_Corrected	552.971
D10	0.08367 mm	D10	0.115596 mm
D32	0.475333 mm	D32	0.504567 mm
DV10	0.211975 mm	DV10	0.213508 mm
DV50	0.768372 mm	DV50	0.990323 mm
DV90	0.997611 mm	DV90	0.998065 mm
RMS	0.09218 mm	RMS	0.10103 mm
65 Degree Nozzle, 1.8 K-factor, 20 psi, 2 ft, 90, Under		65 Degree Nozzle, 1.8 K-factor, 20 psi, 3 ft, 0, Under	
N	6134	N	3525
N_Corrected	8402.48	N_Corrected	4552.09
D10	0.074251 mm	D10	0.078578 mm
D32	0.546865 mm	D32	0.260329 mm
DV10	0.198606 mm	DV10	0.092255 mm
DV50	0.992653 mm	DV50	0.830818 mm
DV90	0.998531 mm	DV90	0.997701 mm
RMS	0.062902 mm	RMS	0.04891 mm
65 Degree Nozzle, 1.8 K-factor, 20 psi, 3 ft, 45, Edge		65 Degree Nozzle, 1.8 K-factor, 20 psi, 3 ft, 90, Edge	
N	529	N	788
N_Corrected	870.46	N_Corrected	1190.49

D10	0.061815 mm	D10	0.068219 mm
D32	0.471739 mm	D32	0.869276 mm
DV10	0.333969 mm	DV10	0.613193 mm
DV50	0.806523mm	DV50	0.991887 mm
DV90	0.997533 mm	DV90	0.998377 mm
RMS	0.063738 mm	RMS	0.104347 mm
65 Degree Nozzle, 1.8 K-factor, 20 psi, 3 ft, 45, Middle		65 Degree Nozzle, 1.8 K-factor, 20 psi, 3 ft, 90, Middle	
N	1029	N	1231
N_Corrected	1065.11	N_Corrected	1392.31
D10	0.099617 mm	D10	0.091406mm
D32	0.586164 mm	D32	0.635858mm
DV10	0.265953 mm	DV10	0.335817mm
DV50	0.982396 mm	DV50	0.956444mm
DV90	0.997925 mm	DV90	0.997859mm
RMS	0.113632 mm	RMS	0.120007mm
65 Degree Nozzle, 1.8 K-factor, 20 psi, 3 ft, 45, Under		65 Degree Nozzle, 1.8 K-factor, 20 psi, 3 ft, 90, Under	
N	4106	N	2925
N_Corrected	5271.1	N_Corrected	3898.32
D10	0.079234 mm	D10	0.076005 mm
D32	0.451675 mm	D32	0.144985 mm
DV10	0.134475mm	DV10	0.066948 mm
DV50	0.992578 mm	DV50	0.157284 mm
DV90	0.998515 mm	DV90	0.642735 mm
RMS	0.061885 mm	RMS	0.038715 mm

There are many patterns and trends that can be found from this information. First, the number of droplets will be analyzed. A general trend that can be seen in this data is that the number of droplets found increases as the picture is taken closer to the center. On the edge, usually the least number of droplets are counted. In the middle, a somewhat higher number is shown. Under the flow, the highest number can be found. When it comes to angle, there are also some patterns related to number of droplets. At 0°, the lowest amount of droplets is counted. At 45°, this number is higher, and at 90° it is greatest. This may relate to the position of the slots and tines. The 45° angle is on a slot, while the other two angles are on tines. It is interesting to see the difference between the two angles that are on tines. The position of the frame arm may be a factor in reducing the number of droplets around the 0° angle. The height of the picture also affected how many droplets were found. When the camera was positioned at 1 ft, the greatest

number of droplets was counted. In order to shorten the testing required, we decided to eliminate testing at 2 ft and focus testing on the 1 ft and 3 ft heights, as there was not a very significant difference between the data at 2ft and 3ft.

To compare how pressure, K-factors, and spray angles affect the shadowgraphy results, another table is necessary. Table 15 shows how a sample set of data changes with a different pressure, K-factor, and nozzle angle. Using the 65° nozzle with a K-factor of 1.8 at 20 psi, the same nozzle will be compared at a higher pressure of 100 psi. Also, a comparison of the K-factor will be shown, with all variables staying the same besides an increase in the K-factor from 1.8 to 7.2. Lastly, the nozzle will be compared by using the data from a 180° nozzle with K-factor of 1.8 at 20 psi. The bolded words and numbers represent the variable that was changed with respect to the first nozzle in blue.

Table 15: Pressure, K-factor, Nozzle Change Comparison

65 Degree Nozzle, 1.8 K-factor, 20 psi, 1 ft, 0, Middle	
N	3795
N_Corrected	4998.1
D10	0.07736 mm
D32	0.381742 mm
DV10	0.152647 mm
DV50	0.723107 mm
DV90	0.996935 mm
RMS	0.069344 mm
65 Degree Nozzle, 1.8 K-factor, 100 psi , 1 ft, 0, Middle	
N	4036
N_Corrected	4973.67
D10	0.082499 mm
D32	0.249738 mm
DV10	0.09963 mm
DV50	0.407136 mm
DV90	0.994546 mm
RMS	0.057821 mm
65 Degree Nozzle, 7.2 K-factor , 20 psi, 1 ft, 0, Middle	
N	2058
N_Corrected	1822.54
D10	0.118279 mm
D32	0.908472 mm

DV10	0.484799 mm
DV50	0.992452 mm
DV90	0.99849 mm
RMS	0.164791 mm
180 Degree Nozzle, 1.8 K-factor, 20 psi, 1 ft, 0, Middle	
N	3529
N_Corrected	4034.88
D10	0.089118 mm
D32	0.304901 mm
DV10	0.118033 mm
DV50	0.525728 mm
DV90	0.995612 mm
RMS	0.067146 mm

Looking at this information, it is simple to see how pressure affects the number of particles. As pressure increases, so does the particle count. This is a rather simple concept, since at higher pressures, more water is passing through at a quicker rate, and so, more particles would be present. An increase in K-factor seems to have the opposite effect on the number of particles. As K-factor increases from 1.8 to 7.2, the particle count drops significantly. This may be due to the fact that a higher K-factor allows for a wider spread. Therefore, in the small section that the pictures were taken, there may have been a more concentrated amount of water at this area when using the smaller K-factor nozzle. The nozzle angle does not seem to have a great affect on the particle count. When the 65 degree nozzle is compared to the 180 degree nozzle in the same position, K-factor, and pressure, the number of particles remains around the same number.

Returning to Table 15, there are few comparisons that can be made with how angle, location, and height affect the D and DV values. They seem to fluctuate randomly, with no consistent patterns or trends. Although, Table 15 helps show some interesting trends related to this data. The D10 value has only a slight increase with pressure increase, but the DV50 value greatly reduces as pressure increases. This may be due to the fact that the average volume of the flow is more distributed with the higher pressure. With an increase in K-factor, both the D10 and DV50 values increase only slightly. This shows that the K-factor does not have a significant impact on the size or volume spread of the particles. With an increase in nozzle angle, the D10 value is not greatly

affected. The DV50 value decreases with an increase in nozzle angle. This can be attributed to the wider angle having a more distributed spread than the more concentrated 65° angle.

With the shadowgraphy results derived from this project, analysis could take months.

Unfortunately, only seven weeks could be spent working on this project, and so, there was a limit on how in-depth the analysis could be. With this, a summary of the results was shown to give an understanding of how six different variables could affect droplets. As location, angle, and height change the number of particles is significantly affected. The D10 and DV50 values seem to have no particular pattern with these changes. When looking into how pressure, K-factor, and nozzle angle affect droplets, interesting trends were also found. Each of these variables changes the number of particles, but seems to also have an effect on the D10 and DV50 values. With this understanding, it can be seen that diameter and volume density change more consistently with changes in nozzle angle and pressure than in location or K-factor alterations.

Citations:

Ren, N., Blum, A., Zheng, Y., Do, C. and Marshall, A., 2009. "Quantifying The Initial Spray From Fire Sprinklers." *Fire Safety Science* 9: 503-514. doi:10.3801/IAFSS.FSS.9-503

Appendix I: Data Handling and Storage

Working on this project with Tyco involved being bound to a confidentiality agreement. With this, privacy was an important aspect of our work. All documents, notes, and data were kept on Tyco's password-protected computers. Only the project team and Tyco employees had access to this information. Today, the files are stored on a flash drive that was given to the project advisor for future work. This will ensure that information is kept secure while still allowing Tyco to make use of the data for related projects. Folders on the flash drive are divided into 'Verticle PIV Testing,' 'Horizontal PIV Testing,' and 'Shadowgraphy.' In each folder are the complete data sets and related pictures.

The files associated with this project area all titled in a similar manner. Each name specifies the type of nozzle, the spray angle, the water pressure, the K-factor, and information about the setup.

Vertical PIV file naming:

Nozzle Type_Spray Angle_Pressure_Rotation Angle_K-factor _Number Of Pictures

Example: D3_65_20_0_1.8_500

Horizontal PIV file naming:

Nozzle Type_Spray Angle_Pressure_K-factor_Height Below Deflector_Number Of Pictures

Example: D3_65_20_1.8_2ft_500

Shadowgraphy file naming:

Nozzle Type_Spray Angle_K-factor_Pressure_Radius_Location In Flow_“Shadow”

Example: D3_65_1.8_20_1ft_0_edge_Shadow

Appendix J: Error Analysis

Since this was one of the first times Tyco was using the LaVision laser system, their employees, as well as this project group were new to the technology. With this, possibilities for error rose, since we did not know how to use all of the software functions. Also, similar to any project, common errors could have occurred throughout the project by incorrect measurements and misinterpretations of the data. There were a few opportunities for error that we noticed and will point out in this section.

First off, in vertical PIV testing, we measured spray angle from the vertical average pictures by hand. The lines we drew were based on visual observation. We used protractor and ruler to measure the angles. This method left room for systematic errors due to the limitations of accuracy using the protractor, as well as random errors that fluctuate from one measurement to the next. The LaVision software had a way to measure spray angle; unfortunately, it was not working correctly. In the future, it would be beneficial to figure out this technique to double-check hand measured results. Also for vertical PIV testing, our ligament distance measurements left room for error. Since there was no defined way to measure ligament distance in the literature, we took our own unique approach. We measured vertically downwards to get the ligament distance breakup, and this may not have been the correct method. Also, ligament distance was measured by hand; this left room for basic mistakes such as incorrect measurements. Ligament distance was difficult to measure since there was subjectivity, so personal interpretations were also taken into account.

When working in the lab with shadowgraphy, there was also room for error. In the shadowgraphy testing, we estimated the edge, middle and under according to the spray angle we got from vertical PIV testing. We used the protractor to estimate the deviation angle from under the nozzle to the edge and used a string to define the radii. The estimation was rough. Therefore, we cannot guarantee the area we looked was on the exactly position. Also, since it was based on our previous spray angle measurements, there was no guarantee those were completely correct to begin with. Another possible error in shadowgraphy testing was related to the camera and equipment. Since the camera needed to actually be in the spray, the lamp and lens inevitably got wet. Sometimes it seemed this occurrence affected the quality of our results. In order to make

sure the pictures we took were clear enough, we often had to adjust the intensity of laser. However, the intensity of laser, in some degree, would influence the results. That is, if the intensity is higher, some of smaller droplets would lose their shadow and cannot be recognized by the computer. Therefore, it is possible that changing the intensity of the laser may have caused some error in the results.

Other errors may have been due to basic fluid dynamic principles. Since we did not calculate friction losses, we would not know the exact pressure entering the nozzle. Even though we controlled the pressure by use of an electrical pressure gauge, head loss inside of the pipe contributed to a pressure loss at the nozzle. This error should be taken into consideration. During our time at Tyco, we attempted to make our results as accurate as possible. Unfortunately, there was some room for error, and these possibilities should be considered in future work.

Appendix K: Tyco Scientific Presentation

The following slides were presented to an audience at Tyco as a technical MQP presentation. This hour-long presentation included a detailed explanation of the project, as well as an extensive question and answer session.



The Group



Nicholas Fast
Mechanical Engineering



Rachel Winsten
Civil Engineering

The Group



Bohan "Jonathan" Hao
Mechanical Engineering



上海交通大学
SHANGHAI JIAO TONG UNIVERSITY



Yueshan "Stella" Chu
Mechanical Engineering

Table of Contents

- Introduction and Purpose
- Background
- Setup
- Particle Image Velocimetry (PIV)
- High-magnification Shadow Imaging (Shadowgraphy)
- Results
- Benefits
- Future Work

Introduction

- Seven week project on sprinkler spray characterization
- Fulfills WPI Major Qualifying Project (MQP) requirements
- In conjunction with Shanghai Jiao Tong University (SJTU)
- Outcomes
 - Conference paper for SUPDET 2012
 - MQP report for WPI
- Presentation is an overview of the study

Purpose

- Create a way to quantify sprinkler characteristics in an effort to develop a more technical approach to sprinkler design
- Groundbreaking research for future spray characterization projects
- Analysis of:
 - Droplet Size
 - Spray Angle
 - Spray Pattern
 - Ligament Distance
 - Droplet Velocity



Background

- Sprinkler Design

- Old testing methods need to be updated

- Fire Modeling

- Input data
- Only as accurate as the information provided
- Characterization improves Fire Dynamics Simulator (FDS) results

- Approval Agencies

- Beginning to use laser testing
- Important to gain understanding for future

Background

- Tyco Type D3 Protectospray Nozzle

- Open, external deflector type nozzle
- Primary goal is preventing excessive heat absorption
- Available spray angles: 65°, 80°, 95°, 110°, 125°, 140°, 160° and 180°
- Available with K-factors: 1.2, 1.8, 2.3, 3.0, 4.1, 5.6 and 7.2

- Limited amount of comparable studies

Background



Different K-factors
(7.2, 3.0, 1.8)



Different Spray Angles
(65°, 125°, 180°)

Laser

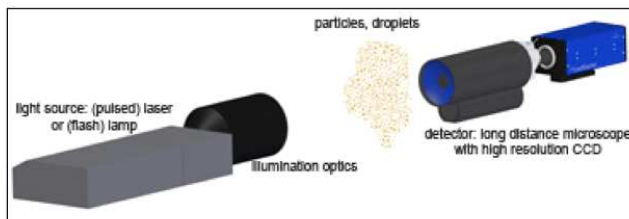
- Two different ways of shooting pictures

- Particle Image Velocimetry (PIV)

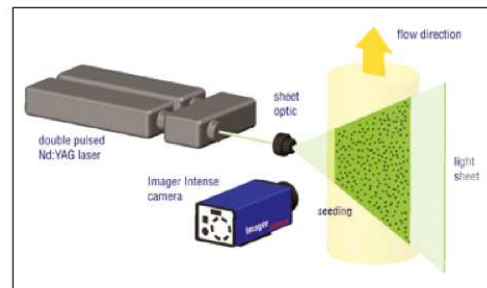
- Both vertical and horizontal slices

- High-magnification Shadow Imaging (Shadowgraphy)

- Small area of focus



Shadowgraphy



PIV

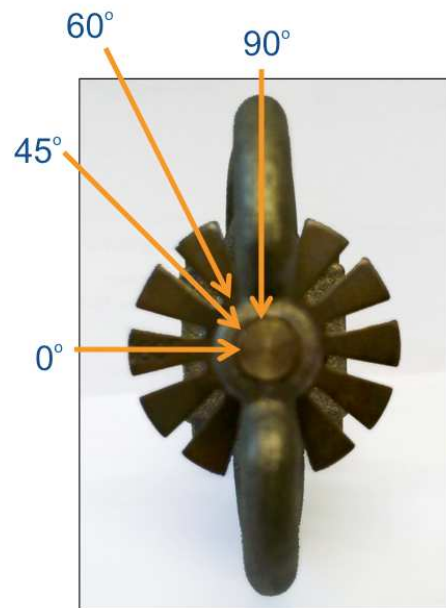
Picture of Vertical PIV testing



Parameters

- Rotation Angles

- Tine: 0°, 60°
- Slot: 45°
- Frame Arm: 90°



Lab Setup

•PIV

- Safety overview- laser, tarps, glasses

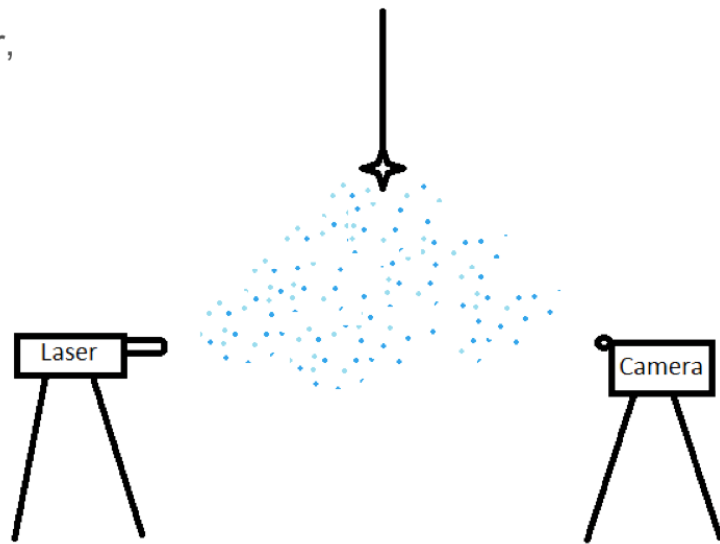
- Vertical

- Laser and camera positions

- Rotating nozzle equipment

- Horizontal

- Laser and camera positions



Vertical PIV setup

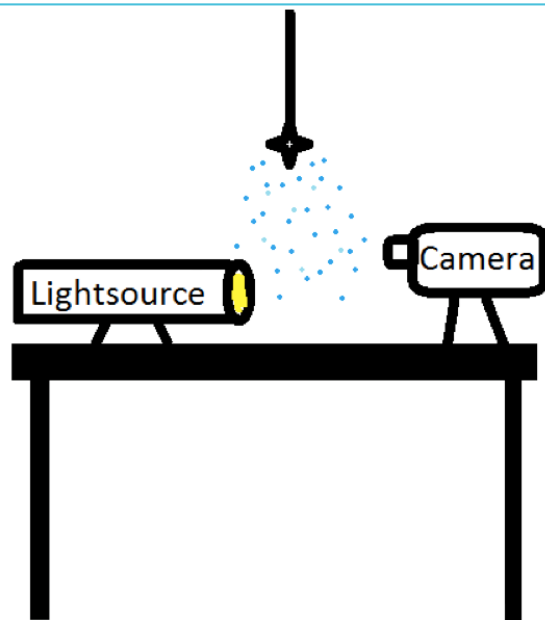
Lab Setup

- Shadowgraphy

- Camera and equipment

- Laser and camera facing each other

- Droplets create shadows



Shadowgraphy Setup

PIV

- Two forms of PIV testing: Vertical and Horizontal

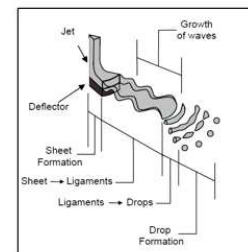
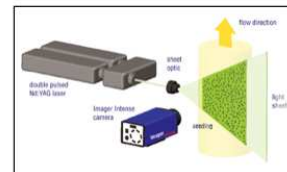
- Vertical provides “profile” of the flow

- **Spray Angle**- angle formed by flow out of nozzle

- **Ligament Distance**- distance between sheet and separate droplets

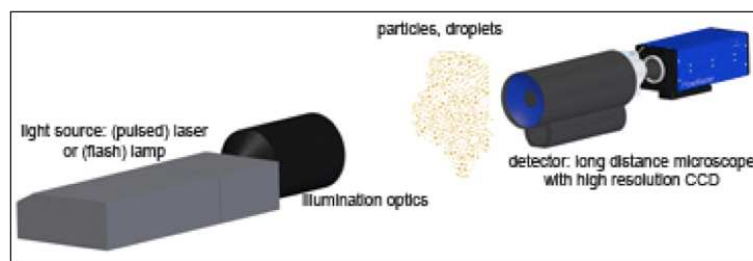
- Horizontal provides “fingerprint” of the flow

- **Flow Geometry (Spray Pattern)**- shape created by flow onto ground

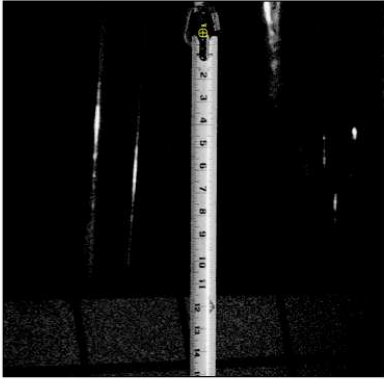


Shadowgraphy

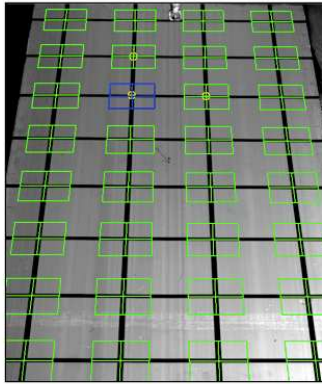
- Highlights a small area of the flow
- Can see very small droplets in the flow
- Uses for Shadowgraphy
 - Droplet Size
 - Velocity



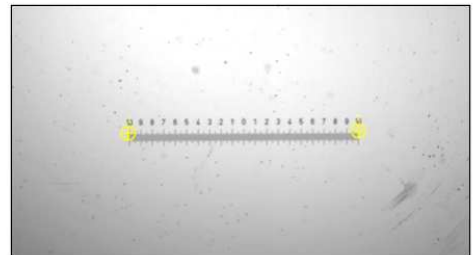
Calibration



Vertical PIV:
Tape measure



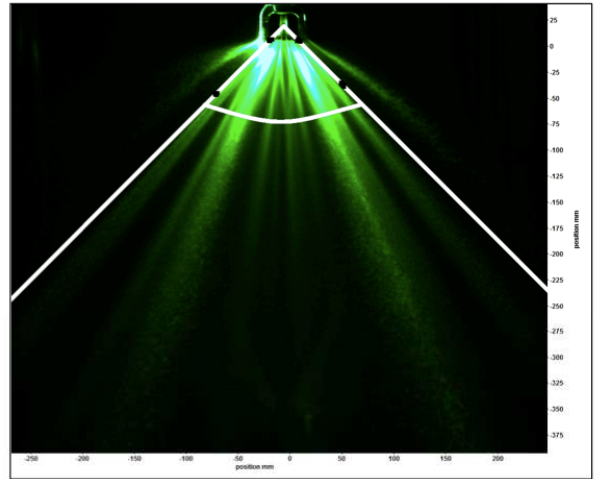
Horizontal PIV:
Styrofoam board



Shadowgraphy:
Calibration lens

Results: Spray Angle

- Method of spray angle measurement
 - Deflector angle vs. measured spray angle
- Two points determine a straight line
 - Point 1: Edge of deflector
 - Point 2: Beginning of change



65°, 20 psi, 1.8 K-factor, 90 degree rotation

Results: Spray Angle

- Pressure does not influence spray angle
- 60° rotation is more consistent with the average

Pressure Rotation	65°(1.8)			125°(3.0)			180°(7.2)	
	20psi	100psi	175psi	20psi	100psi	175psi	20psi	100psi
0°	96°	94°	96°	145°	153°	157°	175°	176°
45°	94°	94°	95°	147°	150°	149°	178°	177°
60°	95°	96°	93°	145°	151°	142°	178°	177°
90°	95°	94°	91°	143°	148°	143°	175°	175°
AVG	95°	94.5°	93.8°	145°	150.5°	147.8°	176.5°	176.3°

Results: Spray Angle

- No obvious trends as K-Factor increases

60 degree

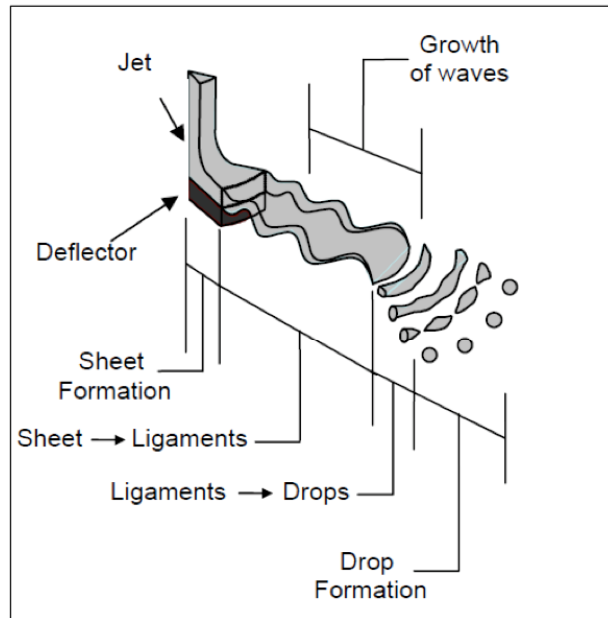
	65°			125°			180°	
K-factor Pressure	1.8	3	7.2	1.8	3	7.2	1.8	7.2
20psi	95°	95°	88°	144°	145°	146°	174°	178°
100psi	96°	98°	93°	145°	151°	149°	175°	177°
175psi	93°	97°		148°	142°			
AVG	94.7°	96.7°	90.5°	145.7°	146°	147.5°	174.5°	177.5°

0 degree

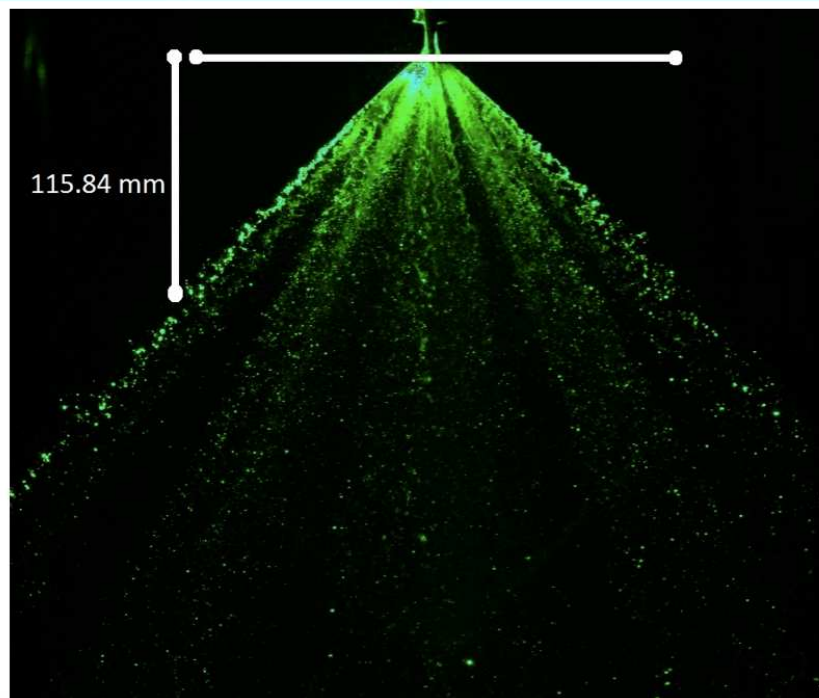
	65°			125°			180°	
K-factor Pressure	1.8	3	7.2	1.8	3	7.2	1.8	7.2
20psi	96°	91°	99°	145°	146°	143°	179°	174°
100psi	95°	95°	94°	144°	150°	149°	177°	175°
175psi	94°	98°		152°	156°			
AVG	95°	94.7°	96.5°	147°	150.7°	146°	178°	174.5°

Results: Ligament Distance

- Characteristic found from Vertical PIV results
- Often ranges between 90-200 mm from nozzle
- Sheet → Ligaments → Drops
- Measured by hand
 - Averages of all group members taken



Results: Ligament Distance



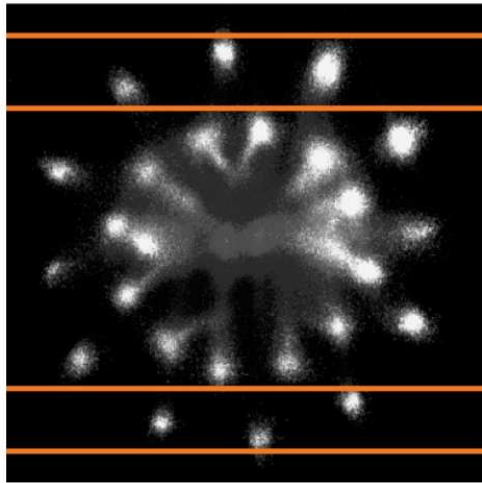
Results: Ligament Distance

- General trends

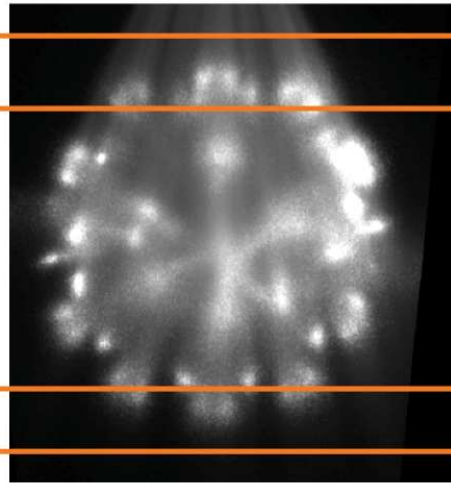
- Pressure increase = ligament distance breakup increases
- Rotation angle affected breakup distance
 - At 45° (on slot) was smallest
 - At 0° and 60° (on tine) was significantly larger

Average Ligament Distance Breakup: 65° nozzle with a K-factor of 1.8				
	0°	45°	60°	90°
20 psi	115.84 mm	97.05 mm	126.3 mm	107.56 mm
100 psi	126.23 mm	106.56 mm	156.78 mm	No Ligament
175 psi	141.75 mm	114.08 mm	180 mm	No Ligament

Results: Horizontal

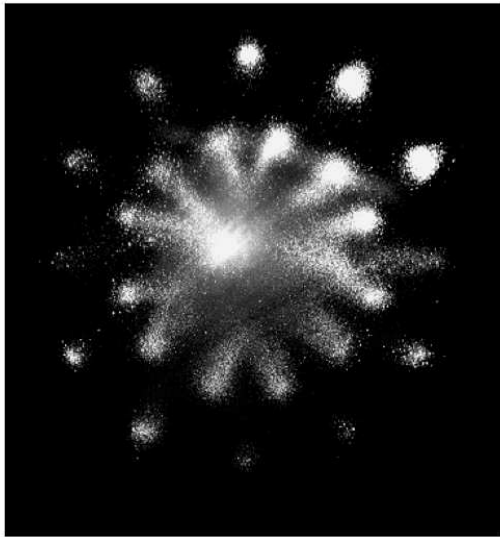


65°, 20psi, 1.8 K-factor, 2ft

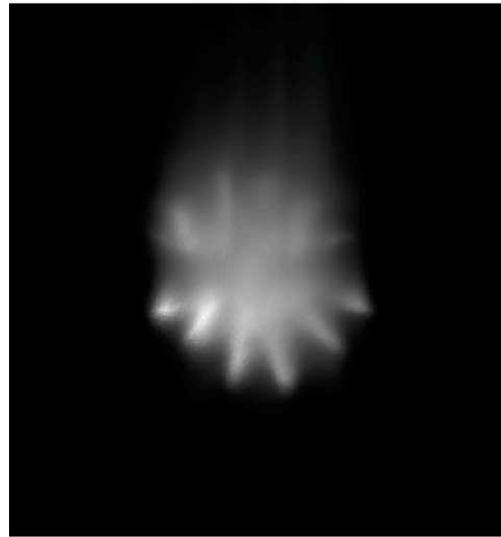


65°, 20psi, 7.2 K-factor, 2ft

Results: Horizontal

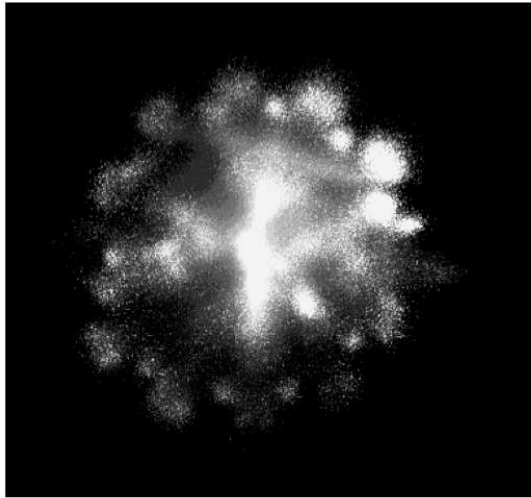


65°, 20psi, 1.8 K-factor, 6ft

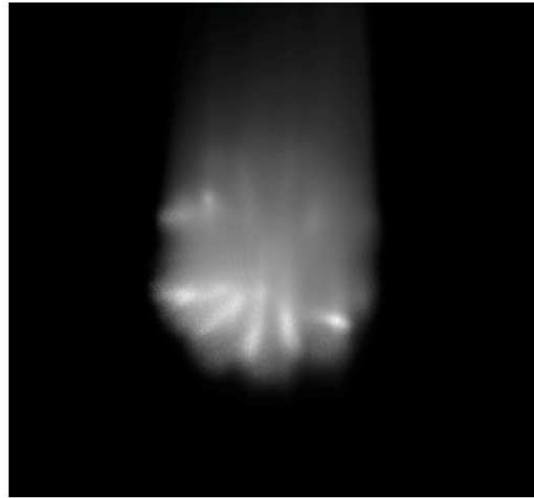


65°, 175psi, 1.8 K-factor, 6ft

Results: Horizontal

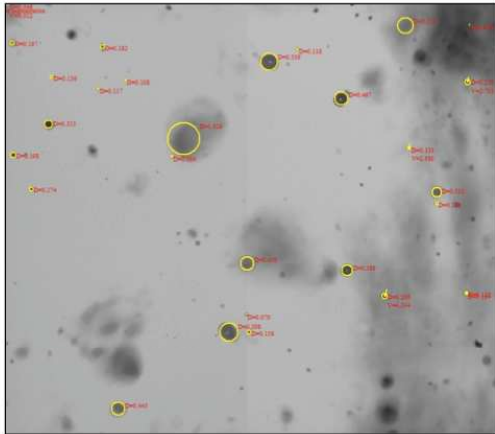


65°, 20psi, 7.2 K-factor, 6ft



65°, 100psi, 7.2 K-factor, 6ft

Results: Shadowgraphy

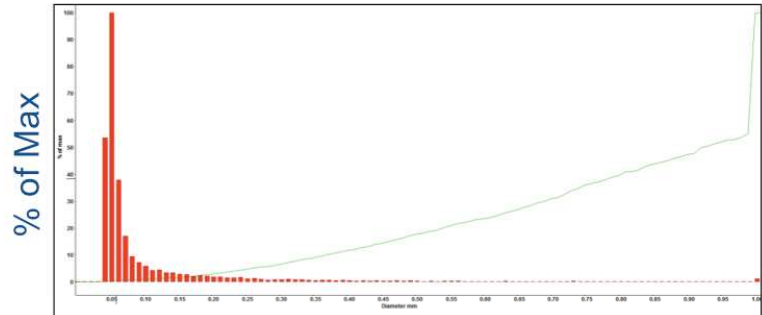
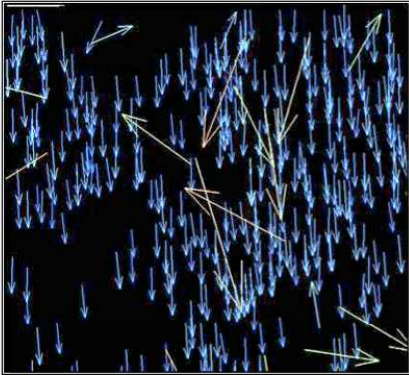


Number of Particles	3348
D10	0.0987
D32	0.6538
DV10	0.3686
DV50	0.9241
DV90	0.9978

- Statistics:

- D10- mean diameter value
- D32- surface volume diameter
- DV“XX”- volume median diameter

Results: Shadowgraphy



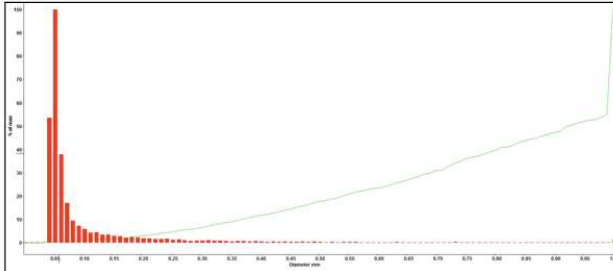
Diameter of Droplet

- Histograms

- X Axis: Diameter of the droplets;
- Y Axis: Percentage of the max volume
- Red Line: Number of the droplets
- Green Line: Cumulative percentage

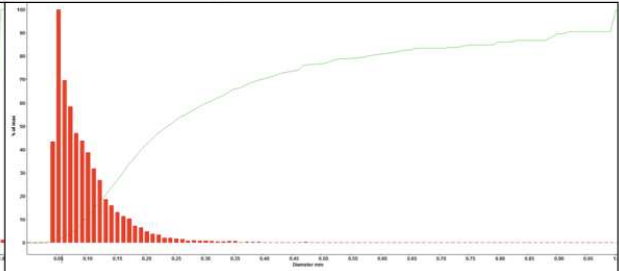
Results: Droplet Size

Low Pressure



Number of Particles	3348
D10	0.0987
D32	0.6538
DV10	0.3686
DV50	0.9241
DV90	0.9978

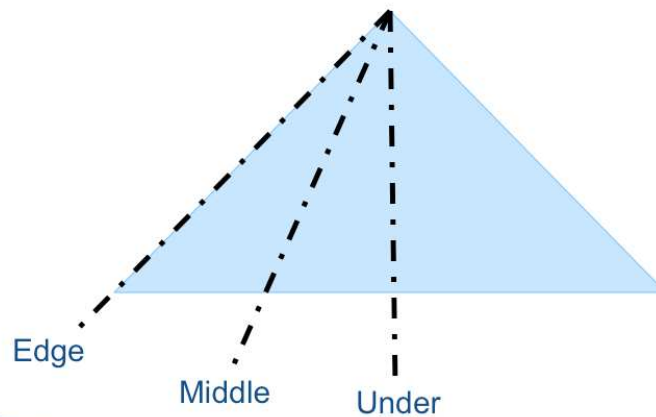
High Pressure



Number of Particles	4504
D10	0.0934
D32	0.2039
DV10	0.0987
DV50	0.2387
DV90	0.0574

Results: Droplet Size

	Edge (Number of droplets/DV50 in mm)	Middle (Number of droplets/DV50 in mm)	Under (Number of droplets/DV50 in mm)
20 psi, 0°	3348/.9241	3795/.7231	6985/.2817
100 psi, 0°	4504/.2387	4036/.4071	6211/.5406



Benefits

- Better understanding of:
 - LaVision laser system
 - Sprinkler characterization
- Learning how to work in a cross-functional environment
- Learning to work in global groups
 - Understanding other cultures and how people work
 - Overcoming differences to achieve a common goal
 - Enhancing everyone's vocabulary

Conclusion

- Ligament distance increases as pressure increases
- Shorter ligament distance at slots than tines
- K-factor and Pressure do not affect spray angle
- Distribution of spray affected by K-factor and pressure

Future Work: Short Term

- Test full range of D3 nozzles
- Use computer software to full potential
 - Measuring spray angle
 - Velocity maps in PIV
- More extensive testing of Shadowgraphy

Future Work: Long Term

- Expanding research to more applications
- Complete spray characterization
- Characterizing effects of surface contact

Acknowledgements

- We would like to thank all the extremely helpful and supportive employees at Tyco and especially give thanks to:

- George Oliver
- Paul Piccolomini
- Melissa Avila
- Chad Goyette
- Zach Magnone
- Prof. Nicholas Dembsey
- Prof. Chen Li
- Patricia Beaulieu





Thank You



Appendix L: Presentation for TFP President George Oliver

As part of the project, a presentation was prepared for the Tyco Fire Protection President George Oliver. This presentation covered a brief overview of the project completed, as well as several slides on group dynamic. With the nature of this joint project (combined effort from SJTU and WPI) learning to work in a global project group was a very big concern and played a large role overall.



The Group



Nicholas Fast
Mechanical Engineering



Rachel Winsten
Civil Engineering

The Group



Bohan "Jonathan" Hao
Mechanical Engineering



上海交通大学
SHANGHAI JIAO TONG UNIVERSITY



Yueshan "Stella" Chu
Mechanical Engineering

Background

- Sprinkler Design

- Testing methods are archaic and need to be updated

- Fire Modeling

- Input data
 - Only as accurate as the information provided
 - Characterization improves Fire Dynamics Simulator (FDS) results

- Approval Agencies

- Beginning to use laser testing
 - Important to gain understanding for future

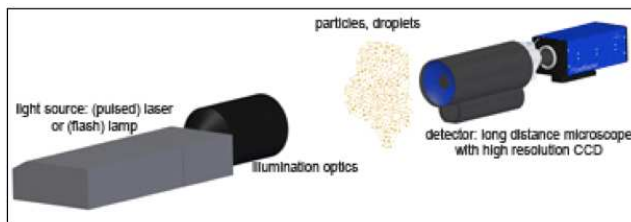
Purpose

- To create a way to quantify sprinkler characteristics in an effort to develop a more technical approach to sprinkler design
- Groundbreaking research for future spray characterization projects
- Analysis of:
 - Droplet Size
 - Spray Angle
 - Spray Pattern
 - Ligament Distance
 - Droplet Velocity

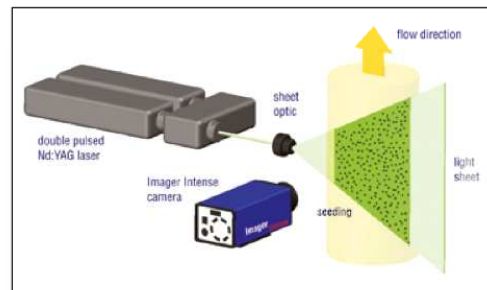


Laser

- Two different ways of shooting pictures
 - Particle Image Velocimetry (PIV)
 - Both vertical and horizontal slices
 - High-magnification Shadow Imaging (Shadowgraphy)
 - Small area of focus



Shadowgraphy

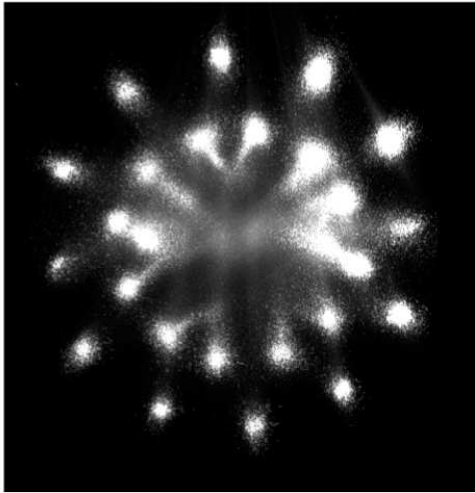


PIV

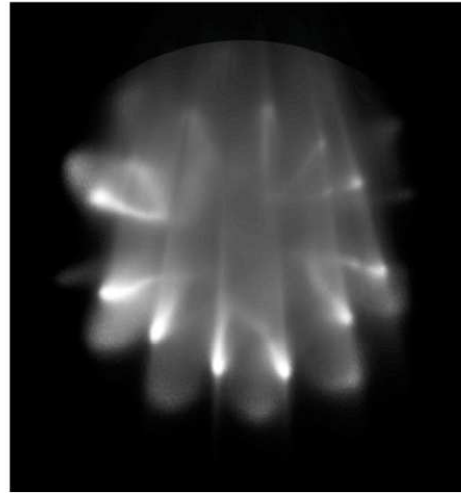
Picture of Vertical PIV testing



Results: Horizontal PIV

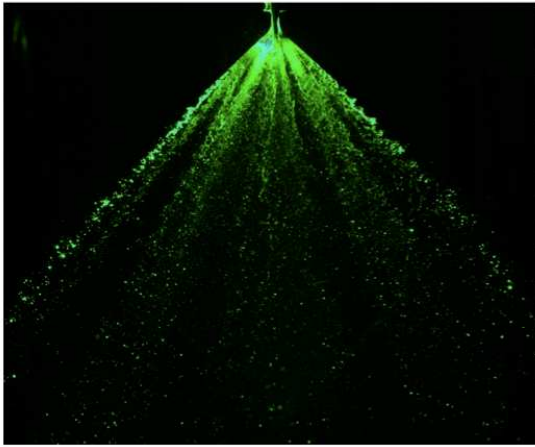


65° Nozzle, 20psi, 1.8K-factor, height of 2ft

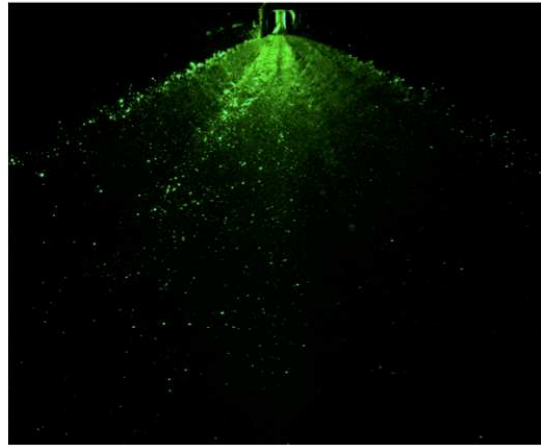


65° Nozzle, 175psi, 1.8K-factor, height of 2ft

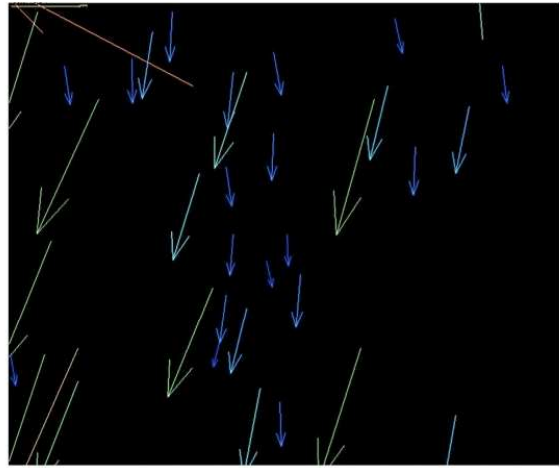
Results: Vertical PIV



65° Nozzle, 20psi, 1.8
K-factor, 0° rotation



125° Nozzle, 20psi, 3.0
K-factor, 60° rotation



10 confidential

161

Results

- K-factor affects the distribution of inner and outer spray patterns
- Pressure increase loses definition around tines and slots
- Distance from nozzle is only a factor at high pressures and higher K-factors
- Comparable results between tests
 - Droplet distribution with higher pressures and droplet size
 - Less flow at edge of 90° rotation in shadowgraphy, also shows in PIV

Benefits to Tyco

- Benefits of testing

- Better understanding of operation of LaVision system
- Developed a basis for understanding sprinkler characterization
- Will help lead to more reliable computer modeling and testing
- Cut down on time and cost required for design cycle

Teaming



Watching TV at the Hotel

Working on the final paper



Overcoming Differences

- An important aspect of being able to work as a team was understanding some of our cultural differences
 - Slowing down English for better comprehension
 - Being straightforward in letting people know if you do not understand
 - Understanding and respecting the differences in the ways that people express themselves

Benefits of a global project team

- Learning how to work in a cross-functional environment
- Learning to work in global groups
 - Understanding other cultures and how people work
 - Overcoming differences to achieve a common goal
 - Enhancing everyone's vocabulary
 - Improving cooperation skills
 - Different views on problems

Team Bonding

- Paw Sox Baseball game
- Red Sox Baseball game
- Tyco-Cranston Golf Tournament
- Dinner in Boston
- Shopping Trips
- WPI campus visit
- Bowling
- Evening bonding time at the hotel
- Group meals
- Cultural Trip to Florida





Getting ready to golf!



Tyco goes bowling!



Having fun at the Sox game!

Florida Trip



Jonathan, Stella and Rachel at Disney World

Acknowledgements

- We would like to thank all the extremely helpful and supportive employees at Tyco and especially give thanks to:
 - George Oliver
 - Paul Piccolomini
 - Melissa Avila
 - Chad Goyette
 - Zach Magnone
 - Prof. Nicholas Dembsey
 - Prof. Chen Li



Thank You

